Transmembrane Ephrin Ligands in Neural and Vascular Development

Thesis by

Hai Wang

In Partial Fulfillment of the Requirements

for the Degree of

Doctor of Philosophy

in Biology

California Institute of Technology
Pasadena, CA

1999

(Submitted August 26, 1998)

Acknowledgement

My special thanks to:

David Anderson, for his encouragement, energy, and support.

My thesis committee: Kai Zinn, Paul Sternberg, Barbara Wold and Ellen Rothenberg, for their advice.

Lab members, campus colleagues and faculties, for their help and friendships. Testu Sato, for cloning tips. Sarah Fashena, for hIgG1Fc expression vector. Liching Lo, for cell techniques. Andy Groves, for in situs. Nirao Shah, for crest preps. Other alumni: Chris Schoenherr, Lukas Sommer, Joe Verdi, Eric Mercer, Susan Birren and Mohendra Rao, for teaching. Sherry Perez, Alice Paquette, for chick embryos. Sebastian Gerety, for computer obsession-sharing. Qiufu Ma, for molecular tricks. Zhoufeng Chen, for gene-knockouts. Amy Greenwood, Pat White, Mariela Zirlinger, Raymond Mongeau, Jae Kim, Sean Morrison, Limin Han, Qiao Zhou, Qi Sun and Yang liu, for sharing. Scott Fraser and Marianne Bronner-Fraser for collaboration. Steve Padilla, Ling Wang, Gina Mancuso, Gaby Mosconi and Lan Dinh, for lab support. Shirley Pease, Robert Vega, Lilia Anonuevo and others, for animal cares. Colorland and Graphic Arts, for excellent photography. Many others, ...

Mom, dad, brother and sister-in-law, for their renewed curiosity in molecular biology.

Abstract

Receptor tyrosine kinases and their ligands play important roles in development. Using an expression cloning approach, I identified two transmembrane ligands - ephrinB1 and ephrinB2 for the receptor tyrosine kinase EphB2. Trunk neural crest cell migration and early motor axon outgrowth are restricted to rostral somite halves. Transmembrane ephrin ligands were localized to the caudal somite halves in both mouse and chick. In vitro functional assays revealed that the ephrin ligands can repulsively guide migrating crest cells and early motor axons that express the receptor EphB2. Targeted gene deletion was used to dissect mouse ephrinB2's role in vivo. By examining multiple markers for hindbrain, somite, migrating crest, and motor axons, I failed to show any obvious phenotypic alterations in the mutant embryos. Related ephrins or unrelated regulators may play redundant roles in the nervous system. Unexpectedly, ephrinB2 mutants die around E10.5 due to severe vascular defects. EphrinB2's unique expression in the blood vessels is restricted to the arteries and not veins. Morever, EphB4, another receptor for ephrinB2, was found restricted to veins and not arteries. Thus, ephrinB2 and its receptor EphB4 revealed a molecular distinction between arteries and veins -- two types of vessels defined by the directions of blood flow. Deletion of ephrinB2 in the arteries resulted in defective arterial angiogenesis in the capillary beds. Embryonic veins also suffered from defective remodeling in the absence of a normal artery development. These results indicated that ephrinB2-EphB4 mediated interactions between arteries and veins is essential for the angiogenesis of both types of vessels. The nature of ligand-receptor signaling between arterial and venous endothelial cells in the capillaries remain unexplored. There are several implications based on our finding. First, more genes are likely expressed differentially in arteries and veins, consistent with the pathological differences between the two types of vessels. Second, the specification of arterial and venous endothelial cells suggests novel embryonic patterning events. Third, the ephrinB2-EphB4 signaling system between arteries and veins is a potential antiangiogenic target for controlling abnormal vascular development in tumor angiogenesis.

Table of Contents

Chapter 1

Introduction

Receptor tyrosine kinases (RTKs) and their ligands play important roles in development. Various evidence suggests that multiple RTKs and their ligands are involved in different aspects of neural crest development, such as cell proliferation, differentiation and migration (For review, see Sieber-Blum and Zhang, 1997). For example, bFGF has been shown to promote the proliferation of the mouse and chick neural crest cells (Bannerman and Pleasure, 1993; Kalcheim and Neufeld, 1990; Murphy et al., 1994). Results from our laboratory have indicated that glia growth factor and its receptor ErbB2 are involved in restricting neural crest stem cells to a glial fate (Shah et al., 1994).

To further dissect the roles of RTKs in the development of the neural crest cells, I used a degenerate RT-PCR approach to survey existing and discover novel RTKs expressed in the neural crest cells. One of the RTKs identified was Nuk/EphB2, a member of the large Eph receptor family (Henkemeyer et al., 1994). At the time of my study (1994), no ligand had been discovered for EphB2 receptor. However, researchers from Amgen had just identified B61/ephrinA1 as a membrane anchored ligand for another Eph family receptor Eck/EphB2 (Bartley et al., 1994). This finding made us think that a similar transmembrane ligand would exist for the EphB2 receptor. Using an expression cloning approach, I have identified two transmembrane ligands for the Nuk/EphB2 receptor - ephrinB1 and ephrinB2. Our subsequent studies focused on the expression patterns and functions of the two ligands in the peripheral nervous system and the vascular system.

A) Ephrin Ligands

Eph family RTKs consist of at least 13 members which are expressed in various developmental compartments such as the nervous system, the immune system, and the vascular system (For review, see Flanagan and Vanderhaeghen, 1998; Gale and Yancopoulos, 1997). The ligands for Eph related RTKs are all membrane achored, and divided into two classes: five members with the GPI membrane linkage and three transmembrane proteins (Gale and Yancopoulos, 1997). Promiscuity is a key feature of the ligand-receptor binding relationship among different members (Gale et al., 1996). GPI linked ligands - ephrin A1 - A5, bind with more or less equal affinities to Eph A class receptors. Transmembrane ligands - ephrinB1 - B3, bind with more or less equal affinities to Eph B class receptors. There is minimal cross binding between the ligands and the receptors of opposite class, with an exception that Sek1/EphA4 can cross react with ephrinB class ligands (Gale et al., 1996). For a summary of nomenclature for the Eph receptors and ephrins, see table 1.

Eph family receptors and ligands display dynamic expression patterns in development, notably in the nervous system. EphA3 and its ligands ephrinA2 and ephrinA5 have been shown to regulate repulsive axon guidance in the retinotectal system (For review, see Drescher et al., 1997). The receptor EphA3/Mek4 is expressed by temporal retinal axons, whereas its ligands, ephrinA2 and ephrinA5, are expressed in posterior tectum (Cheng et al., 1995; Drescher et al., 1995). Axons expressing the EphA3 receptor project from temporal retina to anterior tectum which has the lowest levels of ephrinA ligands. In vitro assays and in vivo perturbations suggested that these 2 ephrinA ligands are repellent molecules for the receptor-bearing temporal retinal axons (Drescher et al., 1995; Nakamoto et al., 1996).

EphB class receptors and their transmembrane ephrinB ligands are also expressed in the nervous system. EphB2/Nuk receptor is expressed by early axons of motor and sensory neurons in the trunk (Henkemeyer et al., 1994). EphB2/Nuk receptor mutant mice, though viable, display commissural axon pathfinding defects (Henkemeyer et al., 1996). Biochemical studies on ephrinB1 and related transmembrane ligands have shown that they can transmit intracellular signaling through cytoplasmic domains (Bruckner et al., 1997; Holland et al., 1996). The EphB type receptors and their transmembrane ligands can mediate bi-directional signaling during cell-cell contact, which make them particularly suited for regulating cell movements and axonagenesis. Our studies have further revealed their dynamic expression patterns in the developing somites and blood vessels. More importantly, our results have suggested their unique roles in regulating cell migration, axon guidance, as well as blood vessel angiogenesis.

Receptors: new name	previous names	Ligands: new name	previous names
EphA1	Eph, Esk	ephrin-A1	B61; LERK-1, EFL-1
EphA2	Eck, Myk2, Sek2	ephrin-A2	ELF-1; Cek7-L, LERK-6
EphA3	Cek4, Mek4, Hek, Tyro4; Hek4	ephrin-A3	Ehk1-L, EFL-2, LERK-3
EphA4	Sek, Sek1, Cek8, Hek8, Tyro1	ephrin-A4	LERK-4; EFL-4
EphA5	Ehk1, Bsk, Cek7, Hek7; Rek7	ephrin-A5	AL-1, RAGS; LERK-7, EFL-5
EphA6	Ehk2; Hek12		
EphA7	Mdk1, Hek11, Ehk3, Ebk		
EphA8	Eek; Hek3		
EphB1	Elk, Cek6, Net; Hek6	ephrin-B1	LERK-2, Elk-L, EFL-3, Cek5-L; STRA1
EphB2	Cek5, Nuk, Erk, Qek5, Tyro5, Sek3; Hek5, Drt	ephrin-B2	Htk-L, ELF-2; LERK-5, NLERK-1
EphB3	Cek10, Hek2, Mdk5, Tyro6, Sek4	ephrin-B3	NLERK-2, Elk-L3, EFL-6, ELF-3; LERK-8
EphB4	Htk, Myk1, Tyro11; Mdk2		
EphB5	Cek9; Hek9		
EphB6	Mep		

Table 1 Nomenclature for the Eph receptor and ephrin families. Previous names are listed by publication date with full-length sequences shown first. Names after a semicolon indicate hypothetical orthologs, or proposals to rename a sequence that had previously been published.

B) Somite Polarity and Crest Migration

In chick and mouse, migrating neural crest cells in the trunk use either of two major pathways. Initially they migrate ventrally through the sclerotome of the rostral somite halves, and later laterally along a path between the dermatome and epidermis (Erickson et al., 1992; Rickmann et al., 1985; Serbedzija et al., 1990). As there are no apparent morphological barriers separating the rostral and caudal somite halves, inhibitory molecules located in the caudal somite halves are believed to regulate this segmental migration process. Early trunk motor axons also avoid the caudal sclerotome tissue when they project ventrally to the peripheral targets (Rickmann et al., 1985). This suggests that neural crest cells and early motor axons maybe regulated by the same or similar molecules, located either in the caudal somite halves with repulsive activities, or in the rostral somite halves with attractive activities. The dermatome tissue initially avoided by migratory neural crest cells is also inhibitory for early motor axons, suggesting that the inhibitors present in the caudal sclerotome may also be expressed in the dorsal-lateral region of the developing somite.

Peanut agglutinin (PNA)-binding glycoproteins located in the caudal somite halves have been implicated in repulsive guidance of both axons and migrating neural crest cells (Davies et al., 1990; Krull et al., 1995). Protein purification of such PNA-binding glycoproteins from early somites have revealed two active inhibitory components of 48 and 55 Kd (Davies et al., 1990). However, their molecular nature has not been elucidated so far. Other molecularly defined candidates located in the caudal somite halves such as collagen IX and T-cadherin have also been shown to exhibit inhibitory activities in vitro toward crest cell attachment and migration, as well as neurite outgrowth (Fredette et al., 1996; Ring et al., 1996). Additional axon collapsing molecules such as collapsin-1 have been shown to be located in early developing dermatome (Shepherd et al., 1996), consistent with the initial avoidance by crest cells of the lateral migratory pathway.

EphrinB2 is expressed in either a polarized or segmented fashion in a number of neural tissues. For example, it is expressed in the dorsal but not in the ventral half of the neural tube (H. W. and D. J. A., unpublished data). It is restricted to even-numbered hindbrain rhombomeres r2, r4, and r6, but not odd-numbered r3 and r5 (Bergemann et al., 1995). A previous study has reported that ephrinB2 was expressed in the two newly generated somites in the caudal trunk region (Bergemann et al., 1995). However, the authors missed an interesting polarized expression pattern of ephrinB2 in the developing somites. Our results showed that ephrinB2 is restricted to caudal somite halves in mouse and rat embryos (Wang and Anderson, 1997). We also showed that EphrinB1/Lerk2 was transiently expressed in early developing dermamyotome (Wang and Anderson, 1997). The fact that two related ephrin transmembrane ligands were located in two regions avoided by neural crest cells and early outgrowing motor axons suggested ephrin-mediated signaling may participate in the inhibitory regulation of their migratory process.

To confirm the expression pattern of rodent ephrinB2 in chick system, I cloned chick ephrin homologs. Surprisingly, it was the chick ephrinB1 that was restricted to the caudal somite halves, and not chick ephrinB2 (Wang and Anderson, 1997). This alteration of expression pattern suggest that the two functionally equivalent ligands (ephrinB1 and ephrinB2) were used interchangeably during evolution of the two animal species.

We and others have then shown that the transmembrane ephrin ligands and their Eph receptors are involved in the repulsive guidance of trunk neural crest cell migration and motor axon outgrowth in vitro (Krull et al., 1997; Wang and Anderson, 1997). Similar conclusions have been reached on the roles of EphB1 and ephrinB2 in the migration of branchial neural crest cells in vivo (Smith et al., 1997).

C) Blood Vessels in the Circulatory System

The vascular system circulates blood and blood cells in addition to supply oxygen and other nutrients to a growing embryo. The circulatory system is composed of arteries and veins, defined by the direction of blood flow and their physiological differences. The initial formation of endothelial cells and their primary plexi from angioblasts is termed vasculogenesis (Sabin, 1917). The subsequent splitting, sprouting, and formation of new blood vessels from existing ones is termed angiogenesis (Risau, 1997). Neovascularization describes angiogenic events that occur in adults, such as wound healing and tumor vascularization.

Several RTKs and their ligands have been implicated in the vasculogenesis and angiogenesis of the blood vessels. Flk1 receptor tyrosine kinase is one of the earliest markers of hemangioblasts, precursors for both blood cells and angioblasts in the yolk sac (Breier et al., 1995; Dumont et al., 1995; Yamaguchi et al., 1993). Targeted deletion of Flk1 in mice results in defective blood-island formation and vasculogenesis (Fong et al., 1995). Angioblasts are not formed in Flk1 mutants. A Flk1 related receptor, Flt1, has also been shown to play a role in vasculogenesis in the embryo and yolk sac (Shalaby et al., 1995). In contrast to the phenotype of Flk1 mutants, angioblasts were formed in Flt1 mutants that displayed a later blockage in the formation of vascular plexus. VEGF, the endothelial cell growth factor, is a ligand for both Flk1 and Flt1. The colocalized expression patterns of VEGF and its two receptors in early embryonic stages suggest that VEGF is essential for the activation of Flk1 and Flt1 (Breier et al., 1992; Breier et al., 1995). Indeed, VEGF knockout embryos suffered from abnormal blood vessel development, and lethality occurred even in the absence of a single VEGF allele (Carmeliet et al., 1996; Ferrara et al., 1996). Embryos generated by aggregation of ES cells with tetraploid embryos showed

progressive phenotypes depending on whether ES cells are heterozygous or homozygous deficient for VEGF.

A second family of RTKs and ligands involved in vascular development is consisted of receptor Tie1 and Tie2, and a soluble ligand angiopoietin1 (Ang-1) for Tie2. Tie1 and Tie2 are endothelial specific receptors, whereas Ang1 is expressed by peri-endothelial cells (Davis et al., 1996; Maisonpierre et al., 1993; Sato et al., 1993). Tie1 and Tie2 play distinct roles in blood vessel formation. Gene targeting analysis of Tie1 suggested that it was not required for early vasculogenic aspect of the vessel formation. Instead, it was necessary for establishing structural integrity of the endothelial lining of the blood vessels (Sato et al., 1995). Tie1 mutants suffered from late embryonic vessel leakage and subsequent haemorrhage. Analysis of Tie2 deficient embryos showed that it was important in angiogenic aspect of the vessel formation, particularly in remodeling of the primary plexi, and heart vascular trabeculation (Dumont et al., 1994; Sato et al., 1995). Ang1, a recently identified soluble ligand for Tie2, has also been a subject of deletional analysis. The Ang1 mutants displayed later defects in angiogenesis compared with Tie2 mutants. Remodeling of the vessels and formation of tight-junctions between endothelial and pericytes are compromised in the absence of Ang1 (Suri et al., 1996). Together, these recent progress in vascular research has elucidated the roles of several RTKs and their ligands in the blood vessel development.

One aspect of the vascular system that has received little attention is related to the endothelial heterogeneity within the vascular system. Endothelial cells of the three major types of vessels, arteries, veins and lymphatics, share many of the signaling molecules mentioned above. However, the physiological and pathological differences among the mature arteries, veins and lymphatics seem to argue against a complete homogeneity among the different populations of endothelial cells.

The initial formations of the arteries, veins and lymphatics was first described at the beginning of this century (Evans, 1909; Sabin, 1909; Sabin, 1917; Sabin, 1920). Aortas as

the first arteries form bilaterally next to the neural tube. The bifurcated aorta at caudal trunk region fuse in the middle of the trunk before connecting to the heart, which is then connected to anterior carotid arteries projected to the head. At the caudal trunk level, cardinal veins form away from the central axis. Small cardinal veins are initially located above the mesonephoro tubules originated from lateral mesoderm. Bifurcated posterior cardinal veins fuse before they connected to the heart, and the heart is then connected to the anterior cardinal veins projected to the head. Lymphatic vessels appear in later embryonic stages, and mature during neonatal period. They absorb interstitial fluid (lymph) and collect peripheral lymphocytes, and carry them back to the heart and the circulation. Lymphatics are believed to have a venous origin, being derived from vessel sacs and sprouts of the large central veins (Sabin, 1909). Different embryonic locations of the arteries, veins and lymphatics suggest their endothelial contributes are likely differentially specified according to their original local environments. This hypothesis on the origins of different embryonic vessels have not been clearly proposed or tested in the recent research of molecular vascular biology.

Through an unexpected vascular phenotype observed in the ephrinB2 knockout mice, we discovered an interesting expression pattern of ephrinB2 ligand (Wang et al., 1998). Its expression is restricted to arterial endothelial cells, and not venous ones. More interestingly, by examining the expression patterns of several EphB type receptors for ephrinB2, we found that EphB4 receptor was only expressed in venous endothelial cells, and not arterial ones. The complementary expression patterns of ephrinB2 ligand and EphB4 receptor implied an interaction between arterial and venous endothelial cells during vessel formation. The defective angiogenesis of arteries and veins in the ephrinB2 mutants suggested that such interactions between the two types of vessels are essential for the formation of the capillary beds. Our findings on the molecular distinction of arterial and venous endothelial cells have raised a series of interesting questions, and prompted us to design ongoing experiments to provide answers.

Chapter 2

Expression Cloning of Transmembrane Ephrin Ligands

A) Survey of crest expressed receptor tyrosine kinases

To study the roles of receptor tyrosine kinases (RTKs) in the development of neural crest cells, I used a degenerate RT-PCR approach to survey existing and discover novel RTKs expressed in the neural crest cells. Previous studies have indicated that bFGFR, ErbB2 and ErbB3 receptors transmit growth and glia-differentiation signals to neural crest stem cells (Bannerman and Pleasure, 1993; Kalcheim and Neufeld, 1990; Murphy et al., 1994; Shah et al., 1994). By identifying novel or previously less-characterized RTKs expressed in neural crest cells, we may gain additional insights into their developmental potentials. Furthermore, orphan RTKs can be used as bait for cloning novel protein ligands through biochemical purification or expression library screens.

For my RT-PCR experiments, I designed multiple degenerate primers. The amino acid sequences for the primers were based on the most conserved motifs of intracellular kinase domains of the RTK-superfamily.

For the 5' region, I made only one primer covering a motif highly conserved in all RTK subfamilies.

RTK5' H R D L A A/T R

For the 3' region, multiple primers were designed based on motifs conserved in any given RTK subfamilies, but slightly different between them. This way, the combination of

the 5' primer and a given 3' primer would preferentially amplify members of a given RTK subfamily.

RTK3'-1 K W L A L E

preferred subfamily members: tif/sky/brt/arl/ufo (GAS6 as ligand), tyro3

RTK3'-2 KW M/I A L/I E

preferred subfamily members: sea/ron/met, EGFR, neu, ret,

RTK3'-3 K W M A P E

preferred subfamily members: FLK1, FLT1, FLT4, PDGFR, FGFR, KIT, CSFR

RTK3'-4 R W T A P E

NOTE: R= "GCI"

preferred subfamily members: EPH Eck, Sek, Myk1, Nuk, Elk, ...

RTK3'-5 R W T A/S P E

NOTE: R=" AG A/G"

preferred subfamily members: MEK, HEK

RTK3'-6 R W M P/A P E

preferred subfamily members: TRK, ROL1, ROL2, IRR

RTK3'-7 R W T A/S W E

preferred subfamily members: NEP/PTK3/DDR, TYRO10, IGF1R

RTK3'-8 R W T A I E

preferred subfamily members: TIE1, TIE2/TEK

Degenerate PCR was performed on cDNA reversed transcribed from mRNA of primary neural crest cells isolated from 1 to 2 day cultured explants. Annealing temperature was varied between 40 to 44^{0}C. PCR products of 175 to 180 base pairs were purified and cloned. Sequence analysis of the PCR products amplified from different sets of primers revealed 11 members of different RTK subfamilies. Several RTKs previously implicated in the crest development were found, such as bFGFR, ErbB2 and ErbB3.

Several receptors that were less characterized at the time were also found. One was Nep, an RTK expressed in the neuroepithelia and early dorsal root ganglia (Zerlin et al., 1993). Nep and tyro10 were two related orphan RTKs identified during 1993 to 1994. They were distinguished by a structural domain in their extracellular portions homologous to discoidin 1 protein of the slime mold Dictyostelium discoideum (Poole et al., 1981). This discoidin 1 domains were also found in other vertebrate proteins such as coagulation factors V and VIII, and a neural recognition molecule in Xenopus call A5 (Eaton et al., 1987; Jenny et al., 1987; Takagi et al., 1987). Nep and tyro10 are now renamed as DDR1 and DDR2, respectively. I went on to produce soluble Nep extracellular domain as a fusion protein to human IgG-Fc. In addition, I performed decoration studies with Nep-Fc fusion proteins. The details are presented in Appendix I.

Another RTK found in my survey was Nuk/EphB2. Nuk/EphB2 was then a recently discovered RTK of the Eph subfamily (Henkemeyer et al., 1994). Nuk was expressed in hindbrain rhombomeres, early motor axons and migratory neural crest cells. The functions of Nuk in the peripheral nervous system were not studied, nor have its ligand been identified. The extracellular domain of Nuk contained one Ig-like domain and two

fibronectin III repeats (Henkemeyer et al., 1994). Such features suggested that Nuk could potentially interact with novel types of extracellular protein ligands.

Various studies at the time indicated that activation of Eph family RTKs did not lead to cell proliferation in vitro and in vivo, unlike that observed for many other types of RTKs (Lhotak and Pawson, 1993; Pandey et al., 1995). This suggested that Eph family receptors would probably regulate other aspects of cell behavior, such as differentiation, survival or migration. In mid-1994, researchers from Amgen purified a soluble ligand for an Eph family member – Eck/EphA2 (Bartley et al., 1994). It was B61, a known GPI-anchored membrane molecule (Holzman et al., 1990). B61 exists in both membrane and soluble forms. The two forms may activate Eck receptor with different affinities. We were excited by this finding, mainly because we thought a similar membrane anchored ligand could exist for Nuk/EphB2 receptor. A ligand for Nuk receptor would provide insight into the development of neural crest cells, especially considering that Eph family receptor activation would not lead to a conventional proliferative response.

B) Expression cloning of ligands for Nuk/EphB2 receptor

The technique for cloning such molecule would be expression cloning. Expression cloning of a membrane ligand utilizes the soluble extracellular domain (ECD) of a receptor as an affinity probe. Usually, the receptor ECD is fused to a protein tag, such as IgG-Fc or alkaline phosphotase. The fusion protein is then used like an antibody to decorate freshly isolated or transfected cells. Several approaches of mammalian expression cloning are illustrated in Figure 1. An entire plasmid expression library constructed from appropriate cell lines or tissue source can be used to transfect mammalian cells such as COS or 293 cells. Transfected cells will be screened with receptor-tag fusion proteins, and positive cells can be harvested and plasmids recovered for further screening. Alternatively, the entire library can be divided into 50 to 100 pools. Individual pools of plasmids can be transfected

and screened. Positive pools will be subdivided and rescreened until a single positive plasmid is isolated.

To construct a soluble affinity probe, I took Nuk extracellular domain and fused it in frame to human IgG1 Fc. The joint between the two domains was the hinge region of the IgG Fc, which contained two cysteins responsible for protein dimerization. The fusion molecule was cloned into a mammalian expression vector pCEP4 (Invitrogen). Human kidney 293 cells were used for transfection and harvest of conditioned media. Western blot analysis of the conditioned media with anti-Fc antibodies revealed that the fusion proteins were dimers under non-reducing condition (Figure 4). The conditioned media were typically stored at 4^0C for several weeks for cell and section staining. Alternatively, Nuk-Fc fusion proteins were purified through protein-A columns (Pierce), aliquoted, and stored at -80^0C.

Since Nuk is expressed at high levels in the developing neural tube and placenta, we reasoned that its membrane anchored ligand(s) would be co-expressed in those tissues. To construct expression library from these tissues, I isolated mouse neural tubes and placenta from E12 to E14 stage embryos. RNA was extracted with oligo-dT cellulose (Fastrack Kit, Invitrogen). First and second strand cDNA synthesis, adapter ligation, size selection, and plasmid library construction in pCDNA3 (Invitrogen) were then performed with reagents from Gibco-BRL.

An efficient plasmid library construction strategy was utilized by using a pair of inverted non-palindromic BstX1 sites in pCDNA3 vector (Invitrogen). The principle resembles the PCR TA-cloning technique. The linearized vectors and linker-ligated cDNA inserts could only ligate with each other, with minimal self-ligation, thus increasing the cloning efficiency. To apply this technique to other larger plasmids was difficult, since most of them did not contain a pair of inverted BstX1 sites, nor can they accommodate one (most of larger plasmids or phagemids have internal BstX1 sites). I searched for other non-palindromic restriction enzymes and found an 8-base pair recognition and 3 base pair stuffer site by SfiI. Most of the larger plasmids do not have internal SfiI sites. I was able to

construct an inverted pair of non-palindromic SfiI sites into some of them. Notably, I made a size selected plasmid cDNA library from a neural crest cell line (Monc1) into a yeast two-hybrid vector called pACTII.

I have successfully used the placenta library to screen for Nuk ligand-encoding cDNAs. The initially ligated placenta plasmid library was electroporated into bacteria to generate pools of 1000 plasmids. Plasmid minipreps were made from 100 such pools. Individual pools of plasmids were calcium-phosphate transfected into human kidney 293 cells which, after 2 days of transfection, were stained with Nuk-Fc containing conditioned media. HRP-conjugated secondary antibodies against human IgG-Fc were used to detect the positive 293 cells. Single positive cells were identified in several pools (Figure 2). Those positive pools of plasmids were transformed into bacteria and subdivided into smaller pools of, for example, 50 plasmids. Through a series of subdivisions and transfections, I have cloned out several plasmids encoding two independent genes of Nuk ligands.

Sequence analysis revealed that one molecule was Lerk2/ephrinB1, a transmembrane ligand for Elk receptor, that had just been published (Davis et al., 1994). The other gene encoded a novel ligand with high homology to Lerk2/ephrinB1. This second ligand was later published under the name Htk-Ligand, now called EphrinB2, by researchers at Genentech in May 1995. Although not published, my results detailed here on the cloning, sequence analysis and affinity assays were independent studies.

Sequence alignments revealed homologous domains between ephrinB1 and ephrinB2 (Figure 3). The signal peptide sequences are underlined for both ligands. The ephrinB2 signal peptide contains six charged residues (4 Rs, 1 K and 1 D). Subsequent production of soluble ephrinB2 extracellular domain was difficult. The secretion of ephrinB2-Fc fusion proteins by 293 cells in conditioned media was much less than that of ephrinB1-Fc. The production of ephrinB2 extracellular domain in the baculovirus system was also very poor. To overcome this problem and make a larger amount of soluble ephrinB2 in the baculovirus-insect cell system, I replaced ephrinB2's signal peptide with

that of acidic glycoprotein gp67 of baculovirus. gp67 is the most abundant envelope surface glycoprotein of AcNPV baculovirus. The gp67 signal peptide greatly increased the secretion and production of soluble ephrinB2 in conditioned media, resulting in concentration of more than 10μg/ml.

Boxed in the figure 3 are four cysteins conserved in most ephrin ligands. Near the underlined transmembrane domains are the variable sequences unique for ephrinB1 and ephrinB2. Intracellularly, the two ligands share highly conserved sequences near c-terminal (highlighted in pink color). Unlike those GPI anchored ephrin ligands (ephrinA type), ephrinB1 and ephrinB2 are capable of signaling through their non-catalytic intracellular domains (Bruckner et al., 1997; Holland et al., 1996). Six tyrosine residues (highlighted in yellow color) near the c-terminals of ephrinB1 and ephrinB2, were shown to be phosphorylated during receptor-triggered ligand activation.

To extend our studies of ephrinB1 and ephrinB2 in the chick system, I designed degenerate primers based on the conserved motifs around cysteins and intracellular domain. The 5' primer was based on a.a. sequence "FTIKFQE," and the 3' primer, "NIYYKV-stop." Day 3 chick embryos were used as the cDNA source, and PCR products were cloned and sequenced. Two different gene fragments were identified as chick homologs of mouse ephrinB1 and ephrinB2, based on sequence relationships. A cross table of identities between mouse and rat ephrins was published in a Neuron paper (See Chapter 3).

Scatchard analysis was used to determine the binding affinity and dissociation constant (Kd) between Nuk/EphB2 receptor and its ligand ephrinB2. Full length ephrinB2 cDNA was transfected into 293 cells in 48 well culture plates. Soluble Nuk-Fc was added for binding at various concentrations, and then detected by I^{125} labeled secondary antibodies (Figure 4). Half maximal binding of cell-bound ephrinB2 was achieved at0.5 nM Nuk-Fc. Thus, the Kd for dissociation of Nuk/EphB2 from ephrinB2 is around 0.5 nM, indicating a relatively high affinity. The dissociation constant between Nuk/EphB2 and ephrinB1 was similarly around 1nM based on published data (Beckmann et al., 1994).

To produce soluble ligand proteins, I fused the extracellular domains of ephrinB1 and ephrinB2 to human IgG Fc. Transient expression of ephrinB1-Fc fusion construct resulted in a high level of secretion by 293 cells. Figure 5 shows a non-reducing western blot of the conditioned media containing varies Fc-fusion proteins, Myk1/EphB4-Fc (lane 4), Nuk/EphB2-Fc (lane 5), Lerk2/ephrinB1-Fc (lane 6), and control Fc (lane 7), compared with a series of defined amounts of human IgG1 Fc (lane 1-3).

Under non-reducing condition, Myk1/EphB4-Fc and Nuk/EphB2-Fc were dimers of around 200 Kd (land 5), Lerk2-Fc/ephrinB1 a dimer around 120 Kd (lane 6), and control Fc a dimer around 50 Kd (land 7). The concentrations of these soluble proteins in the conditioned media from transient transfections were around 0.2 μg/ml for Myk1/EphB4-Fc, 1 μg/ml for Nuk/EphB2-Fc, 4 μg/ml for Lerk2/ephrinB1-Fc, and 15 μg/ml for control-Fc. This result suggested that secretion was decreased with increasing sizes of the fusion proteins. Myk1/EphB4-Fc and HtkL/ephrinB2-Fc (not shown) have very small amounts of secretion by 293 cells, around 0.2-0.3 μg/ml, probably due to their non-optimal signal sequence peptides (discussed above). To produce larger amount of Myk1/EphB4-Fc and HtkL/ephrinB2-Fc, I have switched to the baculovirus insect cell system, with good success.

Figure 1. Model diagram of mammalian expression cloning.

Several common approaches in mammalian expression cloning are illustrated here and tested by me. The first and original approach is using monoclonal antibody to screen surface antigens expressed by transfected cells. I have used mAb-192 to detect p75 low affinity NGF receptor (See Appendix 2). The second way is to used receptor-Fc fusion proteins to detect surface antigen. EphrinB2 transmembrane ligand was cloned using EphB2-Fc receptor fusion proteins (See this chapter). The third way is to used Fc fusion proteins to detect secreted molecules deposited in extracellular matrix or trapped in intracellular compartments such as ER or golgi. I have used Nep-Fc fusion proteins to decorate tissue sections and reveal its collagen ligands in connective and cartilage tissues (See Appendix I).

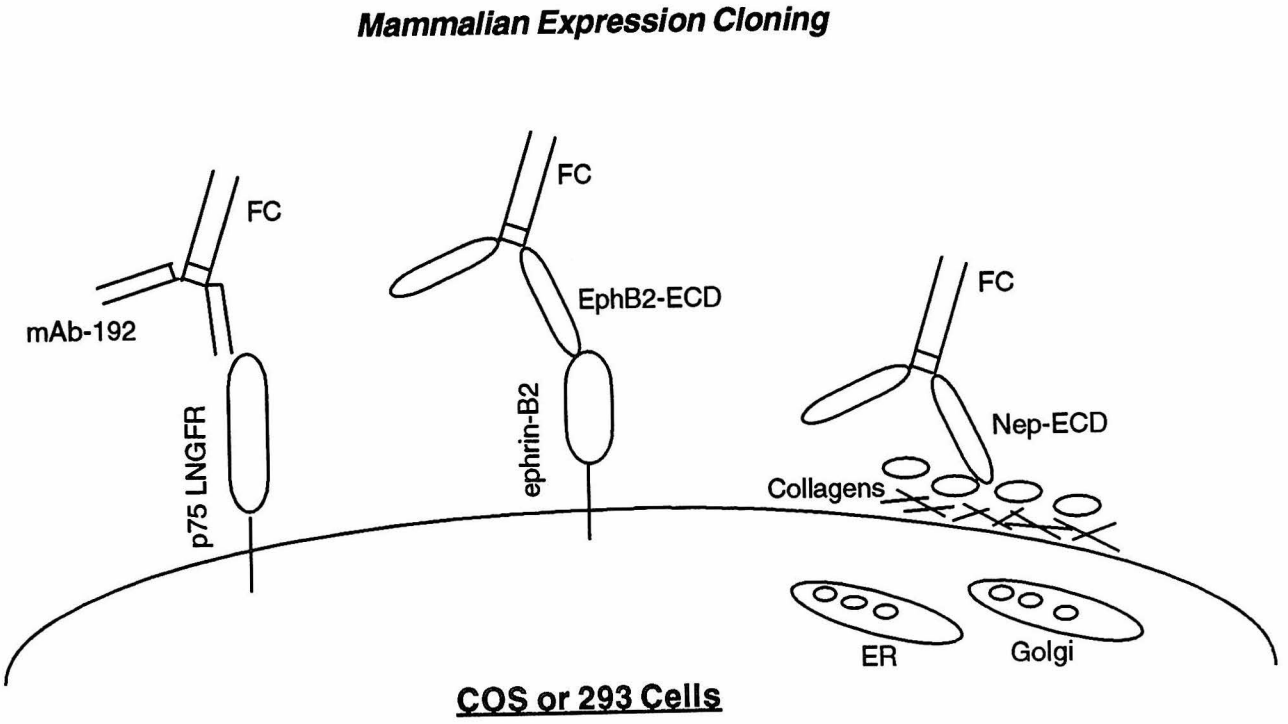

Figure 2. Expression cloning of membrane ligands for Nuk/EphB2 receptor. Monolayers of 293 cells were transfected with placenta expression library constructed in pCDNA3 (Invitrogen). Two days post transfection, cells were stained with 1μg/ml Nuk-Fc fusion protein containing conditioned medium. Bound Nuk-Fc proteins were detected with HRP conjugated secondaries against IgG1 Fc (Jackson). **A** and **B**, single positive cells identified in the independent primary pools (1000 plasmids/pool). **C**, confirmation of Nuk-Fc staining in the secondary pools (50 plasmids/pool). **D**, enrichment of positive cells transfected with tertiary pools (5 plasmids/pool).

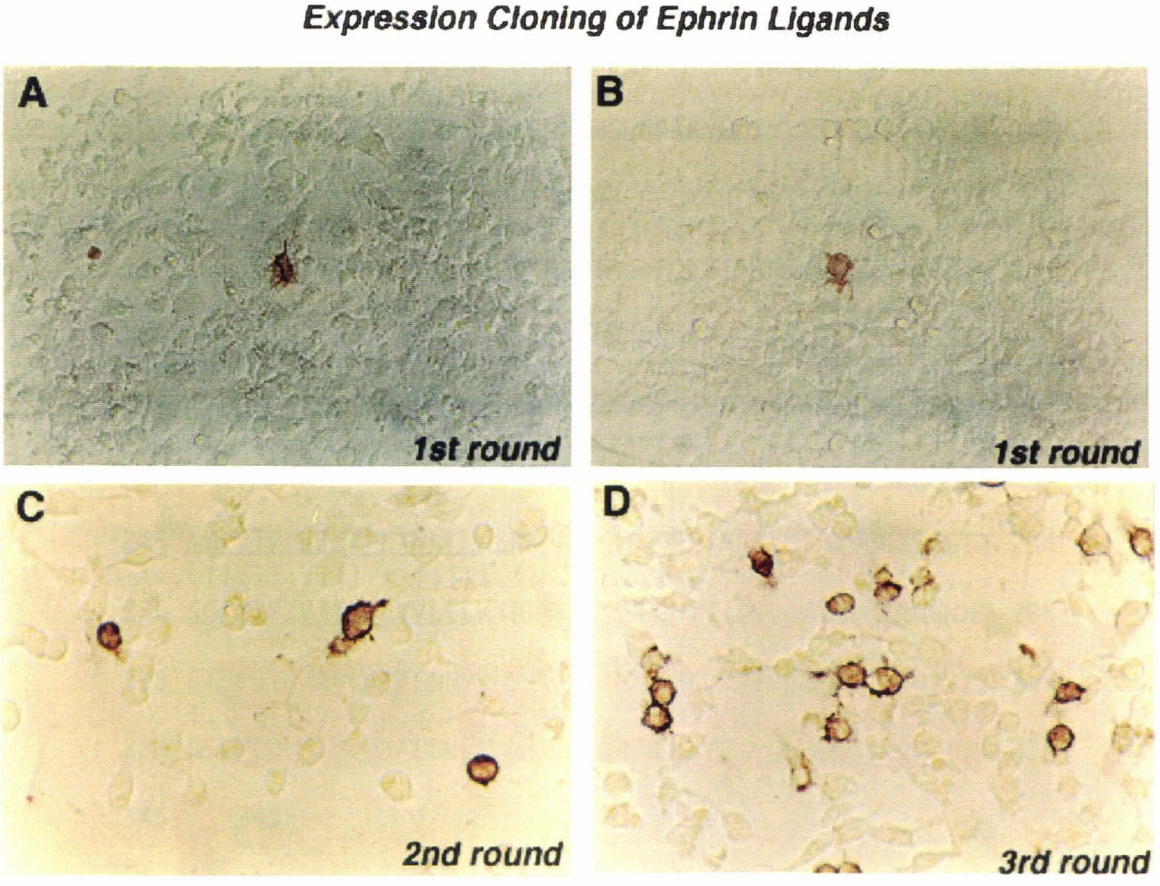

Figure 3. Sequence alignment of transmembrane ephrinB1 and ephrinB2. Peptide sequences of the two mouse ligands are aligned with GCG - GAP program. Signal peptides and transmembrane domains are underlined. Conserved cysteins are boxed. High homology regions of the intracellular domains are highlighted with pink color. Six conserved tyrosine residues are highlighted with yellow color.

Figure 4. Binding of Nuk-Fc to ephrinB2. Monolayers of 293 cells in 48 wells were transfected with full length ephrinB2 expression vector, and stained with defined amount of Nuk-Fc. I^{125} conjugated secondaries against Fc were used to measure bound cpm. Half maximal binding was achieved at around 0.5 nM, suggesting a high affinity with Kd of 0.5 nM.

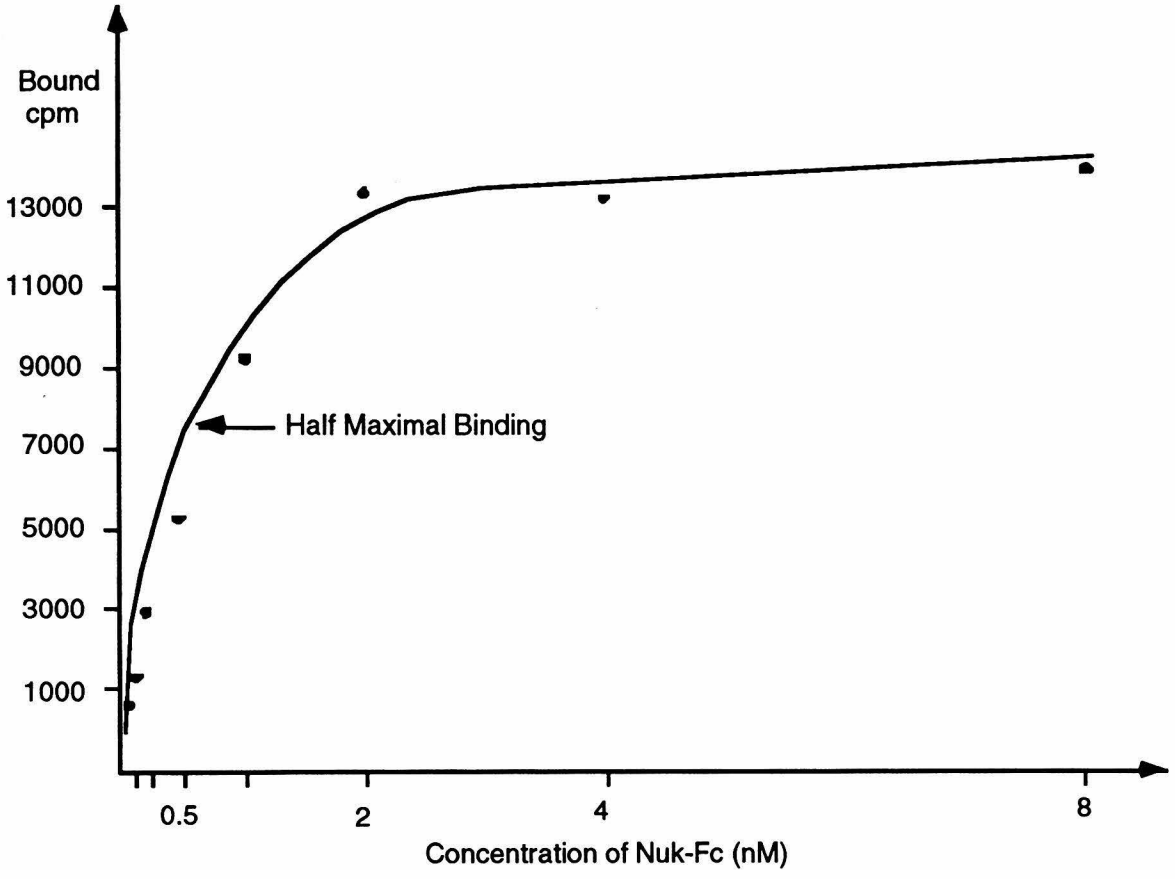

Figure 5. Western blot analysis of Myk1/EphB4-Fc, Nuk/EphB2-Fc, Lerk2/ephrinB1-Fc, and Fc proteins. 5-day conditioned Media from 293 cells transfected with varies expression vectors were subjected to blotting, under non-reducing condition, with HRP-conjugated polyclonal antibodies against human IgG1 Fc. Lane 1-3 were varying amounts of control human IgG1 (containing Fc domains) dimeric proteins, with MW of 185 Kd. Lane 1, 100ng. Lane 2, 50ng. Lane 3, 20ng. Myk1/EphB4-Fc and Nuk/EphB2-Fc (lane 4 and 5, respectively) were dimers around 200 Kd. Lerk2/ephrinB1-Fc (lane 6) was a dimer around 120 Kd. Control Fc (lane 7) was a dimer around 50 Kd. The amount of conditioned media loaded for each fusion protein was, 100 µl for Myk1/EphB4-Fc and Nuk/EphB2-Fc, 600 µl for Lerk2/ephrinB1-Fc, and 20 µl for control Fc. The estimated concentration of each fusion protein in the conditioned media was, around 0.2 µg/ml for Myk1/EphB4-Fc, 1 µg/ml for Nuk/EphB2-Fc, 4 µg/ml for Lerk2/ephrinB1-Fc, and 15 µg/ml for control-Fc.

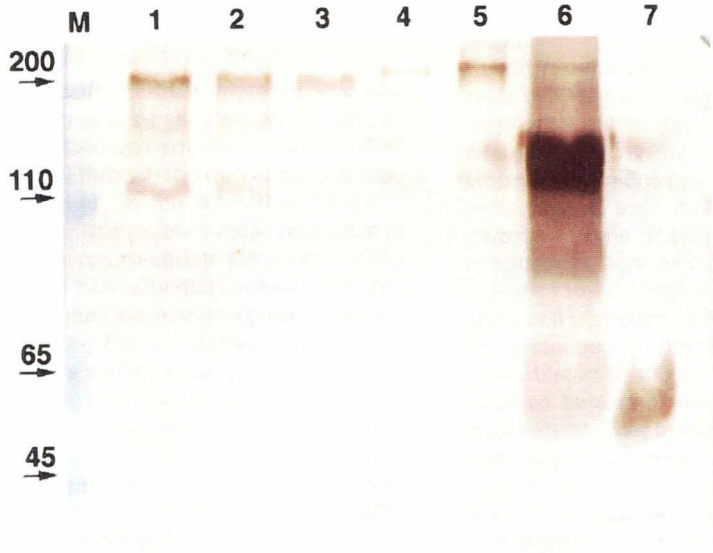

Neuron, Vol. 18, 383–396, March, 1997, Copyright ©1997 by Cell Press

Eph Family Transmembrane Ligands Can Mediate Repulsive Guidance of Trunk Neural Crest Migration and Motor Axon Outgrowth

Hai U. Wang and David J. Anderson*
Division of Biology 216–76
*Howard Hughes Medical Institute
California Institute of Technology
Pasadena, California 91125

Summary

In vertebrate embryos, neural crest cell migration and motor axon outgrowth are restricted to rostral somite halves by repulsive factors located in the caudal somite compartment. We show that two Eph family transmembrane ligands, Lerk2 and HtkL, are expressed in caudal somite halves, and that crest cells and motor axons express receptors for these ligands. In several independent in vitro assays, preclustered ligand-Fc fusion proteins can repulsively guide both crest migration and motor axon outgrowth. These repulsive activities depend on a graded or discontinuous presentation of the ligands when tested in the context of permissive substrates, such as laminin or fibronectin. These results identify Lerk2 and HtkL as potential determinants of segmental pattern in the peripheral nervous system.

Introduction

The neural crest provides a model system for studying cell migration in vertebrates. At early stages of peripheral nervous system development, trunk neural crest cells selectively migrate through the rostral but not caudal halves of the somites, in the sclerotomal portion (Rickmann et al., 1985). This patterned cell migration is in turn determined by a rostro-caudal patterning of the somites: caudal somite halves contain substances that inhibit crest cell migration (Stern and Keynes, 1987; reviewed by Tosney, 1991; Bronner-Fraser, 1992). Early trunk motor axons also avoid growing through caudal somite halves, indicating that somite patterning controls both crest cell migration and motor axon outgrowth (Keynes and Stern, 1984).

As there are no apparent morphological barriers separating the rostral and caudal somite halves, molecules differentially expressed between these halves have been suggested to control this segmental patterning process (Davies et al., 1990; Oakley and Tosney, 1991; Ranscht and Bronner-Fraser, 1991). Two such molecules, collagen IX and T-cadherin, recently have been shown to inhibit neural crest migration and/or neurite outgrowth in vitro (Fredette et al., 1996; Ring et al., 1996). Peanut agglutinin (PNA)–binding glycoproteins have also been implicated in repulsive guidance of both axons (Davies et al., 1990) and neural crest migration (Krull et al., 1995), but the active species have not so far been identified. Other molecules, such as fibronectin, have been shown to promote neural crest cell migration, but these are not differentially expressed in the rostral or caudal somite halves and thus appear to function in a primarily permissive manner (Tucker et al., 1988).

Eph family ligands and their receptors recently have been implicated in the control of axon guidance, particularly in the central nervous system (reviewed by Tessier-Lavigne, 1995; Brambilla and Klein, 1995; Friedman and O'Leary, 1996; Orike and Pini, 1996). These ligands can be divided into two binding specificity subgroups, correlating with the mode of membrane attachment (GPI-linked or transmembrane). Within each subgroup, all ligands can bind and activate all receptors of the same subgroup (Brambilla et al., 1995; Gale et al., 1996a). RAGS and ELF-1, two GPI-linked ligands expressed in developing tectum, can function as repulsive guidance molecules for retinal axons both in vitro (Cheng et al., 1995; Drescher et al., 1995) and in vivo (Nakamoto, et al., 1996), and a human homolog of RAGS (AL-1) modulates axon bundling in vitro (Winslow et al., 1995). The role of the three transmembrane ligands (Gale et al., 1996b) in the development of the nervous system has not yet directly been addressed. Knockouts of Nuk, a receptor for these ligands (Brambilla et al., 1995; Gale et al., 1996a), produce commissural axon pathfinding defects (Henkemeyer et al., 1996). However, it is not yet clear whether this reflects a function for this molecule as a receptor for Eph ligands, or in some other capacity (e.g., cell adhesion).

Here, we identify functional roles for two such transmembrane ligands, HtkL (Elf-2/Lerk5) and Lerk2 (Elk-L/Cek5-L) (reviewed in Pandey et al., 1995a), in restricting both cell migration and axon outgrowth during early segmental patterning of the PNS. HtkL and Lerk2 are expressed in developing somites of both rat and chick embryos in regions avoided by migratory crest cells and motor axons, such as the caudal half sclerotome and dermomyotome. In several independent in vitro assays, preclustered ligand-Fc fusion proteins exhibit repulsive activities toward both motor axon outgrowth and neural crest cell migration. Such repulsive activities require a discontinuous or graded presentation of the ligands when tested in the context of permissive substrates, such as laminin or fibronectin. Taken together, these data indicate that transmembrane as well as GPI-linked Eph ligands can regulate axon guidance, and, further, that transmembrane ligands also can guide cell migration. The results of in vivo perturbations, performed in independent studies, are consistent with this conclusion (Krull et al., unpublished data; Smith et al., unpublished data). Eph-related receptor–ligand signaling systems are thus likely to be key components in the segmental patterning of the PNS.

Results

Detection of Eph-Related Receptors for the Ligands Lerk2 and HtkL in Explanted Trunk Neural Crest Cells and Motor Axons

We initially performed a survey of receptor tyrosine kinases expressed in rat trunk neural crest cells via RT-

PCR. Using degenerate primers against conserved kinase domains, and cDNA from one-day primary neural crest explants, we detected expression of multiple distinct receptors such as bFGFR, erbB2, and erbB3 (data not shown). Included in this group was Nuk, an Eph-related receptor previously shown to be expressed by outgrowing neural tube–derived axons (Henkemeyer et al., 1994). Using an expression cloning approach, we identified two Eph family ligand molecules for the Nuk receptor (H. W. and D. J. A., unpublished data). During the course of these studies, the cloning of these two ligands, referred to as Lerk2 (Elk-L/Cek5-L) and HtkL (ELF-2/LERK5), was reported elsewhere (for review, see Pandey et al., 1995a). Lerk2 and HtkL are homologous transmembrane molecules that bind to Nuk with a Kd of approximately 1 nM, as determined using soluble ligand-Fc fusion proteins (Brambilla et al., 1995; Gale et al., 1996a; H. W. and D. J. A., unpublished data).

To confirm the presence of receptor proteins for Lerk2 and HtkL on trunk neural crest cells, we stained one-day cultured rat crest explants with soluble ligand-Fc fusion proteins. Specific surface labeling of neural crest cells by ligand-Fc but not control Fc proteins was detected (Figures 1A and 1B). A similar receptor decoration experiment was also performed on axons growing from E10.5 trunk neural tube explants cultured on a laminin substrate. Such axons could also be decorated by either Lerk2 or HtkL ligand-Fc fusion proteins (Figure 1E and data not shown), whereas no labeling was detected with control Fc protein (Figure 1F). That many of these axons derive from motor neurons was demonstrated by labeling with antibodies to c-ret, a receptor tyrosine kinase exclusively expressed by motor neurons in the neural tube (Figure 1G) (Lo and Anderson, 1995).

Our in vitro cell surface–labeling results could reflect the expression of multiple Eph-related receptors in explanted neural crest cells and motor axons, since transmembrane ligands Lerk2 and HtkL bind to four receptors in one subgroup: Nuk, Myk-1/Htk, Sek-4, and Elk (Brambilla et al., 1995; Gale et al., 1996a). In addition, Lerk2 and HtkL crossreact to Sek-1 within the other receptor subgroup (which binds the GPI-linked ligands [Gale et al., 1996a]). We therefore used semiquantitative, gene-specific RT-PCR to determine which Eph-related receptors within the Nuk subgroup are expressed in rat neural crest cells. The results indicated that in 24 hr neural crest explants Nuk mRNA is expressed at a higher level than Sek-4, Sek-1, and Myk-1 mRNAs, while the Elk receptor was not detected (Figure 1C, lanes 1–5). These results suggest that Nuk is the predominant receptor for transmembrane Eph family ligands expressed in rat neural crest cells under these culture conditions. This conclusion is in agreement with other data showing that Sek-4, Sek-1, and Myk-1 are mainly expressed outside the nervous system in the trunk region at this stage (Becker et al., 1994; Irving et al., 1996; H. W. and D. J. A., unpublished data). Since the cell population in our neural tube explants is heterogeneous, we were unable to characterize the expression of specific receptors in motor axons by RT-PCR. However, as mentioned above, Henkemeyer et al. (1994) demonstrated by immunocytochemistry that these axons express at least Nuk protein.

Lerk2 and/or HtkL Are Expressed in Somite Regions Avoided by Trunk Neural Crest Cells and Motor Axons in Rat and Chick Embryos

We next examined the expression patterns of Lerk2 and HtkL in E10–E11 rat embryos, a stage when neural crest cells are migrating. In the developing somites, Lerk2 is localized in the dermomyotome, beginning with the most posterior (i.e., most newly formed) somite (Figures 2A, 2F (arrow), and 2M). Such newly formed somites also express HtkL at high levels (Figure 2B, asterisks), as previously reported (Bergemann et al., 1995). However, detectable signals are also observed at this stage in more anterior somites, albeit at lower levels (Figure 2B). Within each somite, moreover, HtkL is preferentially concentrated in the caudal half sclerotomes (Figure 2B; cf. [G] versus [H], asterisks; [L]); by contrast, Lerk2 is not expressed in caudal half sclerotome. Expression of HtkL occurs throughout axial levels where migrating neural crest cells are located, as detected by expression of erbB3 mRNA (Meyer and Birchmeier, 1995) (cf. Figure 2B versus Figure 2D). Moreover, the onset of HtkL expression (Figure 2B, asterisks) occurs just prior to neural crest cell emigration into immediately anterior somites (Figure 2D, asterisks). Similarly, HtkL (as well as Lerk2) expression in this posterior region of the embryo precedes motor neuron differentiation, as detected by expression of SCG10 mRNA (Figure 2E, arrow). Additional HtkL expression is observed in the dermomyotome of both caudal and rostral somite halves (Figures 2G and 2H, arrows), another region avoided by migrating neural crest cells, and in early limb bud (Figure 2B). Expression of both Lerk2 and HtkL in dermatome has disappeared by E12.5, but Lerk2 expression persists in the myotome (not shown).

To determine whether the restricted somitic expression patterns of HtkL and Lerk2 have been evolutionarily conserved, we cloned large portions of their chick homologs. Chick Lerk-2 and rat Lerk-2 were more homologous to one another (77% amino acid identity) than to either chick or mouse HtkL, and vice versa (Figure 3A). One of these chick transmembrane Eph ligands is indeed expressed in caudal somite halves (Figures 3C and 3E; see also Krull et al., 1997); however, it is c-Lerk2, rather than HtkL, as is the case in rat. As in rat, the metameric pattern of c-Lerk2 expression is complementary to that of both neural crest migration (Figure 3D) and motor axon extension (Figure 3F). c-Lerk2 is also expressed in the dermatome of both somite halves (Figures 3B and 3C, arrows), another region expressing HtkL in rat (cf. Figure 2H, arrow). In contrast, expression of c-HtkL is detected in endothelial cells of the aorta and in between the somites (data not shown and Krull et al., 1997).

To confirm that Nuk is expressed in vivo by migrating neural crest cells at the same time that its ligands are expressed in the somites, we performed whole-mount in situ hybridization for Nuk mRNA in rat embryos. Neural crest cells start to enter the somites in the caudal trunk at the 5–6 somite level, and a metameric pattern of migrating cells extends anteriorly (Figure 2D). A similar metameric pattern of Nuk mRNA was also detected throughout the rostro-caudal axis by whole-mount in

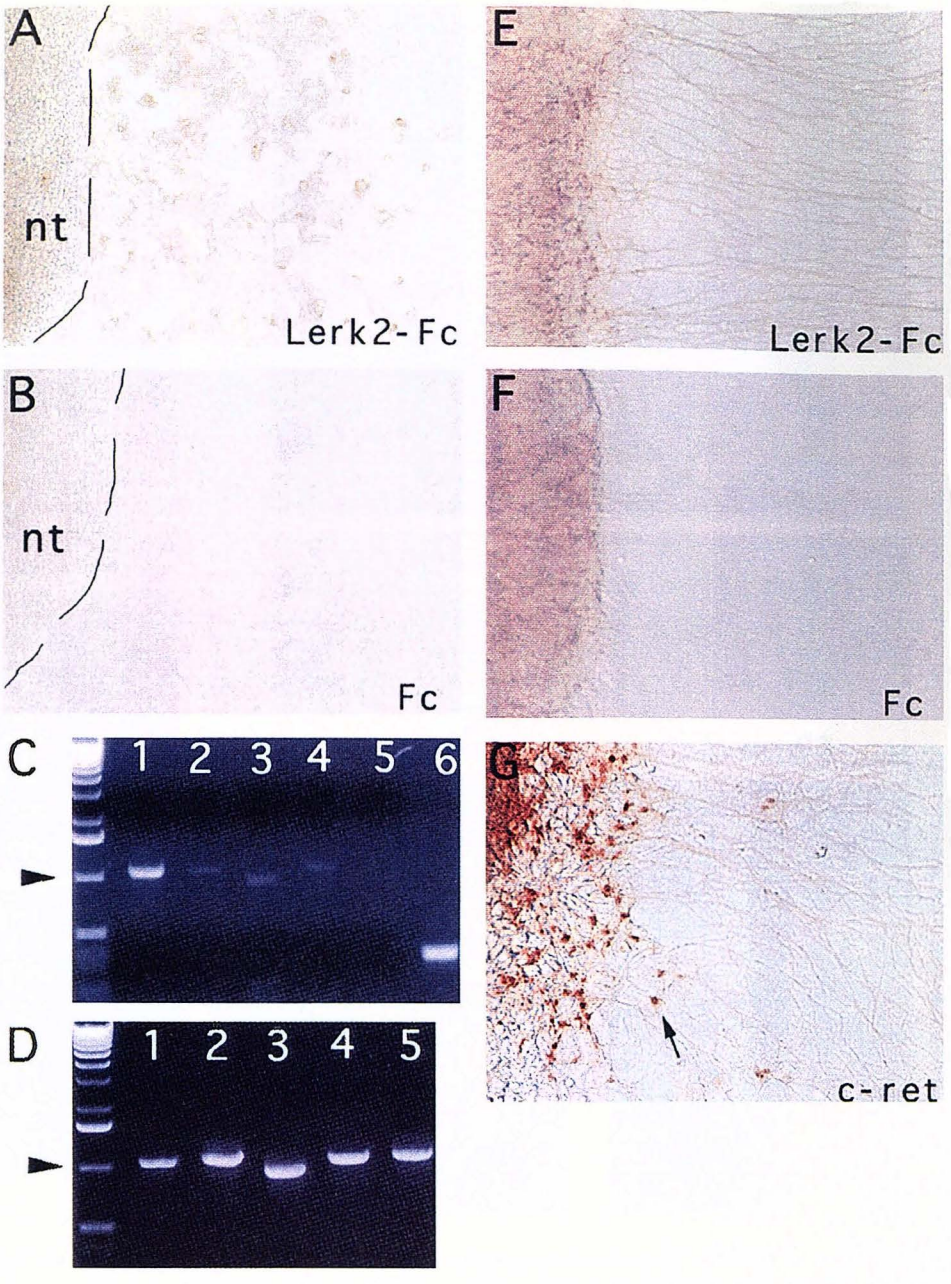

Figure 1. Detection of Eph-Related Receptors for Lerk2 and HtkL in Explanted Rat Neural Crest and Neural Tube Axons

One-day neural crest (A and B) or neural tube (E and F) explants from E10.5 rat embryos were stained with Lerk2-Fc (A and E) or Fc (B and F) proteins. Neural crest cells were labeled by Lerk2-Fc (A), but not by control Fc (B). The edges of the neural tube (nt) are outlined in (A) and (B). In a semiquantitative RT-PCR assay (C), cDNA made from one-day neural crest explants was amplified with gene-specific primers for Nuk (lane 1), Sek-4 (lane 2), Myk-1 (lane 3), Sek-1 (lane 4), Elk (lane 5), and β-actin (lane 6). 27 cycles of PCR amplification were used to keep the reaction below saturation. A separate PCR reaction (D) showed equal levels of amplification of 1 ng plasmid DNA containing cDNAs for Nuk (lane 1), Sek-4 (lane 2), Myk-1 (lane 3), Sek-1 (lane 4), and Elk (lane 5), using the same sets of primers used in (C). This control indicates that each primer set amplifies its template with approximately equivalent efficiency under the conditions used. 1 kb DNA markers are indicated by arrowheads. Neural tube explants were cultured on a polylysine/laminin substrate to promote axon outgrowth. Specific axon labeling was observed with Lerk2-Fc (E), but not with Fc (F). Axons and cell bodies (arrow) were identified as motorneurons by labeling with anti- c-ret antibodies (G). HtkL-Fc gave similar results to that of Lerk2-Fc in both crest cell and motor axon staining (not shown).

situ hybridization (Figure 2C). In longitudinal sections, Nuk mRNA was restricted to rostral half somites (Figure 2K, "r") in a pattern reciprocal to that seen for HtkL (Figure 2L, "c"). In transverse sections, clusters of Nuk-expressing cells were detected next to the neural tube (Figure 2I, arrows), in the same regions that contained erbB3-expressing neural crest cells on adjacent sections (Figure 2J, arrows). These data suggest that Nuk

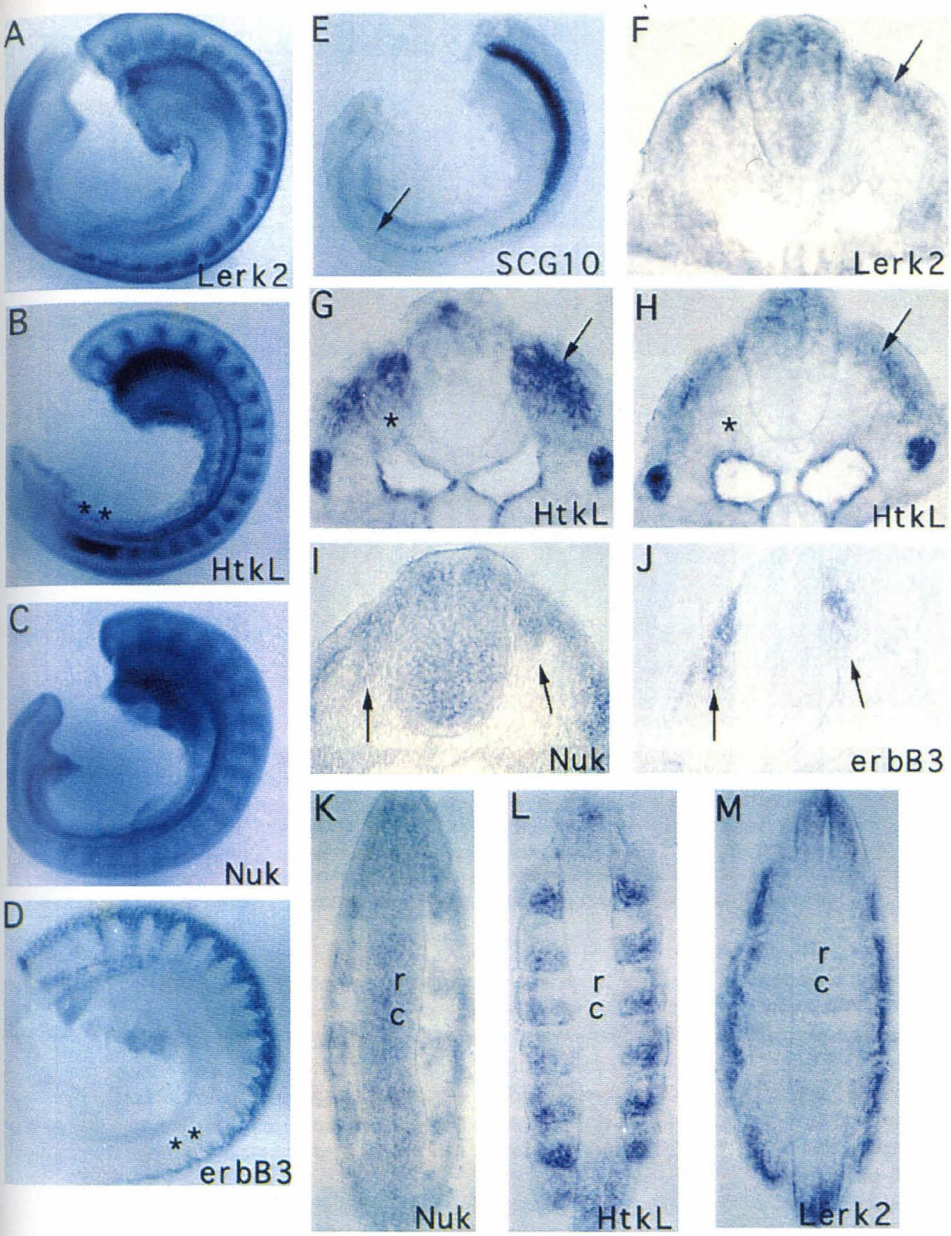

Figure 2. Lerk2 and HtkL Are Expressed in Somite Regions Avoided by Trunk Neural Crest and Motor Axons in Rat Embryos

25-somite stage rat embryo trunks (25) were subjected to whole-mount in situ hybridization using the indicated probes.

(A) Lerk2 labels the dermomyotome and dorsal neural tube.

(B) HtkL is expressed strongly in the early limb bud and in the newly formed somites (asterisks) as well as the more mature (anterior) ones. The HtkL signals are concentrated in the caudal halves of each somite (see also [G] and [L]).

(C) Nuk is expressed in rostral somite halves along the A–P axis. Additional signals are present in the underlying neural tube (see also [I] and [K]).

(D) Neural crest migration, visualized by expression of erbB3 mRNA (Meyer and Birchmeier, 1995), occurs in a similar metameric pattern as Nuk expression (see also [I] and [J]). Neural crest cells start to enter the somites at 5 to 6 somite level (D, asterisks), anterior to the region containing the highest level of HtkL expression (B, asterisks).

(E) SCG10 marks newly formed motor neurons along the ventral neural tube. The earliest born motor neurons are found at the 2- to 3-somite level (arrow), indicating the axon extension into the somites probably occurs in the region just anterior to the highest level of HtkL expression (B, asterisks).

(F–J) Transverse sections from the embryos shown in (A)–(D). (F) Lerk2 is expressed in the dermomyotome and dorsal neural tube. HtkL is expressed in the sclerotome in the caudal somite half (G, asterisk), but not in the rostral half (H, asterisk). Additional HtkL signals are seen in the dermomyotome (arrow in [G] and [H]), aorta, and mesenephoros. ([I] and [J]) Transverse sections through rostral somite halves at the forelimb level. Migrating neural crest cells detected by expression of erbB3 (J, arrows) are located in a region expressing Nuk on an adjacent section (I, arrows). Additional Nuk signals are observed in the ectoderm and throughout the neural tube.

(K–M) Longitudinal sections show the reciprocal patterns of Nuk (K) and HtkL (L) expression in the rostral (r) and caudal (c) somite halves, respectively, and Lerk2 signals (M) in the dermomyotome.

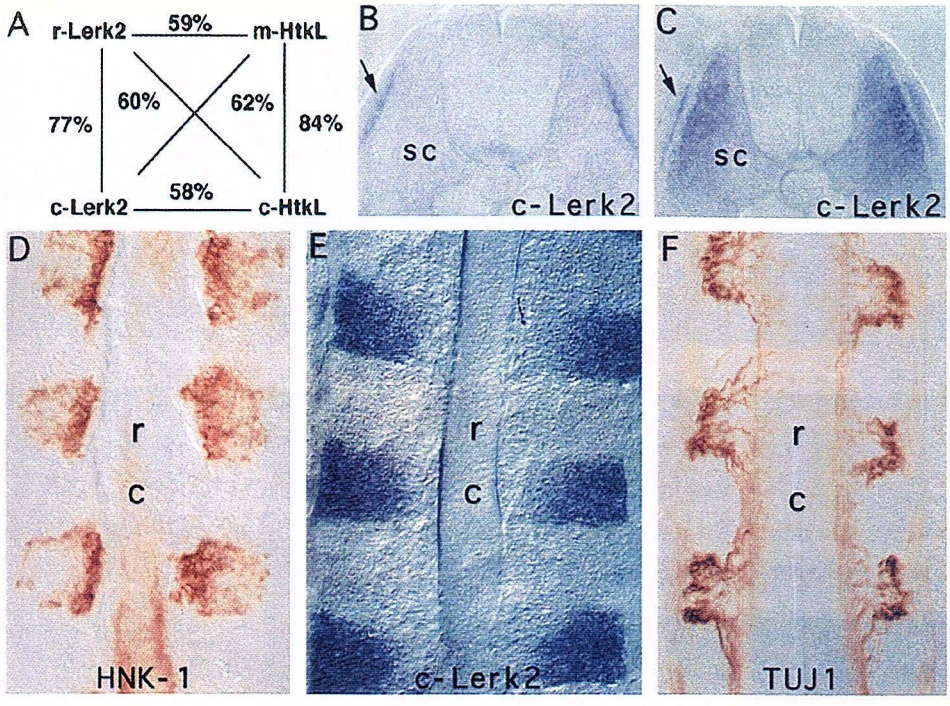

Figure 3. Caudal Half Sclerotome Expression of Chick Lerk2

(A) Percentage of a.a. identities between chick and rat/mouse ligands. Fragments of chick HtkL and Lerk2 used for the alignment, representing 65% to 70% of the full coding sequence, are homologous to a.a. 118–337 of mouse HtkL (Bennett et al., 1995) and a.a. 112–345 of rat Lerk2 (Fletcher et al., 1994) respectively. In stage-16 embryos (25 somite), c-Lerk2 is expressed in dermatome of both rostral and caudal somite halves (B and C, arrow), and in the caudal half sclerotome (C, "sc"). At the same stage, crest cells (D) and motor axons (F) decorated by HNK-1 and TUJ1 antibodies, respectively, are seen in rostral somite halves ("r"), compared with caudal half restricted c-Lerk2 expression (E, "c") in longitudinal sections. For additional data, see Krull et al., unpublished data.

mRNA is expressed by migrating neural crest cells in vivo as well as in vitro (Figure 1C). However, it is likely that Nuk is also expressed by cells of the rostral sclerotome (Figure 2K). This additional somitic expression may account for the slight difference in the pattern of Nuk and erbB3 mRNA expression within rostral half somites seen in whole mounts (cf. Figure 2C versus Figure 2D).

HtkL and Lerk2 Exhibit Repulsive Activities toward Neural Crest Cell Migration in Stripe and Transfilter Chemotaxis Assays

Since Lerk2 and HtkL are expressed in somitic regions known to be inhibitory for neural crest migration, we hypothesized that these ligands might restrict crest cell migration via contact-mediated repulsion. To test this idea, we used stripe assays similar to those developed to study axon guidance (Vielmetter et al., 1990), but coated the substrate with immobilized, purified ligand proteins, rather than cell membrane suspensions. Ligand-Fc fusion proteins were immobilized in alternating narrow stripes on nitrocellulose-coated (Lemmon et al., 1989) plastic cover slips, via binding to anti-Fc antibodies precoated in stripes together with fibronectin, using a special silicone matrix (see Experimental Procedures). The anti-Fc antibodies not only orient the ligand-Fc fusion proteins, but also cluster them, thereby increasing their ability to activate receptors as shown previously using soluble reagents (Davis et al., 1994).

When E10.5 rat neural tubes were plated at a right angle to the stripes, the emigrating neural crest cells encountered delineated boundaries of ligand-Fc or Fc proteins on a fibronectin substrate ("+" lanes in Figures 4A–4C). Cells at the leading edges of the explants (where neural crest cells are most dispersed) tended to avoid ligand-containing stripes (Figures 4A and 4B; Table 1), but not control Fc–containing stripes (Figure 4C). Cells adjacent to the neural tube (bottom of each panel) did not show such restricted migration, perhaps because the high cell density in this region prevents contact between cells and the substrate-immobilized ligand, or because "population pressure" driving expansion of the

Table 1. Percentage of Cells in Stripes Coated with Fc or Ligand-Fc Proteins

	alternating stripes coated		every stripe coated	
	(+)	(−)	(+)	(+)
HtkL-Fc	20.7% ± 1.9	79.3% ± 1.9	51.2% ± 2.5	48.8% ± 2.5
Lerk2-Fc	25.8% ± 1.1	74.2% ± 1.1	49.5% ± 3.5	50.5% ± 3.5
Fc	49.3% ± 2.7	50.7% ± 2.7	49.3% ± 3.4	50.7% ± 3.4

Cells in the distal one-third of each explant that spans 15–20 stripes were counted after DAPI staining. The average number of cells in adjacent stripes is calculated as percentage of the total. The data are averaged from 2 random explants per experiment, and the numbers represent the mean ± SEM from 3 independent experiments. (+) corresponds to stripes coated with Fc or ligand-Fc proteins, and also to lanes illustrated by a "+" in Figure 4. (−) indicates the stripe was coated with fibronectin only.

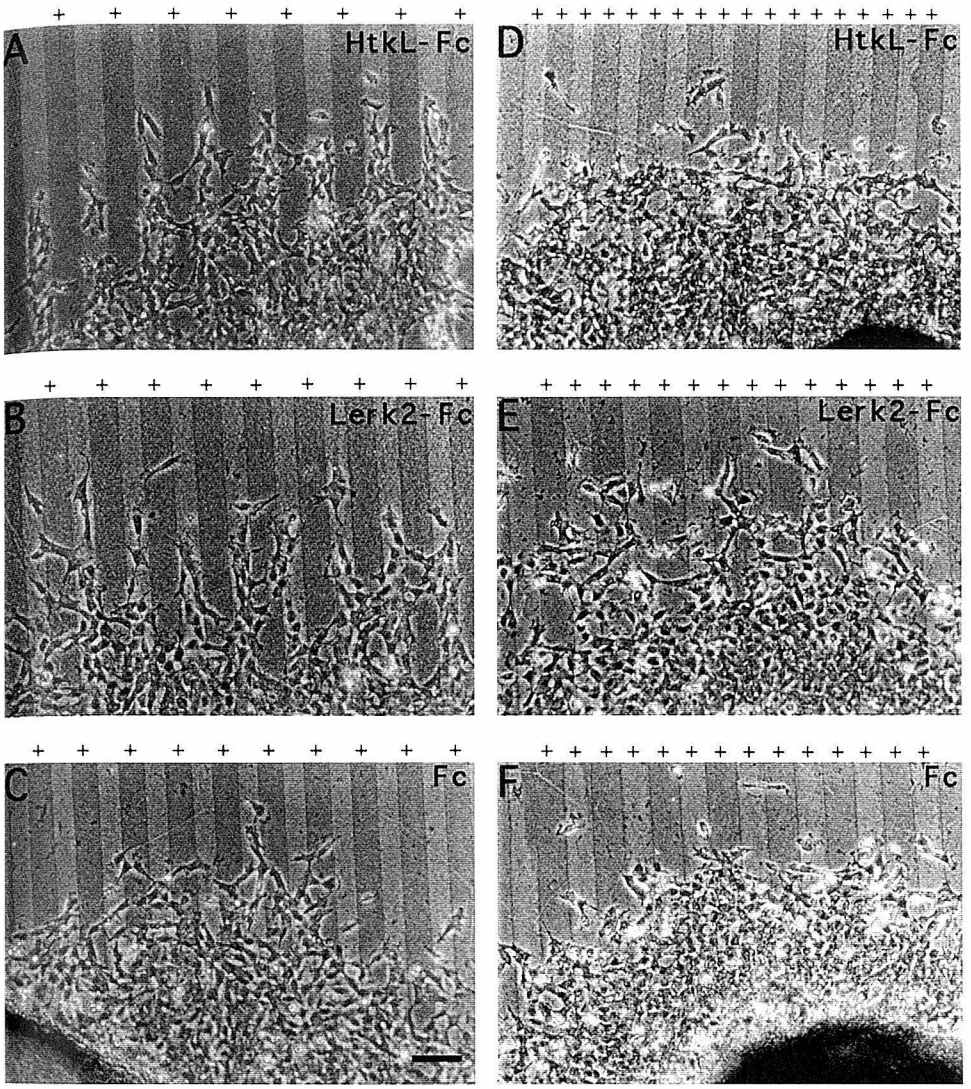

Figure 4. HtkL-Fc and Lerk2-Fc Fusion Proteins Inhibit Rat Neural Crest Cell Migration in a Stripe Assay

Crest explants were cultured on coverslips coated with ligand-Fc or Fc stripes. Each stripe is about 50μm wide.

(A–C) HtkL-Fc, Lerk2-Fc, or Fc, respectively, was coated in alternating stripes marked by "+" and subsequently visualized with alkaline phosphatase-conjugated anti-Fc antibodies after fixation of the explants.

(D–F) HtkL-Fc, Lerk2-Fc, or Fc, respectively, was coated in all stripes marked by "+." The darker lanes were coated first and visualized by anti-BSA antibodies (see Experimental Procedures). Crest cell migration was biased toward ligand-free zones by coating alternating stripes ("+") with HtkL-Fc (A) or Lerk2-Fc (B), but not with Fc (C). This guidance was not observed when either ligand was coated in all stripes (D and E). More than 30 explants were examined for the experiments depicted in each panel, and consistent patterns of cell migration were observed. Quantification of the data is presented in Table 1. Scale bar = 100 μm.

explant overrides the guidance cues on the substrate. Quantification of these stripe assays indicated that, on average, 75–80% of the crest cells in the distal one third of each explant were present in between the ligand-coated lanes, whereas there was no such bias in the distribution of the cells when alternating lanes were coated with control Fc protein (Table 1, left side). Interestingly, when all stripes were coated with Fc or fusion proteins, the cells were uniformly distributed across the stripes, irrespective of whether ligand fusions or control Fc were used (Figures 4D–4F; Table 1, right side). These data suggest that neural crest cell migration is restricted at boundaries between ligand-containing and ligand-free regions in vitro, consistent with the distribution of neural crest cells and ligands observed in vivo (Figure 2).

To examine the effects of ligands on neural crest cell migration using an independent assay, we employed a transfilter chemotaxis system (modified Boyden chamber) (Moiseiwitsch and Lauder, 1995). In this assay, preclustered ligand- or control-Fc fusion proteins were added at various concentrations to the bottom wells of a multiwell chamber. Dissociated primary neural crest cells were added to upper wells separated from the lower ones by an 8 μm porous filter, and allowed to migrate for 6 hr, after which they were fixed and the number of cells that migrated to the bottom side of the filter was determined. There was a statistically significant ($p < 0.05$) concentration-dependent reduction of cell migration by preclustered HtkL-Fc detectable at concentrations as low as 10 ng/ml (Figure 5, black bars/

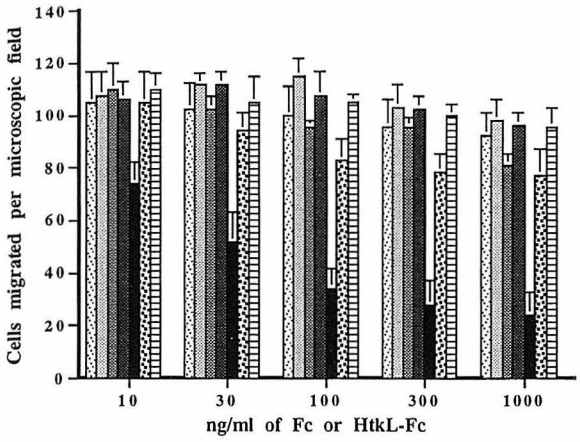

column	1	2	3	4	5	6	7
icon							
top well	--	Fc	--	HtkL-Fc	--	clustered HtkL-Fc	clustered HtkL-Fc
bottom well	Fc	Fc	HtkL-Fc	HtkL-Fc	clustered HtkL-Fc	clustered HtkL-Fc	--

Figure 5. HtkL-Fc Fusion Proteins Inhibit Rat Neural Crest Cell Migration in a Transfilter Chemotaxis Assay

Various concentrations of unclustered or clustered Fc or HtkL-Fc were added to the bottom, top, or both wells of a chemotaxis chamber as indicated. "−" indicates that the well contains culture media only. Cells that migrated to the bottom side of the porous filter membrane (8 μm pore size) were counted under a 200× microscopic field. Clustered HtkL-Fc reduces crest cell migration in a concentration-dependent manner when added to the bottom wells (black bars, column 5). However, this effect is not observed if clustered HtkL-Fc is present in only the top well (column 7), and is much weaker if equal concentrations are present on both sides of the filter (column 6). The results represent the mean ±SEM of three independent experiments. In each experiment, 5 random fields per well and duplicate wells were scored for each concentration of HtkL-Fc or control Fc.

column 5), but not by control Fc or unclustered HtkL-Fc (Figure 5, columns 1 and 3, respectively).

To determine whether this reduction of cell migration depended on a graded presentation of ligand, preclustered HtkL-Fc was added to both the top and bottom wells at equal concentrations (Figure 5, column 6). No significant reduction of migration was observed at concentrations below 300 ng/ml ($p > 0.05$). At 300 and 1000 ng/ml, some small but statistically significant ($p \leq 0.05$) reduction was observed relative to controls, but the effect was not nearly as strong as when the ligand was initially presented on the opposite side of the filter from the cells (Figure 5, cf. column 5 versus column 6). Moreover, no significant reduction of migration was observed when preclustered ligand was added to the top but not the bottom chamber (Figure 5, column 7). These data are consistent with the results of the stripe assays and suggest that inhibition of crest cell migration in vitro requires a discontinuous or graded presentation of the ligand, consistent with the distribution of ligand expression in vivo.

Repulsive and Growth-Cone Collapse Activities of HtkL and Lerk2 on Trunk Motor Axons

The sites of HtkL and Lerk2 expression in vivo include the caudal sclerotome, the dermatome, and early limb buds (Figures 2 and 3), all of which regions are putative barriers to early axon outgrowth (Davies et al., 1990; Oakley and Tosney, 1991). We therefore sought to determine whether Lerk2 and HtkL can play an inhibitory role in guiding motor axon outgrowth as well as neural crest migration. We first tested the ability of clustered ligand-Fc fusion proteins to induce growth-cone collapse of rat motor axons, using two different functional assays. In the first assay, preclustered ligand-Fc proteins were added to the culture medium at various concentrations, and the proportion of spread versus collapsed growth cones was determined in a population of axons fixed after one hr. Both ligands induced a concentration-dependent inhibition of growth-cone spreading, with a half maximal dose around 300 ng/ml (3nM) or 500 ng/ml (5nM) for HtkL- or Lerk2-Fc, respectively (Figure 6A). At saturation, approximately 70% of the growth cones were collapsed (Figure 6A), even if both ligands were combined (not shown). This may indicate that not all axons in the explant express functionally significant levels of receptors for the ligands, as suggested by the transient nature of Nuk expression on motor axons in vivo (Henkemeyer et al., 1994). In a second assay, time-lapse video microscopy was used to image individual growth cones, for 10 min before and 30 min after addition of soluble preclustered ligand-Fc proteins (Figures 6B and 6C). This analysis confirmed that preclustered ligands indeed induced growth-cone collapse (Figure 6C). The percentage of collapse responses recorded by time-lapse was 12% for control Fc (n=17 growth cones imaged), 74% for Lerk2-Fc (n=19 growth cones imaged), and 77% for HtkL-Fc (n=22 growth cones imaged).

Finally, we asked whether the ligands could exhibit repulsive guidance activity toward motor axons when presented in a stripe format. As in the crest migration stripe assays, ligands were presented as purified proteins immobilized using anti-Fc bound to nitrocellulose-coated coverslips, rather than as membrane suspensions from transfected cells (Drescher et al., 1995; Nakamoto et al., 1996). Motor axons avoided growing in alternating lanes containing either HtkL- or Lerk2-Fc fusion proteins (Figures 7A and 7B, "+" lanes), but not lanes containing control Fc protein (Figure 7C). No obvious avoidance was observed, however, when all lanes contained ligand-Fc (Figures 7D and 7E) or control Fc (Figure 7F) protein. These results are consistent with a contact-mediated mechanism for repulsive guidance, as previously indicated by time-lapse videomicroscopic analysis of motor axon outgrowth in vivo (Oakley and Tosney, 1993). Taken together, these data indicate that HtkL and Lerk2 not only induce growth-cone collapse, but can exhibit repulsive guidance activity toward motor axons in vitro.

Discussion

In higher vertebrates, migrating neural crest cells and growing motor axons avoid the caudal compartment of the somites (Keynes and Stern, 1984; Rickmann et al., 1985). Previous studies suggested that this reflects the activity of one or more inhibitory guidance factors present in the caudal sclerotome (Davies et al., 1990; Krull et al., 1995; Hotary and Tosney, 1996). We have discovered

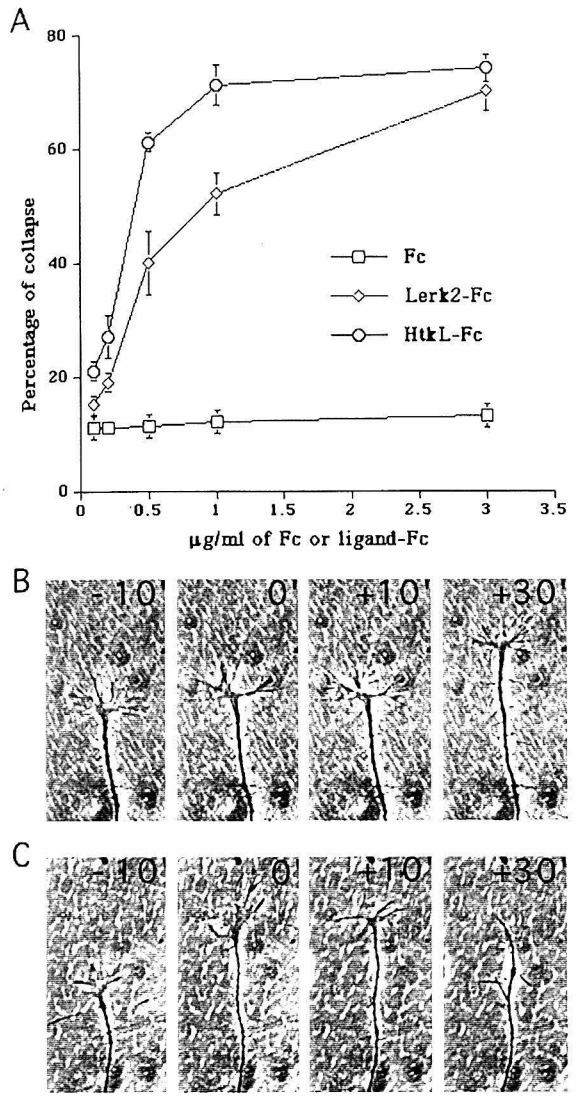

Figure 6. HtkL-Fc and Lerk2-Fc Fusion Proteins Induce Growth-Cone Collapse of Rat Neural Tube Explant Axons

(A) Overnight neural tube explants were incubated with various concentrations of clustered Lerk2- or HtkL-Fc proteins at 37°C for 1 hr. The explants were then fixed and scored for the percentage of collapsed growth cones (as judged by the absence of well-spread lamellipodia and filopodia at the axon termini. In contrast to control Fc (open squares), Lerk2- (open diamonds) or HtkL-Fc (open circles) induced a dose-dependent collapse response. The half maximal dose is around 500ng/ml (5nM) for Lerk2-Fc, and 300ng/ml (3nM) for HtkL-Fc. Neither ligand can induce collapse of more than 80% of the growth cones in the 1 hr period tested, nor can both ligands combined (not shown). 100 random growth cones were counted per experiment at each concentration point, and 3 experiments were performed for each ligand-Fc or Fc protein. Individual growth cones extended from overnight neural tube explants were time-lapsed to observe their response to Lerk2-Fc (B), HtkL-Fc (not shown), or Fc (C). Lerk2-Fc or HtkL-Fc induced growth-cone collapse, usually within 30 min after reagent addition. Preclustered Fc or ligand-Fc proteins were added to the culture medium at 1 μg/ml. One growth cone was recorded at a time. The percentages of collapses observed are given in text.

that two Eph family transmembrane ligands, HtkL and Lerk2, are expressed in somite regions avoided by migratory crest cells and motor axons, and that with minor twists these expression patterns are evolutionarily conserved. Using several independent functional assays, we have demonstrated that both ligands exhibit repulsive guidance activities toward migrating neural crest cells and growing motor axons, and that these repulsive activities require a discontinuous, not uniform, presentation of the ligands. Taken together, these results suggest that HtkL and Lerk2 may play a key role in the early segmental patterning of the PNS. Similar conclusions have been reached in independent and complementary in vivo studies (Krull et al., unpublished data; Smith et al., unpublished data).

Conserved Somite Expression Patterns of HtkL/Lerk2 in Rat and Chick Correlate with Their Proposed Functional Roles in Patterning the PNS

Migrating neural crest cells in the trunk use either of two major pathways. Initially they migrate ventrally through the rostral sclerotome, and later laterally along a path between the dermatome and epidermis (Serbedzija et al., 1990; Erickson et al., 1992). Somite manipulation experiments have shown that the ventral pathway is determined by the intrinsic rostral–caudal polarity of the somite (Teillet, et al., 1987; Bronner-Fraser and Stern, 1991). We have shown that in rat embryos HtkL and Lerk2 are expressed in the caudal sclerotome and early dermatome, precisely the inhibitory regions suggested to restrict early crest migration (as well as motor axon outgrowth; see below). Moreover, the timing of their expression is also appropriate for an inhibitory role in restricting crest migration: the dermatome and the caudal sclerotome expression of the two ligands precedes crest cell migration (Figure 2). In addition, the expression level of these ligands in the dermatome is much reduced in later stages, coincident with the onset of crest migration dorsal to the dermatome (data not shown).

The somitic expression patterns of Eph transmembrane ligands exhibit not only appropriate spatial and temporal characteristics in rat, but are also evolutionarily conserved (Figure 8). In early chick embryos, the ortholog of Lerk2, rather than that of HtkL, is restricted to the caudal half sclerotome and dermatome. Despite this difference, chick-Lerk2 is expressed in places that are inhibitory for neural crest migration and motor axon outgrowth at the appropriate stage of development. The fact that these ligands exhibit indistinguishable binding affinities and selectivities toward their cognate receptors (reviewed in Pandey et al., 1995a) suggests that they may have been used interchangeably in evolution. Similarly, avian neural crest cells express Qek10 (Krull et al., 1997), the homolog of Sek4 in mammals, while rat neural crest cells express primarily Nuk; however, Nuk and Sek4 exhibit indistinguishable binding affinities and specificities toward their ligand subgroup (Brambilla et al., 1995; Gale et al., 1996a). The conserved expression patterns of these ligands and their receptors in avian and mammalian embryos strongly supports the idea that they function in patterning the PNS in vivo.

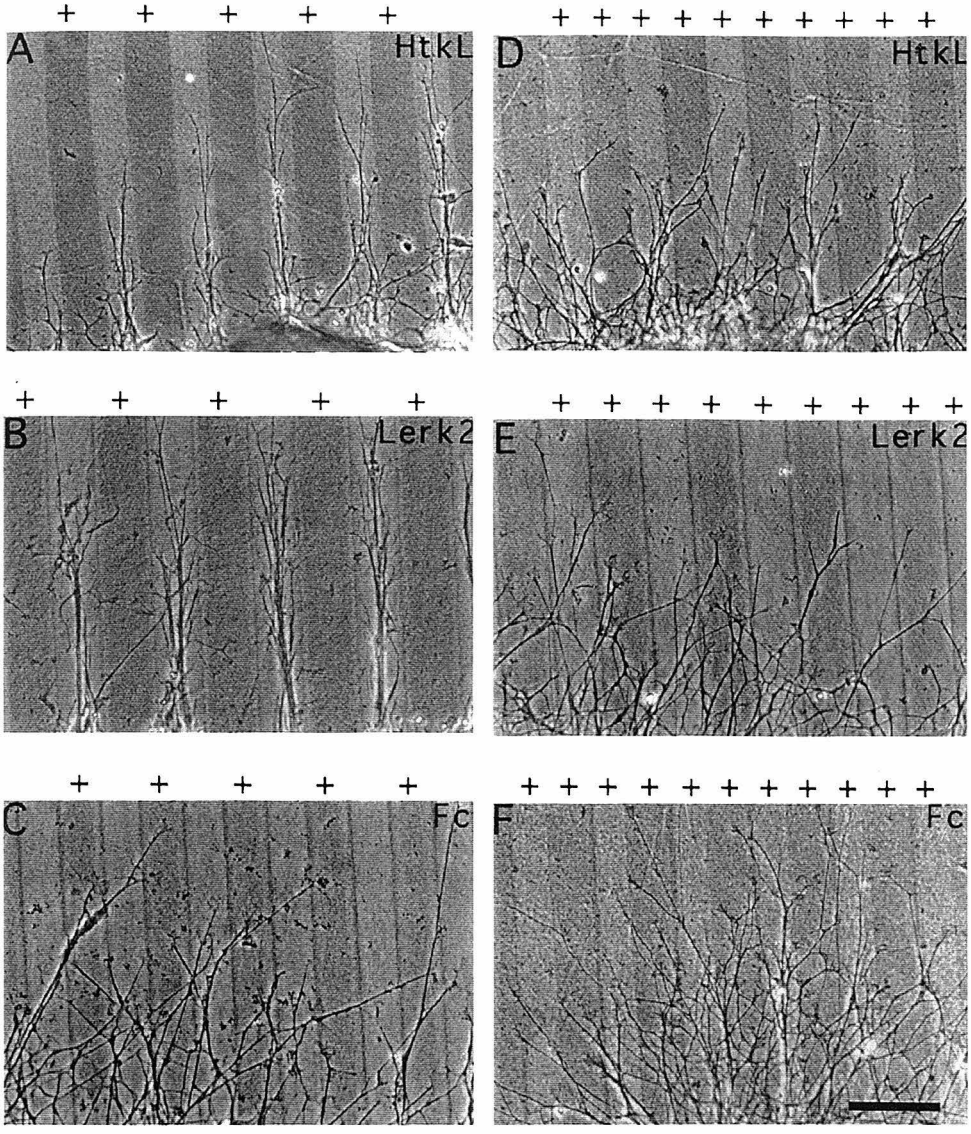

Figure 7. HtkL-Fc and Lerk2-Fc Fusion Proteins Inhibit Rat Motor Axon Outgrowth in a Stripe Assay

Neural tube explants were cultured on coverslips coated with ligand-Fc or Fc stripes in the presence of laminin.

(A–C) HtkL-Fc, Lerk2-Fc, or Fc, respectively, was present in alternating stripes (marked by "+") and visualized with alkaline phosphatase-conjugated anti-Fc antibodies after fixation of the explants.

(D–F) HtkL-Fc, Lerk2-Fc, or Fc, respectively, was present in all stripes (marked by "+"). The darker lanes in (D)–(F) were coated first and visualized by anti-BSA antibodies (see Experimental Procedures). Motor axon outgrowth was guided to noncoated stripes by HtkL-Fc (A) or Lerk2-Fc (B), but not by Fc (C). This guidance was not observed when either ligand was present in all stripes (D and E). At least 30 explants were performed for each panel, and consistent axon outgrowth patterns were observed. Scale bar = 100 μm.

Repulsive Guidance of Neural Crest Migration by HtkL and Lerk2

A number of molecules have been identified as candidates for restricting pathways of neural crest migration in vivo. PNA-binding glycoproteins present in caudal half somites have been shown to prevent migration of neural crest cells into this compartment (Krull et al., 1995), but their molecular identity is not yet known. Similarly, in the dorsolateral migration pathway, unidentified glycoconjugates have been implicated in transiently preventing premature entry of neural crest cells into this route (Oakley et al., 1994). Collagen IX, a chondroitin sulfate proteoglycan present in the caudal sclerotome, has recently been shown to inhibit crest cell migration in vitro (Ring et al., 1996). Other molecularly defined candidates have been shown to exhibit restricted expression in caudal half somites, such as versican and T-cadherin (Ranscht and Bronner-Fraser, 1991; Landolt et al., 1995), but there are so far no functional data supporting the idea that these proteins guide neural crest migration.

We have demonstrated repulsive guidance of migrating rat neural crest cells by HtkL or Lerk2 in two independent functional assays. In the chemotaxis assay, preclustered HtkL-Fc fusion proteins added in soluble form to the bottom wells of a Boyden-like chamber inhibited

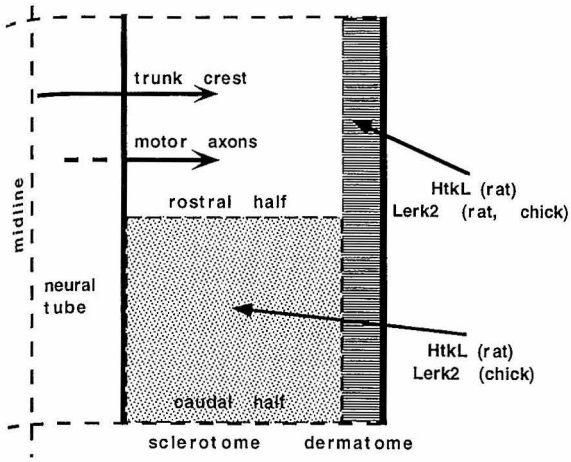

Figure 8. Summary Diagram of HtkL and Lerk2 Expression in Developing Somites

A longitudinal schematic section of a single somite shows the rostral and caudal halves of the sclerotome and the dermatome. Trunk neural crest cells and motor axons selectively migrate through the rostral sclerotome. HtkL and Lerk2 are restricted to somite regions avoided by crest cells and motor axons, and appear to be used interchangeably in rat and chick. In the rat, Lerk2 expression persists in the myotome (not illustrated).

the transfilter migration of crest cells. In the stripe assay, substrate-bound HtkL-Fc or Lerk2-Fc proteins caused crest cells to preferentially migrate in the ligand-free zones. Interestingly, when the ligands were presented uniformly (in every stripe, for example, or in both wells of the chemotaxis chamber), little or no repulsive influence on crest cell migration was observed. These data suggest that the ligands can mediate a repulsive guidance or repellent function, and are not simply inhibitors of cell migration or motility. A similar conclusion has been reached for GPI-linked ligands that mediate axon guidance (Nakamoto et al., 1996). One explanation for this phenomenon is that rapid desensitization occurs when the cells are exposed to uniformly presented ligands.

The action of Eph ligands in vitro appears to be distinct from that of other inhibitors of crest migration studied previously that can exert their effect when applied uniformly to cells in the presence of permissive substrates (Perris and Johansson, 1987). It is formally possible that Eph ligands might also exhibit such inhibitory effects if tested with lower concentrations of permissive substrate. However, in vivo, migrating neural crest cells are likely to encounter Eph ligands in the presence of substantial amounts of permissive substrate. Moreover, the requirement for a discontinuous distribution of HtkL and Lerk2 in vitro is also in good agreement with the fact that HtkL/c-Lerk2 exhibits a sharp boundary of expression between caudal and rostral somite halves in vivo. A discontinuous expression of HtkL is also seen in hindbrain rhombomeres, where reciprocal expression of HtkL and its cognate receptors may play a role in restricting hindbrain cell mixing (Becker et al., 1994; Bergemann et al., 1995; Xu et al., 1995). The repellent function that these ligands can exhibit in vitro therefore seems well suited to the context in which they are likely to function in vivo. This does not mean that other molecules that act as inhibitors are unimportant in guiding neural crest migration in vivo. Rather, both repulsive and inhibitory activities of different molecules probably contribute to excluding neural crest cells from the caudal somite halves.

Prior functional analysis of GPI-linked Eph ligands in the nervous system has focused on their activity as repulsive axon guidance factors. Our data indicate that transmembrane Eph ligands not only function similarly to repel growing axons, but also can act as chemorepellent molecules for migrating cells. In contrast, the GPI-linked Eph family ligand B61 can act as a chemoattractant for endothelial cells in vitro (Pandey et al., 1995b). Whether this indicates that GPI-linked and transmembrane Eph family ligands exert opposite influences on cell migration, or that the nature of the influence is cell context-dependent, awaits further investigation.

Repulsive Guidance of Motor Axon Outgrowth by HtkL and Lerk2

Recent studies have revealed that chemorepulsion is an important mechanism of motor axon guidance (reviewed in Schwab et al., 1993). For example, the floor plate has been shown to repel trunk motor axons that grow ventrolaterally away from the ventral midline of the spinal cord (Guthrie and Pini, 1995). In the cranial region, floor plate–derived netrin-1 has been shown to repel trochlear motor axons (Colamarino and Tessier-Lavigne, 1995). Motor axon projections also avoid the caudal half somites by contact-mediated inhibition (Oakley and Tosney, 1993; Hotary and Tosney, 1996). Recently, T-cadherin and collagen IX (which are expressed in caudal half somites) were shown to inhibit motorneuron neurite outgrowth in vitro (Fredette et al., 1996; Ring et al., 1996). Our data identify HtkL as an additional candidate for restricting motor axon outgrowth in vivo: it is expressed in caudal half somites, and exhibits both repulsive guidance and growth-cone collapse activities toward motor axons in vitro. Sensory axons also avoid the caudal half somites, and PNA-binding glycoproteins of 48 and 55 Kd in extracts of caudal half somites have been shown to collapse the growth cones of DRG axons (Davies et al., 1990). We have not yet determined whether HtkL or Lerk2 exhibit repulsive guidance activity toward sensory axons, in part because Nuk expression appears transient during sensory axon outgrowth in the somites (Henkemeyer et al., 1994). Nevertheless, it is possible that c-HtkL/c-Lerk2 and the PNA-binding glycoproteins are related, and this will become clear once the latter are characterized.

Trunk motor axons are not only patterned metamerically along the anterior–posterior axis, but are also restricted from growing dorsolaterally toward the dermatome. The recent finding that chick collapsin-1 is expressed in early developing dermatome and is able to collapse the growth cones of motor axons in vitro (Shepherd et al., 1996) supports the idea that the dermatome as well as the caudal sclerotome contains repulsive axon guidance molecules. The observation that HtkL and Lerk2 are expressed in the dermatome suggests that they may play a repulsive guidance role in

this tissue as well. Thus, early trunk motor axons are likely guided by multiple repulsive molecules acting in several spatial dimensions. Together, signals in the floor plate (such as netrin-1), caudal half somites (such as HtkL, T-cadherin and collagen IX), and dermatome (including HtkL, Lerk2 and collapsin-1) may form a three-dimensional repulsive matrix that determines the segmented ventrolateral projection pattern of trunk motor axons.

Eight Eph family ligands have thus far been identified (Gale et al., 1996b). Our results extend the number of these ligands with a demonstrable role in axon guidance from two (Drescher et al., 1995; Nakamoto et al., 1996) to four. They also demonstrate that transmembrane as well as GPI-linked ligands can act as repulsive axon guidance cues. Furthermore, the observation that Eph family ligands can guide motor axons as well as retinal axons implies that these molecules play a diverse role in axon guidance in both the central and peripheral nervous systems. In addition to their expression at initial stages of motor axon outgrowth, HtkL and Lerk2 are expressed later in development in regions such as the limb. This suggests that these ligands may function in maintaining as well as initiating restricted patterns of motor axon growth. It further raises the possibility that potential antagonists of such inhibitory ligands might be useful in promoting nerve regeneration, as has been shown for a myelin-associated inhibitor of axon growth (Bregman et al., 1995).

Function of HtkL and Lerk2 in PNS Patterning In Vivo

The spatio-temporally appropriate and evolutionarily conserved expression patterns of HtkL and Lerk2, taken together with their in vitro activities, provide circumstantial evidence that these ligands are involved in patterning the developing PNS in vivo. In a direct test of this idea, we performed a preliminary examination of neural crest cell migration and early motor axon outgrowth patterns in mouse embryos carrying homozygous mutations in two receptors for these ligands, Nuk and Sek-4 (kindly provided by T. Pawson and R. Klein). No obvious perturbations were observed (data not shown). One explanation for this lack of a clear mutant phenotype is that other Eph receptors are expressed in crest cells or motor neurons that are capable of interacting with HtkL and Lerk2, such as Myk-1, Elk, and Sek-1. All of these can be activated by transmembrane Eph ligands (Gale et al, 1996a), and Myk-1 and Sek-1 are detectably expressed in crest cells (albeit at levels lower than Nuk [Figure 1]). Since the somite expression patterns of HtkL and Lerk2 appear nonoverlapping, ligand knockouts may be more likely to reveal a function for this signaling system in vivo. Consistent with this idea, application of unclustered Elk-L/Lerk-2-Fc as a competitive antagonist of endogenous ligands disrupted the metameric pattern of neural crest migration in whole trunk explants from avian embryos (Krull et al., 1997). These in vivo perturbation experiments complement our in vitro studies and suggest that Eph family ligands that are sufficient to mediate guidance activities in vitro are also involved in restricting crest cell migration in vivo.

Coordination among Functionally Equivalent Eph Family Ligands

HtkL and Lerk2, by virtue of their expression in different regions of the somites, may act in concert to pattern neural crest cell migration and motor axon outgrowth in the peripheral nervous system. Such a coordinated action of functionally equivalent Eph ligands is also observed for RAGS and ELF-1 in the retinotectal system, where both ligands are expressed in the developing tectum in a gradient fashion (Cheng et al., 1995; Drescher et al., 1995). Thus, in each system, the construction of the temporally and spatially dynamic expression pattern needed to guide cells or axons appears to be distributed among functionally equivalent, independent gene products. Perhaps the evolutionary process that leads to the acquisition of such complex expression patterns may be more easily achieved by utilizing multiple, functionally interchangeable ligand-encoding genes, rather than by evolving complex spatial and temporal regulatory mechanisms for a single gene. In this respect, the large size of the Eph receptor and ligand family seems to make them particularly suitable for achieving the complex signaling patterns necessary to organize the developing nervous system.

Experimental Procedures

Production of Fc and Ligand-Fc Fusion Proteins

Human IgG1-Fc expression plasmid (Aruffo et al., 1990) was used to produce soluble Fc proteins. The entire extracellular regions of Lerk2 and HtkL were fused in frame with the first amino acid of the human IgG1-Fc hinge region in pCEP4 expression vector (Invitrogen). Expression plasmid DNA was transiently transfected into human 293 cells using the calcium phosphate precipitation method. Serum-free conditioned medium was then collected for 5 days, passed through a 0.22 μm filter, and either stored at 4°C, or the Fc or ligand-Fc fusion proteins were purified over protein-A columns (Pierce). The concentration of purified Fc or ligand-Fc fusion proteins was determined using MicroBCA protein assay reagents (Pierce), and their purity assessed by Coomassie Blue staining of SDS gels. Recombinant Lerk2- and HtkL-Fc are disulfide-linked dimers of MW ca. 100 Kd.

Gene-Specific RT-PCR for Eph-Related Receptors

RNA was isolated from one-day explants of E10.5 rat neural crest cells (Stemple and Anderson, 1992) using a Rneasy Total RNA kit (Qiagen). About 1 μg of total RNA was reverse transcribed with Superscript Preamplification System (GIBCO) for first-strand cDNA synthesis. For the semiquantitative RT-PCR experiment (Figures 1C and 1D), Eph-related receptor genes and β-actin were amplified from equal amounts of neural crest cDNA at 60°C for 28 cycles in a 50 μl volume. With the same sets of receptor primers, 1 ng of DNA for each receptor-containing plasmid was amplified at 60°C for 21 cycles in a 50 μl volume. The entire products of each reaction were fractionated by electrophoresis.

The PCR primers for Eph-related receptors are: GGT GAG GTC TGC AGT GGC CAT TTG (5′) and AGA CTG GAT CTG GTT CAT CTG GGC (3′) for Nuk, TTT ACC TAT GAG GAT CCC AAT GAG (5′) and CTG GAT ACT GCA GAG GAT CTT CTT (3′) for Sek-4, GAT CCT TTT ACT TAC GAA GAC CCT (5′) and GGC TCC TGG CTT AGC TTC CCA CTT (3′) for Myk-1, GCC AAA GAA ATC GAT GCA TCC TGC (5′) and GAC GCT GCT CAA AAT CTT ATT CTG (3′) for Sek-1, and AAT GAA GCT GTC CGG GAG TTT GCC (5′) and CTC AGG AGG TCT TCT GAT GTC ATC (3′) for Elk. The β-actin primers are CAC ACI TTC TAC AAT GAG CTG CGT (5′) and GGT IAG GAT CTT CAT GAG GTA GTC (3′). To construct plasmids (pBluescript-KS) containing specific receptors, Nuk, Sek-4, Sek-1, and Myk-1 were amplified from neural crest cDNA, and Elk from P1 rat brain.

Whole-Mount In Situ Hybridization and Immunohistochemistry

Whole-mount in situ hybridization followed a protocol by Wilkinson (1992). HNK-1 and TUJ1 whole-mount immunohistochemistry on chick embryos was performed following a protocol by Ohta et al. (1996). The stained embryos were sectioned on a cryostat after freezing in 15% sucrose plus 7.5% gelatin. Photo negatives were scanned using a Polaroid SprintScan-35 into the Adobe Photoshop program, where figure composites were made. In situ probes for Lerk2 and HtkL are full-length coding sequences. The erbB3 (Genebank U29339) probes were amplified with TGC AGC TTG TTA CTC AGT ACT TGC (5′) and GGC TCC TAC ACA CTG ACA CTT TCT (3′). Nuk probes were amplified with oligos described above. The fragments of chick Lerk2 (678 bp) and HtkL (648 bp) (also used for the Figure 3 alignment) were cloned with degenerate oligos: TTC/T ACI ATI AAA/G TTT/C CAA/G GA (5′), and TC/TA IAC T/CTT G/ATA G/ATA IAT G/ATT (3′).

Neural Crest Explant Cultures and Ligand Assays

E10.5 rat trunk neural tubes were isolated and cultured in complete crest media as previously described (Stemple and Anderson, 1992). For Eph-related receptor detection, one-day explants were incubated with Fc or ligand-Fc conditioned media (harvested from transfected 293 cells) for 1 hr at room temperature, fixed, then incubated with biotin-conjugated goat anti-human IgG-Fc secondary antibodies (Jackson), and detected with the ABC-HRP system (Vector).

15 mm-round Thermanox tissue culture coverslips (Nunc) were used for protein coating in the stripe assay with special silicone matrices kindly provided by Dr. F. Bonhoeffer (Max-Planck Institute, Tübingen, Germany). The cover slips were first coated with nitrocellulose dissolved in methanol as previously described (Lemmon et al., 1989). Stripes were prepared according to the procedure of Vielmetter et al. (1990). Briefly, for the first stripes, a mixture of 200 μg/ml fibronectin (Biomedical Technology) and 100 μg/ml goat anti-Fc antibodies were injected into the open channels of the matrix placed onto the coverslip. After a 1 hr incubation at 37°C, unbound proteins were removed by washing twice with PBS. A blocking solution (2 mg/ml of BSA in PBS) was then injected and incubated for 30 min, to saturate the remaining binding sites. The matrix was then removed, and for the second stripes, the coverslip was coated with either 50 μg/ml fibronectin (for alternating stripes containing ligand) or a mixture of 50 μg/ml fibronectin and 50 μg/ml goat anti-Fc antibodies (for every stripe containing ligand) for 1 hr at 37°C. Finally, Fc or ligand-Fc (5 μg/ml) protein in conditioned media was bound to the coverslip via a 2 hr incubation at 37°C. Isolated E10.5 neural tubes were plated perpendicular to the stripes, cultured overnight, and fixed with 4% paraformaldehyde. The darker color of the first stripes seen in Figure 3 was revealed by staining the coverslip with either AP-conjugated goat anti-Fc (Jackson), or goat anti-BSA antibodies (Sigma) followed with AP-conjugated secondary antibodies (see legend to Figure 4).

A 48-well chemotaxis chamber (Neuroprobe) in which upper and lower wells are separated by an 8 μm pore-size polycarbonate membrane was used in the transfilter migration assays. The membranes were coated with a mixture of gelatin and fibronectin (50 μg/ml each in PBS) before the assays. Prior to adding them to the wells, purified Fc or HtkL-Fc fusion proteins (5 μg/ml) were preclustered by incubation with 50 μg/ml polyclonal goat anti-human IgG-Fc antibodies (Jackson) for 1 hr at R. T. in complete crest culture media; these mixes were then diluted accordingly. 25 μl of complete crest culture media, containing preclustered HtkL-Fc or Fc at appropriate concentrations, were first added to bottom wells of the multiwell chamber. The upper wells were then filled with 50 μl media containing neural crest cells at 2×10^5 cell/ml; in some experiments, HtkL-Fc or Fc proteins were included as well. In addition, 10 μg/ml of fibronectin was present in the bottom wells to provide a permissive substrate for transfilter migration. Crest cells were dissociated from 2- to 3-day explants of E10.5 neural tubes with Hank's Ca^{2+}, Mg^{2+}-free medium containing 1mM EDTA. Approximately 60 explants were pooled for each experiment. After a 6 hr incubation at 37°C, the chamber was disassembled, and cells were removed mechanically from the upper side of the filter membrane. After the membrane was fixed in methanol and stained with hematoxylin, the number of cells that migrated to the bottom side was determined by counting in a 200× microscopic field.

Explant Cultures for Axon Outgrowth and Ligand Assays

Small pieces of trunk neural tube (about 0.5 mm in length) were prepared from E10.5 rat embryos using the method described for neural crest explant culture (Stemple and Anderson, 1992). Culture dishes were first coated with poly-lysine (Stemple and Anderson, 1992), then with 5 μg/ml laminin in L15-Air (GIBCO) for 1 hr at 37°C. Neural tube explants were cultured in defined crest culture medium (Stemple and Anderson, 1992). For axon staining, the explants were either incubated with Fc- or ligand-Fc–conditioned media as described above for the neural crest cells, or with c-ret antibodies (Lo and Anderson, 1995). Stripe assay preparation was as described above, except that laminin (100 μg/ml for the first stripe and 50 μg/ml for the second) was used as substrate instead of fibronectin, and poly-lysine was omitted. The extent of ligand-dependent avoidance was lower (although still detectable) if the ligand-Fc fusions were coated in the presence of poly-lysine plus laminin, reflecting the stronger neurite outgrowth–promoting activity of this combined permissive substrate. Neural tube explants were cultured overnight for axon outgrowth, fixed, and developed to visualize the first stripes as described above.

Overnight neural tube explants were assayed for growth-cone collapse responses. To induce Fc or ligand-Fc clustering prior to collapse assays, 5 μg/ml purified Fc or ligand-Fc fusion proteins was first incubated with 50 μg/ml polyclonal goat anti-hIgG-Fc antibodies for 1 hr at R. T. in defined crest culture medium, then added to neural tube explant cultures at various concentrations. After a 1 hr incubation with Fc or ligand-Fc reagents at 37°C , the explants were fixed in 4% paraformaldehyde for 1 hr at R. T., and the number of spread or collapsed growth cones was counted. Time-lapse recording was performed using a charge-coupled device (CCD) camera and the Metamorph program. Photographic image contrast was enhanced using the Adobe Photoshop program.

Acknowledgments

We thank A. Groves and N. Shah for teaching the in situ hybridization and neural crest explant procedures, respectively; S. Fashena for the hIgG1-Fc vector; L. Lo for anti-c-ret antibody; T. Frankfurter for TUJ1 antibody; J. Lauder and J. Moiseiwitsch for advice on the chemotaxis assay; J. Vielmetter and C. Krull for advice on the stripe assay, and C. Marcelle for help in the interpretation of the chick in situs. We are particularly grateful to F. Bonhoeffer for providing silicone matrices for use in the stripe assays. We thank N. Gale and G. Yancopoulos for sharing unpublished results, and S. Kulkarni, T. Pawson, and R. Klein for Nuk/Sek4 mutant embryos. We also thank D. Wilkinson, S. Fraser, and M. Bronner-Fraser for communicating their unpublished results and for comments on the manuscript, and our lab members for discussions and support. D. J. A. is an Investigator of the Howard Hughes Medical Institute.

Received December 27, 1996; revised January 24, 1997.

References

Aruffo, A., Stamenkovic, I., Melnick, M., Underhill, C.B., and Seed, B. (1990). CD44 is the principal cell surface receptor for hyaluronate. Cell *61*, 1303–1313.

Becker, N., Seitanidou, T., Murphy, P., Mattéi, M.-G., Tipilko, P., Nieto, M.A., Wilkinson, D.G., Charnay, P., and Gilardi-Hebenstreit, P. (1994). Several receptor tyrosine kinases genes of the Eph family are segmentally expressed in the developing hindbrain. Mech. Dev. *47*, 3–17.

Bennett, B.D., Zeigler, F.C., Gu, Q., Fendly, B., Goddard, A.D., Gillett, N., and Matthews, W. (1995). Molecular cloning of a ligand for the Eph-related receptor protein tyrosine kinase Htk. Proc. Natl. Acad. Sci. USA *92*, 1866–1870.

Bergemann, A.D., Cheng, H.J., Brambilla, R., Klein, R., and Flanagan,

J.G. (1995). ELF-2, a new member of the Eph ligand family, is segmentally expressed in mouse embryos in the region of the hindbrain and newly forming somites. Mol. Cell. Biol. *15*, 4921–4929.

Brambilla, R., and Klein, R. (1995). Telling axons where to grow: a role for Eph receptor tyrosine kinases in guidance. Mol. Cell. Neurosci. *6*, 487–495.

Brambilla, R., Schnapp, A., Casagranda, F., Labrador, J.P., Bergemann, A.D., Flanagan, J.G., Pasquale, E.B., and Klein, R. (1995). Membrane-bound Lerk2 ligand can signal through three different Eph-related receptor tyrosine kinases. EMBO J. *14*, 3116–3126.

Bregman, B.S., Kunkel-Bagden, E., Schnell, L., Dai, H.N., Gao, D., and Schwab, M.E. (1995). Recovery from spinal cord injury mediated by antibodies to neurite growth inhibitors. Nature *378*, 498–501.

Bronner-Fraser, M. (1992). Environmental influences on neural crest cell migration. J. Neurobiology *24*, 233–247.

Bronner-Fraser, M., and Stern, C. (1991). Effects of mesodermal tissues on avian neural crest cell migration. Dev. Biol. *143*, 213–217.

Cheng, H.-J., Nakamoto, M., Bergemann, A.D., and Flanagan, J.G. (1995). Complementary gradients in expression and binding of ELF-1 and Mek4 in development of the topographic retinotectal projection map. Cell *82*, 371–381.

Colamarino, S.A., and Tessier-Lavigne, M. (1995). The axonal chemoattractant netrin-1 is also a chemorepellent for trochlear motor axons. Cell *81*, 621–629.

Davies, J.A., Cook, G.M.W., Stern, C.D., and Keynes, R.J. (1990). Isolation from chick somites of a glycoprotein fraction that causes collapse of dorsal root ganglion growth cones. Neuron *2*, 11–20.

Davis, S., Gale, N.W., Aldrich, T.H., Maisonpierre, P.C., Lhotak, V., Pawson, T., Goldfarb, M., and Yancopoulos, G.D. (1994). Ligands for the EPH-related receptor tyrosine kinases that require membrane attachment or clustering for activity. Science *266*, 816–819.

Drescher, U., Kremoser, C., Handwerker, C., Loschinger, J., Noda, M., and Bonhoeffer, F. (1995). In vitro guidance of retinal ganglion cell axons by RAGS, a 25kDa tectal protein related to ligands for Eph receptor tyrosine kinases. Cell *82*, 359–370.

Erickson, C.A., Duong, E.D., and Tosney, K.W. (1992). Descriptive and experimental analysis of the dispersion of neural crest cells along the dorsolateral path and their entry into ectoderm in the chick embryo. Dev. Biol. *151*, 251–272.

Fletcher, F.A., Carpenter, M.K., Shilling, H., Baum, P., Ziegler, S.F., et al. (1994). Lerk-2, a binding protein for the receptor-tyrosine kinase Elk, is evolutionarily conserved and expressed in a developmentally regulated pattern. Oncogene *9*, 3241–3247.

Fredette, B.J., Miller, J., and Ranscht, B. (1996). Inhibition of motor axon growth by T-cadherin substrata. Development *122*, 3163–3171.

Friedman, G.C., and O'Leary, D.D.M. (1996). Eph receptor tyrosine kinases and their ligands in neural development. Curr. Opin. Neurobiol. *6*, 127–133.

Gale, N.W., Holland, S.J., Valenzuela, D.M., Flenniken, A., Pan, L., Ryan, T.E., Henkemeyer, M., Strebhard, K., Hirai, H., Wilkinson, D.G., et al. (1996a). Eph receptors and ligands comprise two major specificity subclasses, and are reciprocally compartmentalized during embryogenesis. Neuron *17*, 9–19.

Gale, N.W., Flenniken, A., Compton, D.C., Jenkins, N., Copeland, N.G., Gilbert, D.J., Davis, S., Wilkinson, D.G., and Yancopoulos, G.D. (1996b). Elk-L3, a novel transmembrane ligand for the eph family of receptor tyrosine kinases, expressed in embryonic floor plate, roof plate and hindbrain segments. Oncogene *13*, 1343–1352.

Guthrie, S., and Pini, A. (1995). Chemorepulsion of developing motor axons by the floor plate. Neuron *14*, 1117–1130.

Henkemeyer, M., Marengere, L.E.M., McGlade, J., Oliver, J.P., Conlon, R.A., Holmyard, D.P., Lewtin, K., and Pawson, T. (1994). Immunolocalization of the Nuk receptor tyrosine kinase suggests roles in segmental patterning of the brain and axonogenesis. Oncogene *9*, 1001–1014.

Henkemeyer, M., Orioli, D., Henderson, J.T., Saxton, T.M., Roder, J., Pawson, T., and Klein, R. (1996). Nuk controls pathfinding of commissural axons in the mammalian central nervous system. Cell. *86*, 35–46.

Hotary, K.B., and Tosney, K.W. (1996). Cellular interactions that guide sensory and motor neurites indentified in an embryo slice preparation. Dev. Biol. *176*, 22–35.

Irving, C., Nieto, M.A., DasGupta, R., Charnay, P., and Wilkinson, D.G. (1996). Progressive spatial restriction of Sek-1 and Krox-20 gene expression during hindbrain segmentation. Dev. Biol. *173*, 26–38.

Keynes, R.J., and Stern, C.D. (1984). Segmentation in the vertebrate nervous system. Nature *310*, 413–429.

Krull, C.E., Collazo, A., Fraser, S.E., and Bronner-Fraser, M. (1995). Segmental migration of trunk neural crest: time-lapse analysis reveals a role for PNA-binding molecules. Development *121*, 3733–3743.

Landolt, R.M., Vaughan, L., Winterhalter, K.H., and Zimmermann, D.R. (1995). Veriscan is selectively expressed in embyronic tissues that act as barriers to neural crest cell migration and axon outgrowth. Development *121*, 2303–2312.

Lemmon, V., Farr, K.L., and Lagenaur, C. (1989). L1-mediated axon outgrowth occurs via a homophilic binding mechanism. Neuron *2*, 1597–1603.

Lo, L.-C., and Anderson, D.J. (1995). Postmigratory neural crest cells expressing c-ret display restricted developmental and proliferative capacities. Neuron *15*, 527–539.

Meyer, R., and Birchmeier, C. (1995). Multiple essential functions of neuregulin in development. Nature *378*, 386–390.

Moiseiwitsch, J.R., and Lauder, J.M. (1995). Serotonin regulates mouse cranial neural crest migration. Proc. Natl. Acad. Sci. USA *921*, 7182–7186.

Nakamoto, M., Cheng, H.-J., Friedman, G.C., McLaughlin, T., Hansen, M.J., Yoon, C.H., O'Leary, D.D.M., and Flanagan, J.G. (1996). Topographically specific effects of ELF-1 on retinal axon guidance in vitro and retinal axon mapping in vivo. Cell *86*, 755–766.

Oakley, R.A., and Tosney, K.W. (1991). Peanut agglutinin and chondroitin-6-sulfate are molecular markers for tissues that act as barriers to axon advance in the avian embryo. Dev. Biol. *147*, 187–206.

Oakley, R.A., and Tosney, K.W. (1993). Contact-mediated mechanisms of motor axon segmentation. J. Neurosci. *13*, 3773–3792.

Oakley, R.A., Lasky, D.J., Erickson, C.A., and Tosney, K.W. (1994). Glycoconjugates mark a transient barrier to neural crest migration in the chicken embryo. Development *120*, 103–114.

Ohta, K., Nakamura, M., Hirokawa, K., Tanaka, S., Iwama, A., Suda, T., Ando, M., and Tanaka, H. (1996). The receptor tyrosine kinase, cek8, is transiently expressed on subtypes of motoneurons in the spinal-cord during development. Mech. Dev. *54*, 59–69.

Orike, N., and Pini, A. (1996). Axon guidance: following the Eph plan. Current Biology *6*, 108–110.

Pandey, A., Lindberg, R.A., and Dixit, V.M. (1995a). Receptor orphans find a family. Current Biology *5*, 986–989.

Pandey, A., Shao, H., Marks, R.M., Polverini, P.J., and Dixit, V.M. (1995b). Role of B61, the ligand for the Eck receptor tyrosine kinase, in TNF-α-induced angiogenesis. Science *268*, 567–569.

Perris, R., and Johansson, S. (1987). Amphibian neural crest cell migration on purified extracellular matrix components: a chondroitin sulfate proteoglycan inhibits locomotion on fibronectin substrates. J. Cell Biol. *105*, 2511–2521.

Ranscht, B., and Bronner-Fraser, M. (1991). T-cadherin expression alternates with migrating neural crest cells in the trunk of the avian embryo. Development *111*, 15–22.

Rickmann, M., Fawcett, J.W., and Keynes, R.J. (1985). The migration of neural crest cells and the growth of motor axons through the rostral half of the chick somite. J. Embryol. Exp. Morphol. *90*, 437–455.

Ring, C., Hassell, H., and Halfter, W. (1996). Expression pattern of collagen IX and potential role in the segmentation of the peripheral nervous system. Dev. Biol. *180*, 41–53.

Schwab, M.E., Kapfhammer, J.P., and Brandtlow, C.E. (1993). Inhibitors of neurite outgrowth. Annu. Rev. Neurosci. *16*, 565–595.

Serbedzija, G.N., Fraser, S.E., and Bronner-Fraser, M. (1990). Pathways of trunk neural crest cell migration in the mouse embryo as revealed by vital dye labeling. Development *108*, 605–612.

Shepherd, I., Luo, Y., Raper, J.A., and Chang, S. (1996). The distribution of collapsin-1 mRNA in the developing chick nervous system. Dev. Biol. *173*, 185–199.

Stemple, D.L., and Anderson, D.J. (1992). Isolation of a stem cell for neurons and glia from the mammalian neural crest. Cell *71*, 973–985.

Stern, C.D., and Keynes, R.J. (1987). Interactions between somite cells: the formation and maintenance of segment boundaries in the chick embryo. Development *99*, 261–272.

Teillet, M., Kalcheim, C., and Le Douarin, N.M. (1987). Formation of the dorsal root ganglion in the avian embryo: Segmental origin and migratory behavior of neural crest progenitor cells. Dev. Biol. *120*, 329–347.

Tessier-Lavigne, M. (1995). Eph receptor tyrosine kinases, axon repulsion, and the development of topographic maps. Cell *82*, 345–348.

Tosney, K.W. (1991). Cells and cell interactions that guide motor axons in the developing chick embryo. BioEssays *13*, 17–23.

Tucker, G.C., Duband, J.L., Dufour, S., and Thiery, J.P. (1988). Cell-adhesion and substrate-adhesion molecules - their instructive roles in neural crest cell migration. Development *103*, 82–94.

Vielmetter, J., Stolze, B., Bonhoeffer, F., and Stuermer, C.A.O. (1990). In vitro assay to test differential substrate affinities of growing axons and migratory cells. Exp. Brain Res. *81*, 283–287.

Wilkinson, D.G. (1992). Whole-mount in situ hybridization of vertebrate embryos. In In Situ Hybridization: A Practical Approach, D.G. Wilkinson, ed. (Oxford: IRL Press), pp. 75–83.

Winslow, J.W., Moran, P., Valverde, J., Shih, A., Yuan, J.Q., Wong, S.C., Tsai, S.P., Goddard, A., Henzel, W.J., Hefti, F., et al. (1995). Cloning of AL-1, a ligand for an Eph-related tyrosine kinase receptor involved in axon bundle formation. Neuron *14*, 973–981.

Xu, Q., Alldus, G., Holder, N., and Wilkinson, D.G. (1995). Expression of truncated Sek-1 receptor tyrosine kinase disrupts the segmental restriction of gene expression in the xenopus and zebrafish hindbrain. Development *121*, 4005–4016.

Note Added in Proof

The following two completed bodies of work are being reviewed:

Krull, C.E., Lansford, R., Gale, N.W., Marcelle, C., Collazo, A., Yancopoulos, G.D., Fraser, S.E., and Bronner-Fraser, M. Interactions of Eph-related receptors and ligands confer rostrocaudal pattern to trunk neural crest migration.

Smith, A., Robinson, V., Patel, K., and Wilkinson, D.G. Eph-related receptor tyrosine kinases Sek-1 and Elk and the ligand Htl-L regulate the targeted migration of branchial neural crest cells.

Chapter 4

Neural Analysis of ephrinB2 Mutant Embryos

To confirm the roles of ephrinB2 in the nervous system in vivo, we generated ephrinB2 deficient mice. The details of ephrinB2 gene-targeting are presented in the beginning of the next chapter. This section describes the neural analysis of ephrinB2 mutant embryos, and our interpretation of the results.

EphrinB2 mutant embryos die in utero around E10.5. To examine possible phenotypic alterations in neural crest migration, motor axon projection, somite polarity, and hindbrain segmentation, I used a panel of molecular markers.

EphrinB2 is expressed strongly in hindbrain rhombomeres r1, r2, r4, and r6, but is low or absent in rhombomeres r3 and r5 (Bergemann et al., 1995). Its receptors Nuk/EphB2 and Sek1/EphA4 are conversely restricted to rhombomeres r3 and r5 (Henkemeyer et al., 1996; Mori et al., 1992; Nitto et al., 1992). Ephrin ligands and its receptors (Nuk/EphB2 and Sek1/EphA4) mediated signaling has been investigated through gain-of-function studies either using dominant negative truncated-receptors or using full length ephrin ligands. In Xenopus and zebrafish embryos, expression of truncated Sek1/EphA4, lacking kinase sequences, led to ectopic expression of r3/r5 markers in adjacent even-numbered rhombomeres (Xu et al., 1995). Ectopic activation of Sek1/EphA4 receptor by overexpression of full length ephrinB2 leads to abnormal scattering of neural crest cells originated from even-numbered rhombomeres (Smith et al., 1997).

To examine possible defects in hindbrain segmentation in the ephrinB2 mutant embryos, I performed wholemount in situ hybridization with cRNA probes of krox-20 and Sek1/EphA4, two established markers of odd-numbered rhombomere r3 and r5 (Becker et al., 1994). Figure 1 shows that the r3 and r5 restricted staining of krox-20 and Sek1 in the control embryos. EphrinB2 mutant embryos display identical segmental staining in r3 and

r5. For even-numbered rhombomeres, I took advantage of endogenous ephrinB2 expression in r2, r4, and r6. LacZ signals (Tau-LacZ driven by ephrinB2 endogenous promoter) were observed in the control hindbrain rhombomeres r1, r2, r4, and r6, but low or absent in r3 and r5 (Figure 2). Mutant hindbrain gave same types of segmental patterns of lacZ expression (Figure 2).

EphrinB1 has a strong expression in rhombomere r1 which is also termed metencephalon. Rostral to r1/metencephalon is a narrow neural tube region called isthmus. Isthmus is essentially located at the junction between the metencephalon and the mesencephalon. It was shown to be an organizer region with inducing activities for mes-met structures and associated markers such as Engrail-1 upon transplantation (For review, see Alvarado-Mallart, 1993; Le Douarin, 1993). We and others have shown that ephrinB1 could restricted the migration of neural crest cells of the trunk and the hindbrain (Krull et al., 1997; Smith et al., 1997; Wang et al., 1998). Targeted-deletion of ephrinB1 in r1 could potentially affect the development of isthmus just anterior to r1. The cells of isthmus could disperse abnormally to the posterior r1 or the anterior mesencephalon region. To examine the possibility of isthmus dispersion or enlargement, two isthmus specific markers FGF8 and Pax2 were studied. Wholemount in situs hybridization showed no alteration of the narrow band of signal for either FGF8 or Pax2 in the ephrinB2 mutant embryos, compared to that of the controls (Figure 3).

EphrinB2 has a caudal half-restricted expression in each of the newly developed somites. Our and others' previous studies have suggested ephrinB2 could inhibit crest cell migration and motor axon outgrowth in vitro (Krull et al., 1997; Wang and Anderson, 1997). An additional role of ephrinB2 in developing somites is its ability to set up or maintain the rostral-caudal polarity *within* the somite. To examine a possible defect of somite polarity, I first studied ephrinB2-lacZ expression in the control and the mutant embryos. EphrinB2-lacZ staining revealed no obvious alteration in its caudal somite half-restricted expression pattern in the mutants, compared to that of the controls (Figure 4A,

4B). Delta like-1 (Dll1) is another caudal somite half-restricted molecule, with stronger expression level compared with ephrinB2 (Hrabe de Angelis et al., 1997). Dll1 is essential for the formation of somite polarity in mouse. Dll1 mutant embryos have fused somite halves, subsequent fusion of the DRGs, and misplacement of outgrowing motor axons (Hrabe de Angelis et al., 1997). Dll-1 was examined in the ephrinB2 mutant somites. Though the level of expression was lower than that of the control embryos, Dll-1 signals were still restricted to the caudal somite halves in the ephrinB2 mutants (Figure 4C, 4D).

Even if the formation of somite polarity does not require ephrinB2, neural crest cell migration and motor axon outgrowth could still be affected in the mutants. EphrinB2 could be a necessary inhibitory component in the caudal somite halves. ErbB3 receptor tyrosine kinase is an excellent marker for migrating crest cells in the trunk as well as in the branchial arches (Meyer and Birchmeier, 1995; Wang and Anderson, 1997). Wholemount in situ hybridization of ErbB3 was performed on E9 to E10 embryos. The segmental staining of ErbB3 were not obviously different between the mutant somites and the controls in E9, E9.5 and E10 stages (Figure 5A, 5B). This result suggested that the segmental neural crest migration was largely normal.

I also examined the outgrowth of early motor axons and cranial axons by a monoclonal antibody against neuronal tubulin - TUJ1. In the control embryos, TUJ1 labeled early motor axons projecting ventral from the neural tube, and cranial ganglia axon bundles (Figure 5C, 5D). Additional TUJ1 signals were observed in the longitudinal fibers of the developing somites. In the mutant embryos, the cranial axonal signals were normal, compared to that of the controls. However, in the trunk region, there was a lack of motor axon projection in the mutants, despite strong signals in the somitic fibers. EphrinB2 mutant embryos were consistently smaller, and appeared younger, than their control litter mates due to vascularization defects (see next chapter). The maturation of neural tube and the differentiation of motor neurons may be delayed as a consequence of the malnutrition.

Therefore, at this point, I can not conclude whether the lack of motor axon projection is directly due to the absence of ephrinB2, or a delay in motor neuron differentiation.

Through my examination of varies gene and antibody markers, I have failed to detect obvious phenotypic alterations in different neuronal tissues in the ephrinB2 mutants. The reduced expression of Dll1 in the somites and the lack of motor axon projection may be secondary to a vascularization defect (See next chapter). Our results suggested that there are functionally redundant molecules replacing ephrinB2 in the neuronal tissues. In the hindbrain, ephrinB3, a sister transmembrane molecule of ephrinB2 is also expressed in even-numbered rhombomeres, though at lower level than that of ephrinB2 (Bergemann et al., 1998; Gale et al., 1996). In the developing somites, ephrinB2 is not the only inhibitory molecules for crest cell migration. Several other types of extracellular proteins located in the caudal somite halves such as collagen IX and T-cadherin, have been shown to exhibit inhibitory activities toward crest cell attachment and migration in vitro (Fredette et al., 1996; Ring et al., 1996).

Similar lack-of-phenotype results have been found in mutants lacking Eck and tenascin (Chen et al., 1996; Saga et al., 1992). Eck is an EphA type receptor tyrosine kinase expressed in specific patterns in hindbrain rhombomeres and neural tube (Ruiz and Robertson, 1994). Insertional mutagenesis and targeted mutation of Eck did not create any discernable phenotype in the homozygous embryos or mice (Chen et al., 1996). The normality of the Eck deficient mice suggests that other members of the Eph family can functionally compensate for the loss of Eck. Tenascin is an extracellular matrix protein expressed in numerous restricted patterns during embryogenesis (Saga et al., 1992). The results from tenascin knockout mice suggested that tenascin is not essential for development.

Gene knockout experiments of Eck and tenascin suggest that there are functional equivalent molecules of the same gene family or completely unrelated family, and these redundant genes were not selected against during evolution. Though disappointing, I still

think mutational experiments on closely related or large-family molecules are very informative. Compound mutants can be used to further address their roles in various developmental compartments in which they display dynamic expression patterns.

Figure 1. Hindbrain segmentation in EphrinB2 mutant embryos.

Odd numbered rhombomeres r3 and r5 in E9.5 embryos were revealed by krox-20 (**A** and **B**) and Sek1 probes (**C** and **D**). Heterozygous (**A** and **C**) and homozygous (**B** and **D**) ephrinB2 embryos were compared. Krox-20 signal is stronger in r5 than r3 at this stage (E9.5). Sek1 also shows somitic expression in the newly formed somite (**B** and **D**, asterisk).

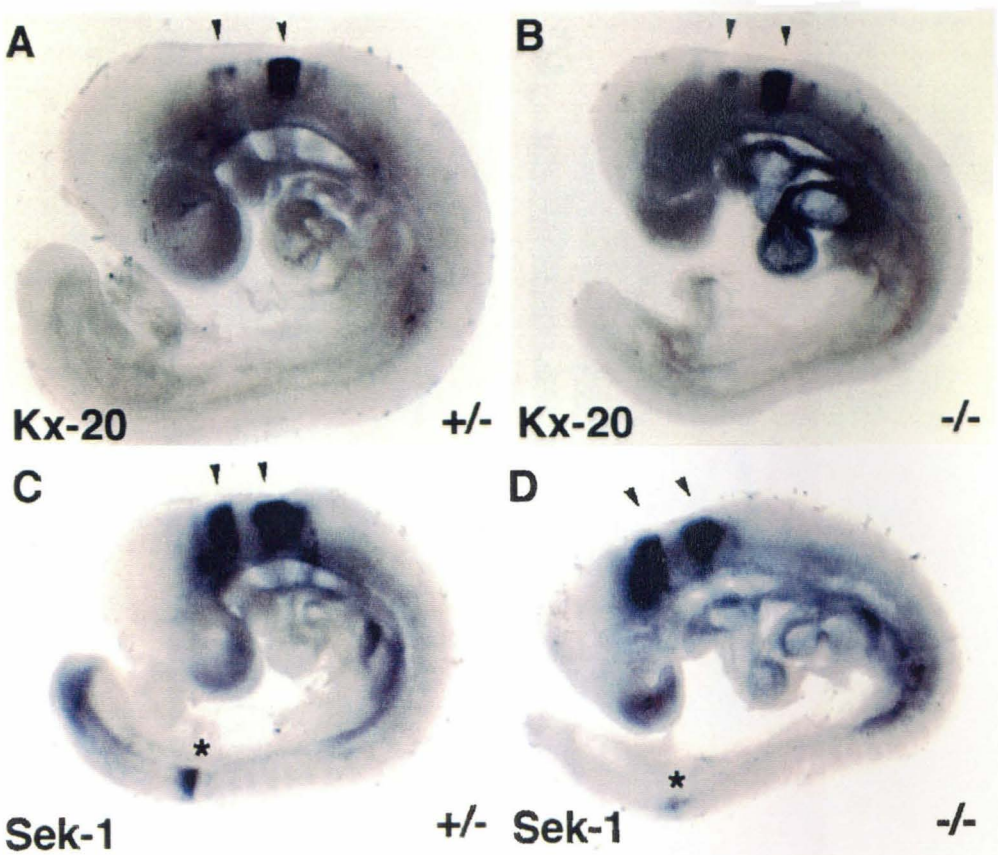

Figure 2. EphrinB-lacZ expression in hindbrain segments.

E9.5 stage embryos was processed for lacZ staining before sectioned to reveal hindbrain segments. EphrinB2-lacZ signals are in rhombomere r1, r2, r4 and r6, but low in r3 and absent in r5. EphrnB2 mutant hindbrain displays identical pattern of staining. Anterior half of otical vesicle and hindbrain crest streams originated from r2 and r4 also show strong expression in both heterozygous and homozygous embryos.

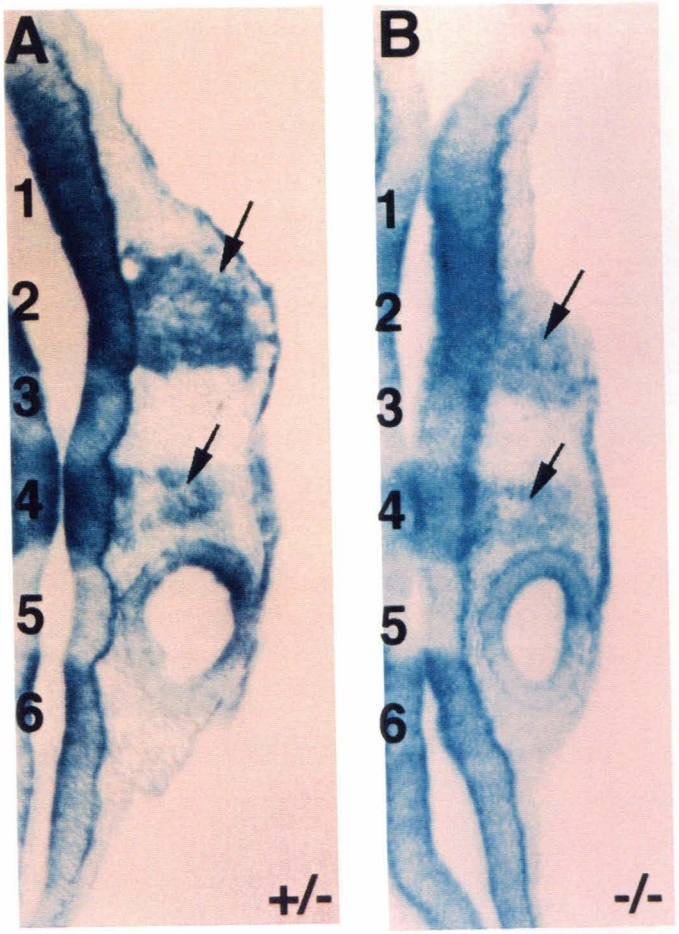

Figure 3. FGF8 and Pax2 expression in isthmus of ephrinB2 mutants.

E9.5 stage embryos were stained with isthmus marker FGF8 (**A** and **B**) and Pax2 (**C** and **D**) in heterozygous and homozygous embryos. Arrowheads point to the isthmus region. Addition expression of FGF8 in the limb bud (**A** and **B**, asterisk), and Pax2 in mesenephoros (**C** and **D**, asterisk) were labeled. Identical expression patterns of FGF8 and Pax2 were observed in heterozygous and homozygous mutants.

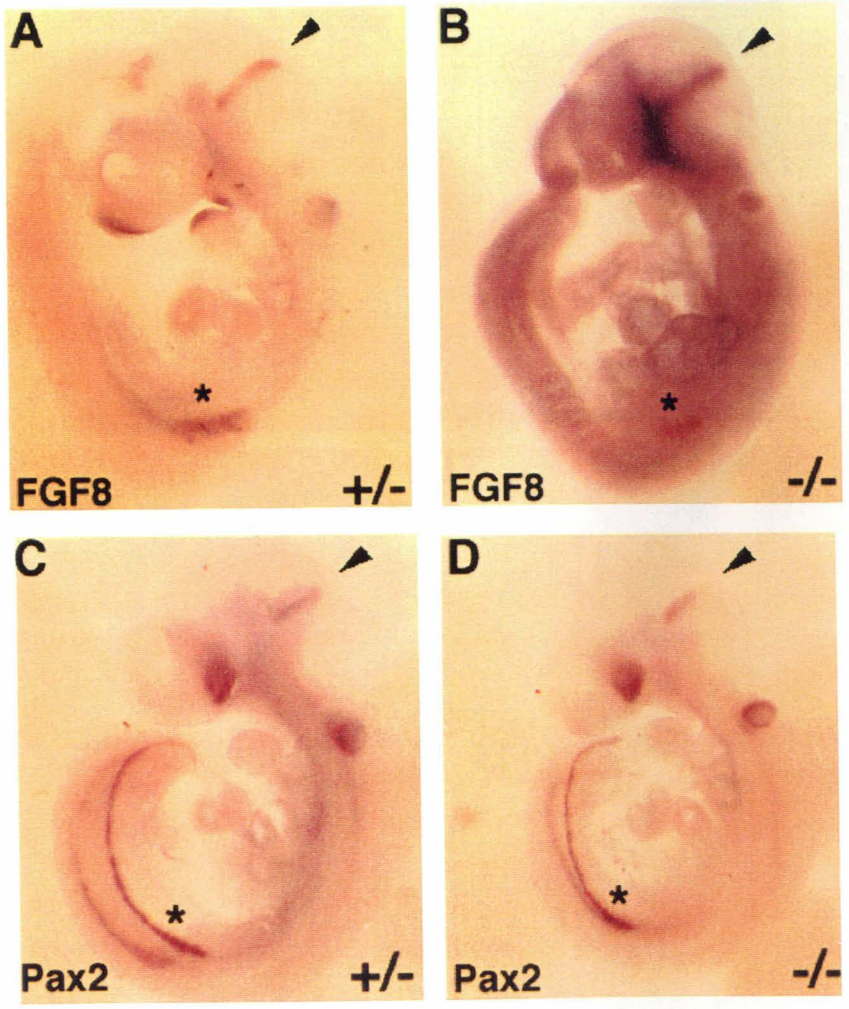

Figure 4. Somite polarity in ephrinB2 mutants.

E9.5 embryo trunks were analyzed for ephrinB2-lacZ (**A** and **B**) and delta like -1 (Dll1) (**C** and **D**) expression in caudal somite halves. One typical somite unit was bracketed, with rostral (r) and caudal (c) halves labeled. Caudal half restricted expression of ephrinB2-lacZ and Dll1 was preserved in the homozygous mutants (**B** and **D**).

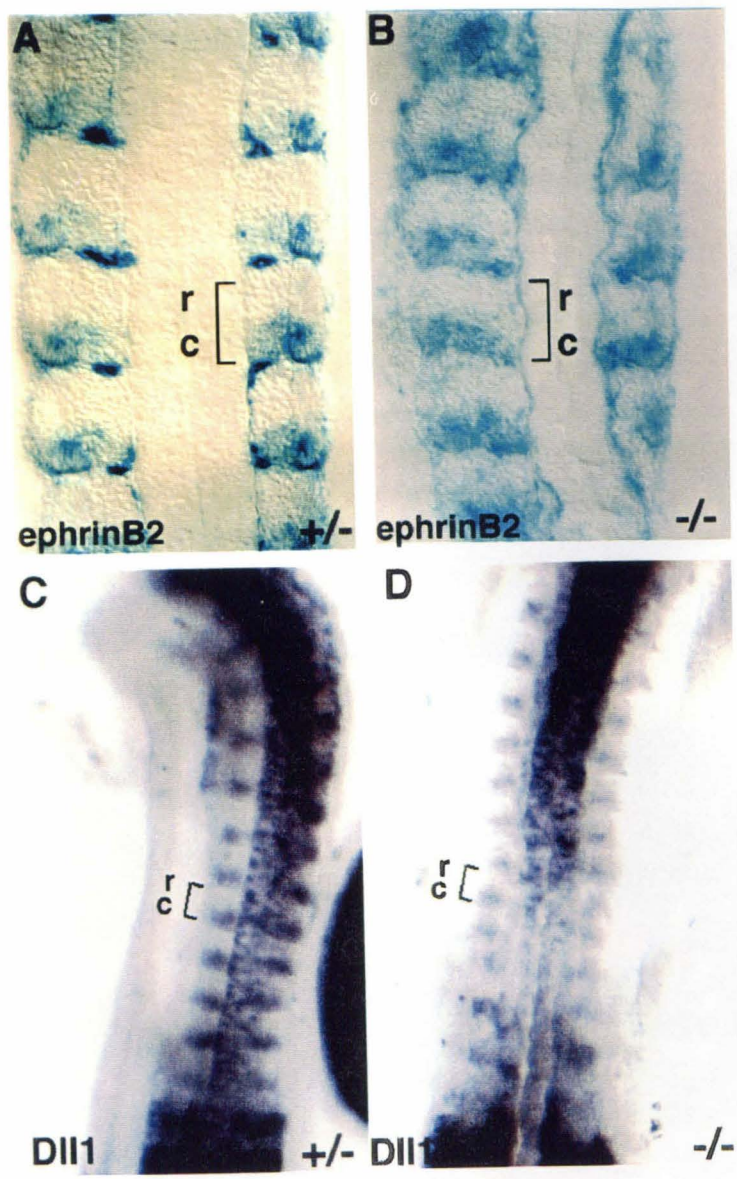

Figure 5. Neural crest migration, early cranial axons, and trunk axons in ephrinB2 mutants. Crest marker ErbB3 is expressed in migratory crest cells in heterozygous (**A**) as well as homozygous mutant (**B**) embryos. Identical crest segmentation was observed. TUJ1 antibody against neural tubulin was used to visualize all early axons in the embryo (**B** and **D**). Cranial bundles (arrows) were normal in the ephrinB2 homozygous mutants. In the trunk region, somite fibers show transient but strong signal for TUJ1 at E9.5 stage (asterisks). Homozygous mutants show less motor axon projection in the trunk compared with heterozygous littermates. However, this may due to a delayed embryonic development from vascularization defects (see next chapter).

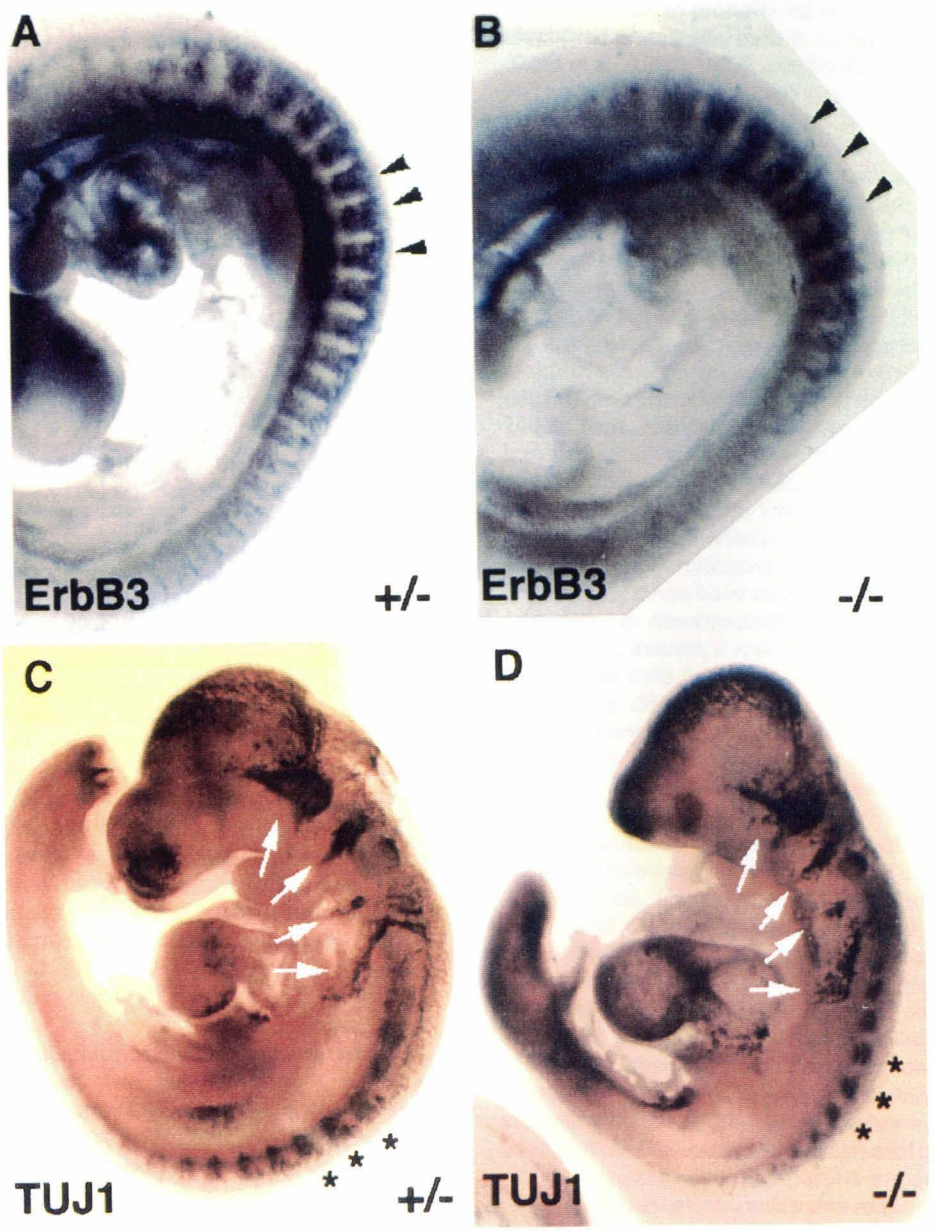

Cell, Vol. 93, 741–753, May 29, 1998, Copyright ©1998 by Cell Press

Molecular Distinction and Angiogenic Interaction between Embryonic Arteries and Veins Revealed by ephrin-B2 and Its Receptor Eph-B4

Hai U. Wang,† Zhou-Feng Chen,* and David J. Anderson*‡
*Howard Hughes Medical Institute
†Division of Biology
California Institute of Technology
Pasadena, California 91125

Summary

The vertebrate circulatory system is composed of arteries and veins. The functional and pathological differences between these vessels have been assumed to reflect physiological differences such as oxygenation and blood pressure. Here we show that ephrin-B2, an Eph family transmembrane ligand, marks arterial but not venous endothelial cells from the onset of angiogenesis. Conversely, Eph-B4, a receptor for ephrin-B2, marks veins but not arteries. *ephrin-B2* knockout mice display defects in angiogenesis by both arteries and veins in the capillary networks of the head and yolk sac as well as in myocardial trabeculation. These results provide evidence that differences between arteries and veins are in part genetically determined and suggest that reciprocal signaling between these two types of vessels is crucial for morphogenesis of the capillary beds.

Introduction

Arteries and veins are defined by the direction of blood flow and by anatomical and functional differences. Despite recent intensive study of blood vessel formation (reviewed in Folkman and D'Amore, 1996; Hanahan, 1997; Risau, 1997), surprisingly little attention has been paid to the question of when and how arteries and veins acquire their distinct properties. Indeed, these differences have been widely assumed to reflect primarily physiological influences such as oxygenation, blood pressure, and shear forces.

Blood vessels are comprised of two cellular layers: an inner layer of endothelial cells, which lines the lumen, and an outer layer of smooth muscle cells. The first tubular structures are formed by the endothelial cells, which subsequently recruit pericytes and smooth muscle cells to ensheath them (Risau and Flamme, 1995). The de novo formation of blood vessels from a dispersed population of mesodermally derived endothelial cell precursors, called angioblasts, is termed vasculogenesis (Sabin, 1917). Vasculogenesis occurs in several independent locations, including the embryo proper, and in extraembryonic membranes such as the yolk sac. In the yolk sac, angioblasts first assemble into a reticulum of primitive tubules called the primary capillary plexus (Risau, 1997). This network of thin tubules then undergoes a succession of morphogenetic events involving sprouting, splitting, and remodeling, collectively called angiogenesis (Risau, 1997), to generate larger, branched vessels. Thus, formation of the yolk sac vasculature occurs by generation of larger from smaller vessels (Evans, 1909). This process is coupled to the interconnection of the embryonic and extraembryonic circulatory systems (Carlson, 1981).

Recent studies have identified a number of receptor tyrosine kinases expressed on endothelial cells and their cognate ligands, which mediate the vasculogenic and angiogenic development of blood vessels (reviewed in Folkman and D'Amore, 1996; Hanahan, 1997). FGF-2 is an endothelial cell mitogen (Folkman and Klagsbrun, 1987) and is able in collaboration with vascular endothelial growth factors (VEGFs) (reviewed in Risau and Flamme, 1995) to promote de novo tubule formation by dispersed endothelial cells in collagen matrices in vitro (Goto et al., 1993). VEGF and its receptors, Flk-1 (VEGF-R2) and Flt-1 (VEGF-R1), are essential for both vasculogenesis and angiogenesis in vivo (Fong et al., 1995; Shalaby et al., 1995). Angiopoietin-1 (Ang-1) and its receptor, TIE2/TEK, are essential for angiogenesis (but not vasculogenesis) and proper heart development (Dumont et al., 1994; Sato et al., 1995; Suri et al., 1996). These ligands are provided to endothelial cells by neighboring mesenchymal cells. Conversely, ligands expressed on cardiac endothelial (endocardial) cells, such as neuregulin, are also essential for heart formation and activate receptors present on neighboring mesenchymal (myocardial) cells (Lee et al., 1995; Meyer and Birchmeier, 1995). Thus, the process of angiogenesis appears to involve bidirectional signaling between endothelial cells and the support cells that eventually will ensheath them (Folkman and D'Amore, 1996).

Although mature arteries and veins have obvious distinctions in their functional properties and disease susceptibilities, it has been assumed that these differences arise later in development as a reflection of vascular physiology. Indeed, it has not even been clear that the endothelial cells lining these two types of vessels are necessarily different. This is reflected in the fact that current models of angiogenesis treat the developing endothelial network as an homogeneous population (Folkman and D'Amore, 1996; Hanahan, 1997; Risau, 1997).

We now show that arterial and venous endothelial cells are molecularly distinct from the earliest stages of angiogenesis. This distinction is revealed by expression on arterial cells of a transmembrane ligand, called ephrin-B2 (Bennett et al., 1995; Bergemann et al., 1995), whose cognate receptor Eph-B4 (Andres et al., 1994) is expressed on venous cells. Targeted disruption of the *ephrin-B2* gene prevents the remodeling of veins from a capillary plexus into properly branched structures. Moreover, it also disrupts the remodeling of arteries, suggesting that reciprocal interactions between prespecified arterial and venous endothelial cells are necessary for angiogenesis. Our results suggest that differences between arteries and veins are in part genetically determined and have important implications for thinking about both the mechanisms of angiogenesis and the

‡To whom correspondence should be addressed.

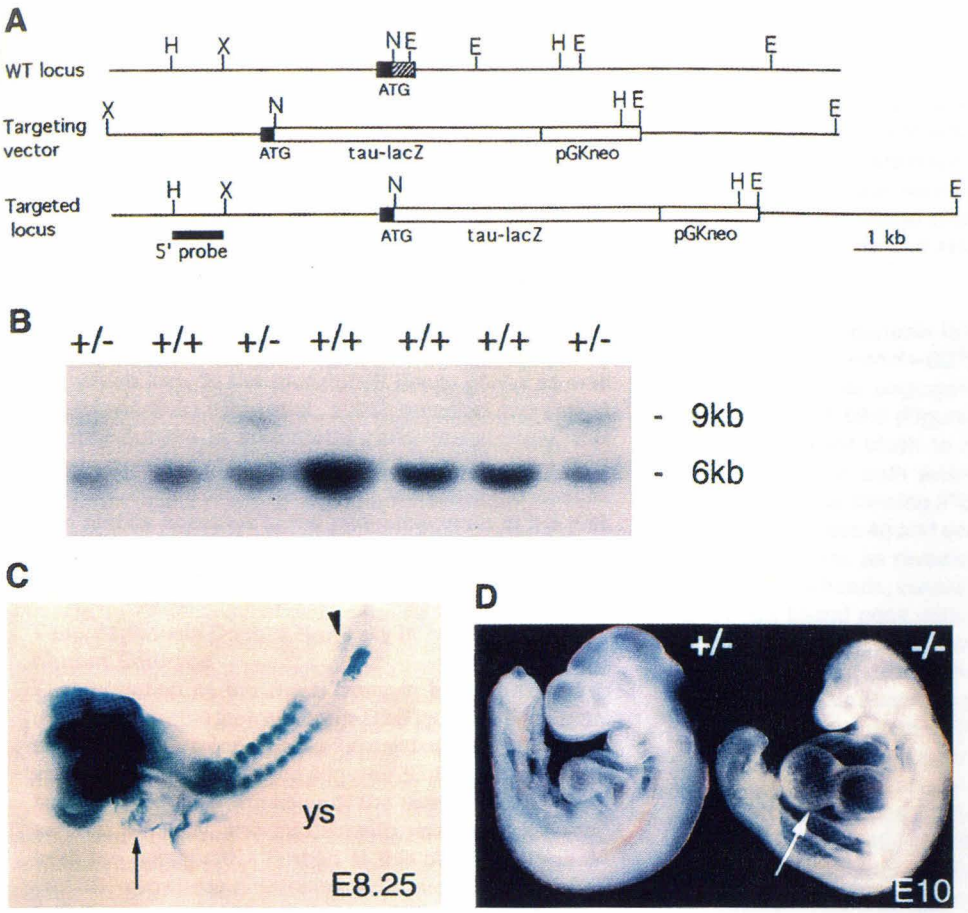

Figure 1. Targeted Disruption of the *ephrin-B2* Gene

(A) Exon-1 structure. Filled box represents 5′ untranslated region. Hatched box starts at the ATG and includes the signal sequence.

(B) Tail DNA of adult mice was subjected to Southern blot analysis with a 1 kb HindIII–XbaI probe. No −/− samples are seen because of the embryonic lethality of the mutation.

(C) LacZ staining of a 7 somite embryo shows early endothelial signals in heart (arrow) and dorsal aorta (arrowhead) but not in yolk sac (ys).

(D) Growth retardation and enlargment of the heart (arrow) are seen in an E10 mutant embryo. All embryos died by E11.

cellular targets of potential therapeutic agents that promote or inhibit this process.

Results

Targeted Mutagenesis of *ephrin-B2* in Mice

Targeted disruption of the *ephrin-B2* gene was achieved by homologous recombination in embryonic stem cells. The targeting strategy involved deleting the signal sequence and fusing a *tau-lacZ* indicator gene in frame with the initiation codon (Figures 1A and 1B). The expression pattern of β-galactosidase in heterozygous (*ephrin-B2*^{tlacZ}/+) embryos was indistinguishable from that previously reported for the endogenous gene (Bennett et al., 1995; Bergemann et al., 1995; Wang and Anderson, 1997) (Figure 1C). While prominent expression was detected in the hindbrain and somites, lower levels were observed in the aorta and heart as early as E8.25 (Figure 1C, arrow). Expression in the yolk sac was first detected at E8.5 (Figure 4B). Heterozygous animals appeared phenotypically normal. In homozygous embryos, growth retardation was evident at E10 (Figure 1D) and lethality occurred with 100% penetrance around E11. No expression of endogenous ephrin-B2 mRNA was detected by in situ hybridization, indicating that the mutation is a null (not shown). Somite polarity, hindbrain segmentation, and the metameric patterning of neural crest migration (in which ephrin-B2 and related ligands have previously been implicated [Xu et al., 1995; Krull et al., 1997; Smith et al., 1997; Wang and Anderson, 1997]) appeared grossly normal in homozygous mutant embryos (data not shown).

Reciprocal Expression Pattern of ephrin-B2 and Eph-B4 in Arteries and Veins

The enlarged heart observed in dying mutant embryos (Figure 1D, arrow) prompted us to examine the expression of *ephrin-B2*^{tlacZ} in the vascular system in detail (see model diagrams, Figures 2A and 2L). Surprisingly, expression was consistently observed in arteries but not veins. In the E9.5 yolk sac, for example, the posterior vessels connected to the vitelline artery, but not the vitelline vein, expressed the gene (Figure 2B). In the trunk, labeling was detected in the dorsal aorta (Figures 2D and 2E, da), vitelline artery (Figure 2D, va), umbilical artery, and its allantoic vascular plexus (Figure 2F, ua,

avp) but not in the umbilical, anterior, and common cardinal veins (Figure 2D, uv; Figure 2E, acv, ccv). In the head, labeling was seen in branches of the internal carotid artery (Figure 2L, ica; Figures 2M–2O, arrows) but not in those of the anterior cardinal vein (Figure 2L, acv; Figures 2N and 2O, arrowheads). In situ hybridization with ephrin-B2 cRNA probes confirmed that the selective expression of *tau-lacZ* in arteries correctly reflected the pattern of expression of the endogenous gene (Figures 2H and 2J, arrows). Expression of ephrin-B1 and -B3 was undetectable in endothelial cells of the trunk and yolk sac at these stages (data not shown).

Examination of the expression of receptors for ephrin-B2, which include the four *Eph-B* family genes as well as Eph-A4/Sek1 (Gale et al., 1996), revealed expression of only Eph-B4 in endothelial cells. Surprisingly, this expression was observed in veins but not arteries (Figures 2G, 2I, and 2K, arrowheads), including the vitelline vein and its branches in the anterior portion of the yolk sac (Figure 2C, vv, arrowheads), as early as E9.0.

Vasculogenesis Occurs Normally in ephrin-B2 Mutant Embryos

The formation of the major vessels in the trunk was unaffected by the lack of ephrin-B2 (Figure 3). The dorsal aorta, vitelline artery, posterior cardinal, and umbilical veins, for example, formed (Figures 3B and 3D), although some dilation and wrinkling of the vessel wall was observed. Similarly, the intersomitic vessels originating from the dorsal aorta formed at this stage (Figures 3A and 3B, arrowheads). Between E8.5 and E9.0, the primitive endocardium appeared only mildly perturbed in mutants (Figure 3B, arrow), while a pronounced disorganization was apparent at E10 (Figure 6F). Red blood cells developed and circulated normally up to E9.5 in both the mutant yolk sac and embryo proper (data not shown).

Extensive Intercalation of Yolk Sac Arteries and Veins Revealed by ephrin-B2 Expression

In the yolk sac, the vitelline artery and its capillary network occupy the posterior region, and the vitelline vein and its capillaries, the anterior region (Figure 2A). At E8.5, a stage at which the primary capillary plexus has formed but remodeling has not yet occurred (Figure 4A), asymmetric expression of *ephrin-B2-tau-lacZ* in heterozygous embryos was evident at the interface between the anterior and posterior regions (Figure 4B). Apparently homotypic remodeling of β-galactosidase$^+$ arterial capillaries into larger, branched trunks clearly segregated from venous vessels was evident between E9.0 and E9.5 (Figures 4D, 4F, and 4H). At this stage, expression of the receptor Eph-B4 was clearly visible on the vitelline veins but not arteries (Figure 2C, arrowheads). Thus, arterial and venous endothelial capillaries are already molecularly distinct following vasculogenesis and prior to angiogenesis.

Strikingly, while textbook diagrams (Carlson, 1981) of the yolk sac capillary plexus depict a nonoverlapping boundary between the arterial and venous capillary beds (Figure 2A), expression of *ephrin-B2-tau-lacZ* allowed detection of a previously unrecognized extensive intercalation between arteries and veins across the entire anterior–posterior extent of the yolk sac (Figures 4F, 4H, 4L, 4N, and 9A). Double labeling for platelet endothelial cell adhesion molecule (PECAM) and β-galactosidase revealed that the interface between the arteries and veins occurs between microvessel extensions (Figure 4H, arrowheads) that bridge larger vessels interdigitating en passant (Figures 4L and 4N, arrowheads; Figure 9B).

Disrupted Angiogenesis in the Yolk Sac of *ephrin-B2^{tlacZ}/ephrin-B2^{tlacZ}* Embryos

Defects in yolk sac angiogenesis were apparent by E9.0 and obvious at E9.5 (Figures 4E, 4G, 4I, and 5). There was an apparent block to remodeling at the capillary plexus stage for both arterial vessels as revealed by β-galactosidase staining (Figures 4D versus 4E, 4F versus 4G, 4H versus 4I) and venous vessels in the anterior region of the sac as revealed by PECAM staining (Figures 4J, arrowheads, versus 4K). Thus, disruption of the *ephrin-B2* ligand gene caused both a nonautonomous defect in Eph-B4 receptor-expressing venous cells and an autonomous defect in the arteries themselves.

This defect was accompanied by a failure of intercalating bidirectional growth of arteries and veins (Figure 4L) across the antero–posterior extent of the yolk sac, so that an interface between *ephrin-B2*-expressing and -nonexpressing zones at the midpoint of the sac was apparent (Figures 4G, 4I, 4M, and 4O). (However, small patches of *lacZ* expression were occasionally visible within the anterior venous plexus [Figures 4M and 4O], suggesting that some arterial endothelial cells may have become incorporated into venous capillaries.) These observations imply a close relationship between the remodeling of the capillary plexus into larger vessels and the intercalating growth of these vessels (see Figure 9B). The large β-galactosidase$^+$ vitelline arteries (Figure 4G, arrow) as well as vitelline veins (Figure 4K, arrowhead) present at the point of entry to the yolk sac of the embryo-derived vasculature (Figure 2A) appeared unperturbed in the mutant, however. This is consistent with the observation that the mutation does not affect formation of the primary trunk vasculature (Figures 3B and 3D). It also argues that the yolk sac phenotype is due to a disruption of intrinsic angiogenesis and is not secondary to a failure of ingrowth of embryo-derived vessels.

Histological staining of sectioned yolk sacs revealed an accumulation of elongated support cells in close association with the endothelial vessels at E10 and E10.5 (Figures 5B and 5C, arrows). In the mutant yolk sacs, these support cells appeared more rounded (Figures 5E and 5F, arrows), suggesting a defect in their differentiation. Moreover, in contrast to heterozygous yolk sacs, where vessels of different diameters began to appear at E9.5 and vessel diameter increased through E10.5 (Figures 5A–5C), capillary diameter appeared relatively uniform and did not increase with age in the mutants (Figures 5D–5F). The mutant capillaries also failed to delaminate from the basal endodermal layer (Figures 5B versus 5E, 5C versus 5F).

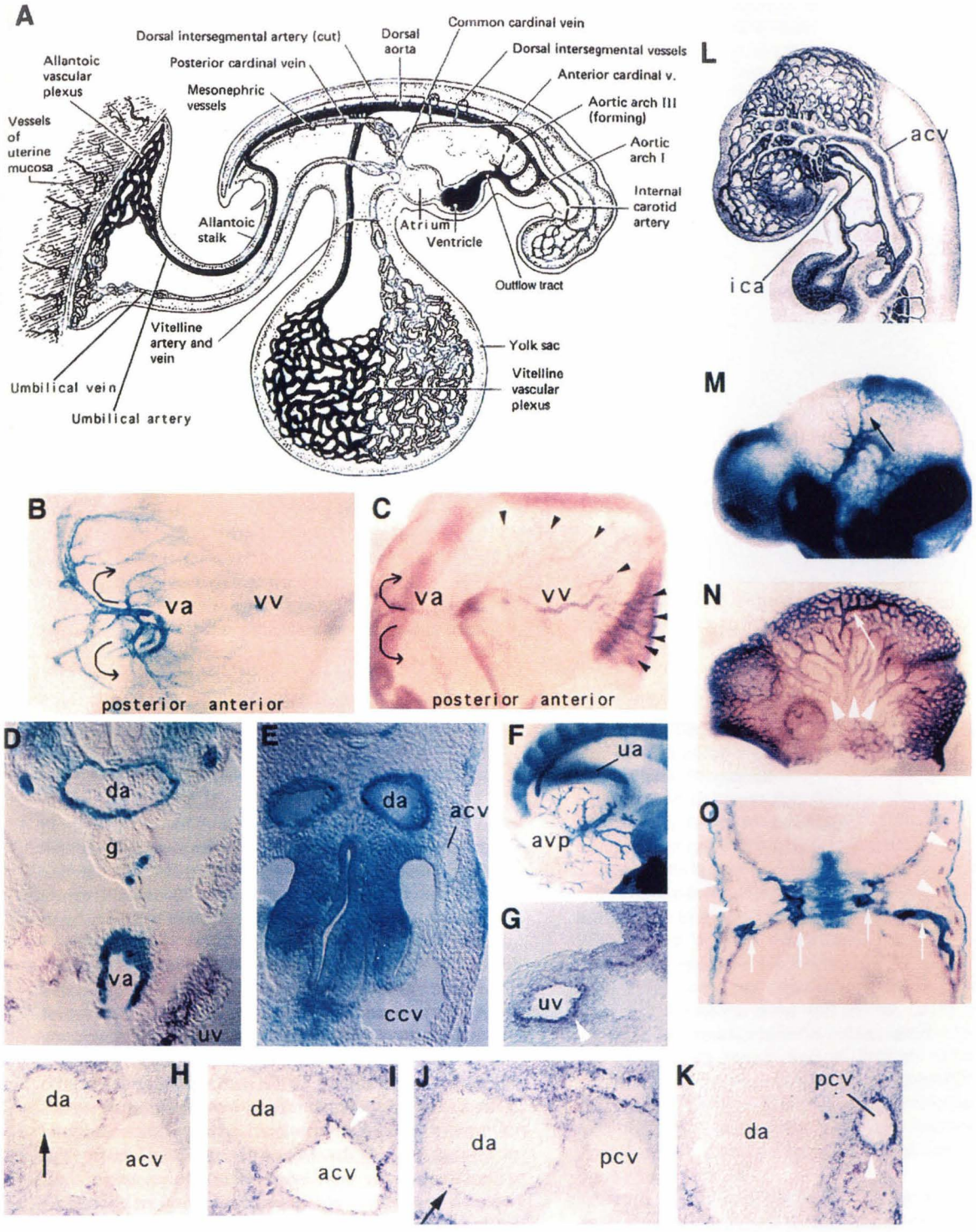

Figure 2. Complementary Expression of ephrin-B2 and Its Receptor Eph-B4 in Embryonic Arteries and Veins

(A) A textbook digram of the circulatory system in a young pig embryo (reproduced from Carlson, 1981).

(B and C) Dorsal whole-mount view of E9.5 (25–30 somites) yolk sac showing expression of ephrin-B2 (detected by lacZ staining) in the vitelline artery (va) (B), or (C) of Eph-B4 (detected by in situ hybridization) in the vitelline vein (vv).

(D) Double staining of lacZ and PECAM-1 in a caudal trunk section. Note expression of ephrin-B2 in the dorsal aorta (da) and vitelline artery (va) but not in the umbilical vein (uv), which is PECAM labeled.

(E) LacZ staining in a rostral trunk section. ephrin-B2 is not expressed in the anterior cardinal vein (acv) or common cardinal vein (ccv).

(F) LacZ staining identifies ephrin-B2-expressing cells in the umbilical artery (ua) and allantoic vascular plexus (avp).

(G–K) In situ hybridization to adjacent sections in the rostral (H and I) or caudal (G, J, and K) trunk region. Expression of ephrin-B2 (H and J) or Eph-B4 (G, I, and K) is detected in the dorsal aorta ([H] and [J], da) or umbilical, anterior, and posterior cardinal veins ([G], [I], and [K],

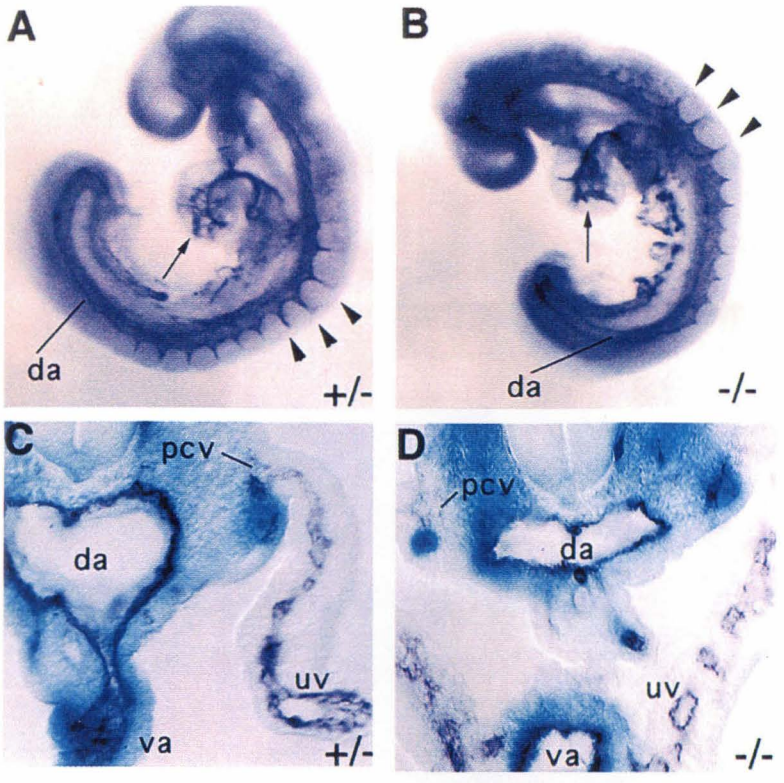

Figure 3. Normal Vasculogenesis in *ephrin-B2* Mutants

(A and B) PECAM-1 staining of 9 somite embryos. Arrows indicate endocardium, and arrowheads, the intersomitic vessels. da, dorsal aorta.

(C and D) LacZ and PECAM-1 double staining of caudal trunk sections of E9.5 embryos. Note the expression of *ephrin-B2-tau-lacZ* in the dorsal aorta (da) and vitelline artery (va), but not the umbilical and posterior cardinal veins (uv and pcv, respectively).

Absence of Internal Carotid Arterial Branches and Defective Angiogenesis of Venous Capillaries in the Head of Mutant Embryos

Similar to the yolk sac phenotype, the capillary bed of the head appeared dilated in the mutant (Figures 6N versus 6M) and apparently arrested at the primary plexus stage (Figures 6F versus 6B). Staining for β-galactosidase revealed that the anterior-most branches of the internal carotid artery failed to develop in the mutant (Figures 6C versus 6D, 6G versus 6H, 6I versus 6J, 6K versus 6L, arrows). Unlike the case in the yolk sac, therefore, the malformed capillary beds must be entirely of venous origin. However, the anterior branches of the anterior cardinal vein formed, although they were slightly dilated (Figure 6E versus 6F, 6K versus 6L, arrowheads). Taken together, these data indicate that, in the head, venous angiogenesis is blocked if the normal interaction with arterial capillaries is prevented. The angiogenic defects observed in the head and yolk sac are unlikely to be secondary consequences of heart defects (see below), since they are observed starting at E9.0, and the embryonic blood circulation appears normal until E9.5.

ephrin-B2-Dependent Signaling between Endocardial Cells Is Required for Myocardial Trabeculae Formation

Examination of ligand and receptor expression in wild-type hearts revealed expression in the atrium of both ephrin-B2 (Figure 7B) and Eph-B4 (Figure 7A). Expression of both ligand and receptor was also detected in the ventricle in the endocardial cells lining the trabecular extensions of the myocardium (Figures 7C, arrows, and 7E). Double labeling experiments suggested that the ligand and receptor are expressed by distinct but partially overlapping cell populations, although the resolution of the method does not permit us to distinguish whether this overlap reflects coexpression by the same cells or a close association of different cells (data not shown). In any case, expression of ephrin-B2 and Eph-B4 does not define complementary ventricular and atrial compartments of the heart, although expression of the ligand appears much higher in the atrium than in the ventricle (Figure 7B).

Heart defects commenced at E9.5 and were apparent in mutant embryos at E10 both morphologically (Figure 1D) and by whole-mount PECAM staining (Figures 7E

uv, acv, and pcv, respectively).

(L) A classical diagram showing the arteries (internal, darker) and veins (superficial, lighter) in the 25 somite stage chick head (reproduced from Evans, 1909); acv, anterior cardinal vein; ica, internal carotid artery.

(M and N) Vessels of the E9.5 mouse head. Darker-colored branches of the internal carotid artery can be singled out in PECAM-1 stained vessels ([N], arrow), which is the only vessel labeled by lacZ staining ([M], arrow).

(O) A cross section of a lacZ- and PECAM-1-double-stained head. Arrows indicate branches of the internal carotid artery, arrowheads indicate branches of the anterior cardinal vein.

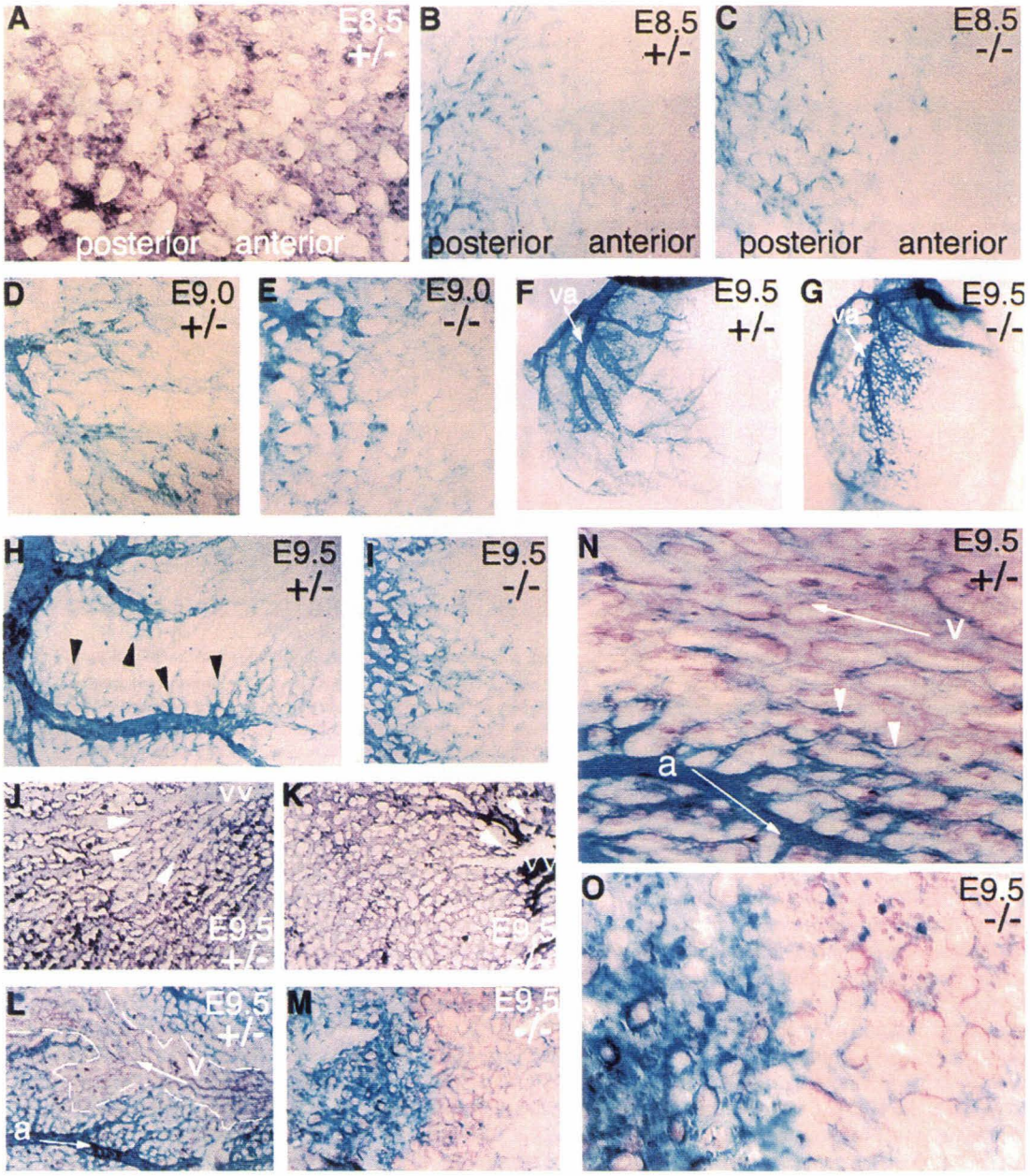

Figure 4. The *ephrin-B2* Mutation Blocks Angiogenesis in the Yolk Sac

(A–C) PECAM-1 (A) and lacZ (B and C) stained E8.5 yolk sacs. The sacs are oriented with the posterior (arterial) and anterior (venous) regions to the left and right, respectively (see also Figure 2A).

(D and E) LacZ-stained E9.0 yolk sacs.

(F and G) LacZ- stained E9.5 yolk sacs. Arrows indicate vitelline arteries (va).

(H and I) Higher magnifications of yolk sacs shown in (F) and (G). Arrowheads in (H) indicate arterial capillaries.

(J and K) PECAM-1 reveals vessels draining back to the vitelline vein (vv). Arrowheads show the conjugation of the veins. Note that the arterial and venous networks in the mutant appear arrested at the capillary plexus stage (cf., [I], [K], and [A]).

(L and M) LacZ and PECAM-1 double labeling reveals the boundaries between arterial (blue) and venous (brown) capillaries. Note the bidirectional (arrows) intercalation of the arteries (a) and veins (v) in the heterozygote (L), which is lacking in the mutant (M).

(N and O) Higher magnifications of the boundaries shown in (L) and (M). Arrowheads in (N) indicate the endings of arterial capillaries.

and 7F, arrows). Sections revealed an absence of myocardial trabecular extensions, although strands of ephrin-B2-expressing endocardial cells were still visible (Figure 7G). Thus, mutation of the ligand-encoding gene caused a nonautonomous defect in myocardial cells similar to the effect of a mutation in the *neuregulin-1* gene (Meyer and Birchmeier, 1995). Paradoxically, however, in this case the Eph-B4 receptor is expressed not on myocardial cells, as is the case for the neuregulin-1 receptors erbB2 and erbB4 (Gassmann et al., 1995; Lee et al., 1995), but rather on endocardial cells. We failed to detect expression of any of the other receptors for ephrin B

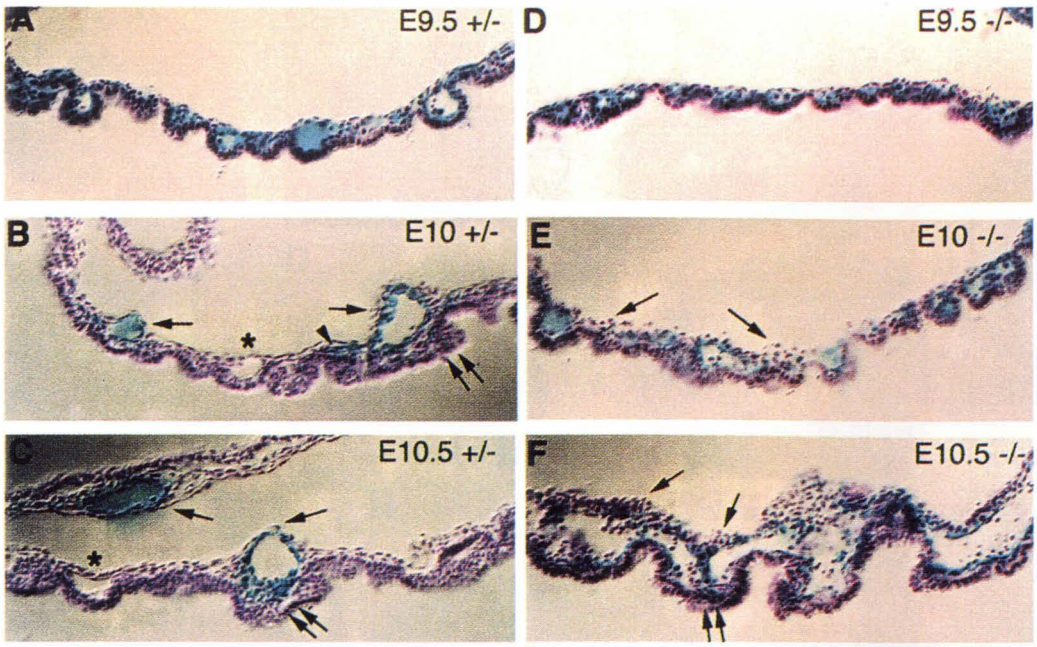

Figure 5. Defective Interactions between Endothelial and Supporting Cells in the Mutant Yolk Sacs

LacZ-stained heterozygous (A–C) and homozygous mutant (D–F) yolk sacs were sectioned and mesenchymal cells surrounding the blood vessels revealed by hematoxylin staining. Single arrows (B–F) indicate elongating mesenchymal cells or pericytes surrounding the endothelial cells at E10 (B and E) and E10.5 (C and F). Note the more rounded morphology of these cells in the mutant ([E] and [F], single arrows). Asterisks (B and C) indicate lacZ-negative veins. Note also the failure of vessels to delaminate from the underlying endoderm (double arrows) in the mutant (cf., [C] versus [F]). Arrowhead in (B) indicates ephrin-B2$^+$ endothelial cells that may be migrating into an arterial vessel. At E10.5 (F), arteries appear dilated, as if fusion of vessels occurred without encapsulation by support cells (C).

family ligands (Eph-B1, -B2, -B3, and -A4) in this tissue (data not shown). This suggests that in the heart, ligand-receptor interactions among endothelial cells may in turn affect interactions with myocardial cells.

ephrin-B2 Is Required for Vascularization of the Neural Tube

In *ephrin-B2^{tlacZ}/ephrin-B2^{tlacZ}* embryos, capillary ingrowth into the neural tube failed to occur (Figures 8A versus 8B). Instead, ephrin-B2-expressing endothelial cells remained associated with the exterior surface of the developing spinal cord (Figure 8B, arrow). Comparison of β-galactosidase to pan-endothelial PECAM and Eph-B4 expression (data not shown) provided no evidence of a separate, venous capillary network expressing Eph-B4 in the CNS at this early stage (E9–E10). Rather, expression of a different ephrin-B2 receptor, Eph-B2, was seen in the neural tube (Figure 8C), as previously reported (Henkemeyer et al., 1994), where no gross morphological or patterning defects were detectable (data not shown). In this case, therefore, the mutation does not appear to cause a nonautonomous phenotype in receptor-expressing cells, rather, only an autonomous effect on ligand-expressing cells.

Discussion

The study of blood vessel formation was primarily an anatomical and descriptive subject since the beginning of this century (Evans, 1909). Only in the last few years have the molecular mechanisms underlying this process begun to emerge (Risau and Flamme, 1995; Folkman and D'Amore, 1996; Risau, 1997). While explosive progress has been made in identifying growth factors and receptors that control vasculogenesis and angiogenesis (Hanahan, 1997), none of these advances have illuminated the problem of vessel identity. Indeed, in the absence of markers to distinguish vessel types, both classical (Evans, 1909; Carlson, 1981) and modern (Folkman and D'Amore, 1996; Risau, 1997) views of blood vessel formation have treated developing capillary networks as a uniform structure. The expression pattern of ephrin-B2 and its receptor Eph-B4 establishes a new concept in angiogenesis: arterial and venous endothelial cells have distinct identities from the earliest stages of blood vessel formation. The essential role of ephrin-B2 in angiogenesis, moreover, suggests that reciprocal interactions between arteries and veins are intrinsic to the vessel remodeling process.

Vessel Identity Is Established at the Earliest Stages of Angiogenesis

The extent to which an artery-specific molecular marker changes our view of the basic ontogenetic anatomy of the embryonic vasculature is illustrated by the case of the yolk sac. Textbook diagrams (Carlson, 1981; Gilbert, 1997) of the yolk sac capillary bed indicate a nonoverlapping apposition of arterial and venous capillaries at the midline of the structure (Figure 2A). Strikingly, however, lacZ staining of *ephrin-B2^{tlacZ}/+* embryos revealed that this inferred structure is completely wrong. By distinguishing small arteries from veins, we were able to

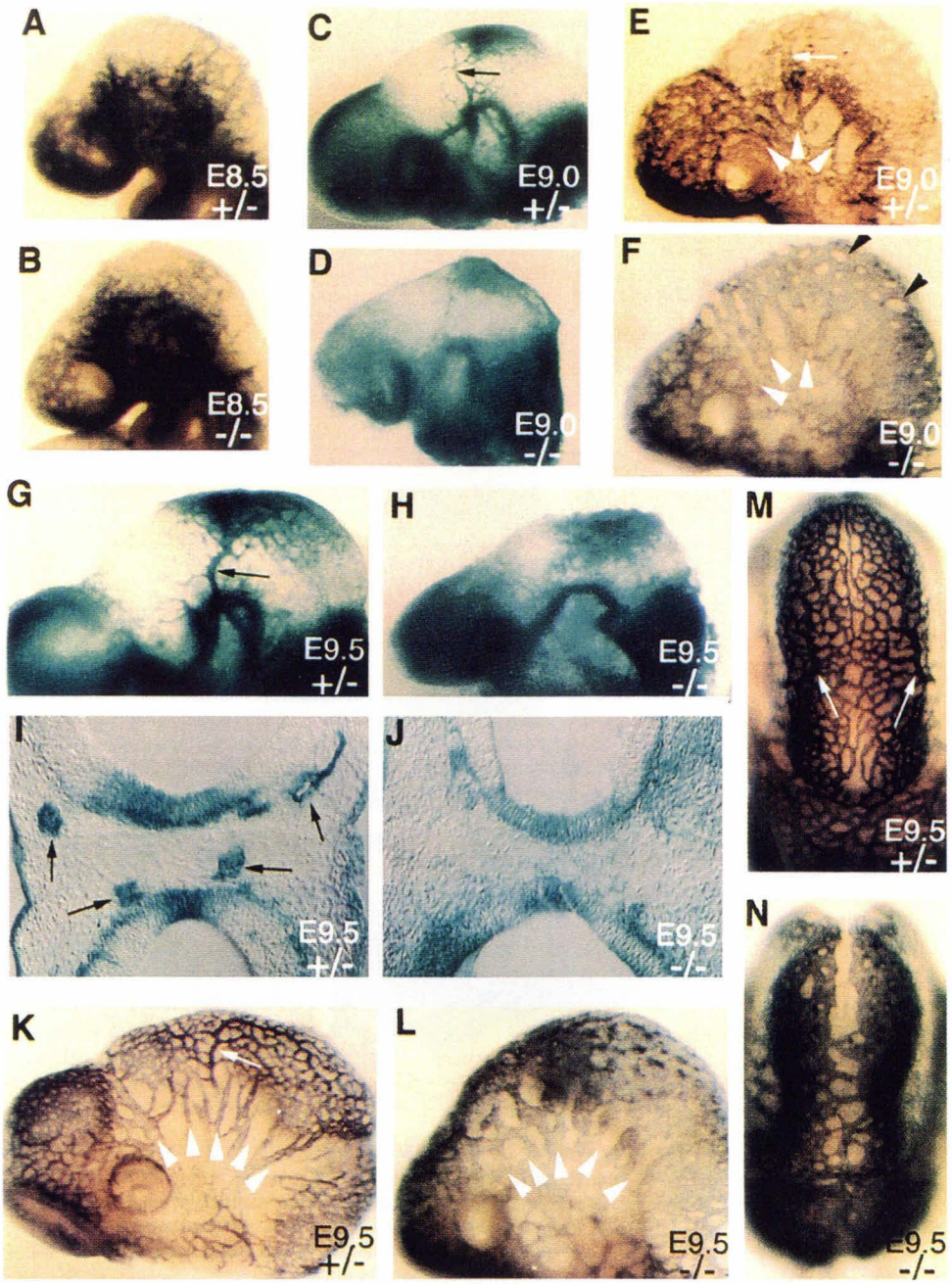

Figure 6. Defective Angiogenesis in the Head

(A and B) PECAM-1-stained E8.5 heads. (C–F) LacZ- or PECAM-1-stained E9.0 heads. (G and H) LacZ-stained E9.5 heads. (I and J) Sections of lacZ-stained heads shown in (G) and (H). Arrows (I) indicate branches of the internal carotid artery. Side (K and L) or dorsal (M and N) views of PECAM-1-stained E9.5 heads. Darker-colored branches of the internal carotid artery can be singled out in PECAM-1-stained vessels of heterozygous embryos (arrows in [E], [K], and [M]). Arrowheads indicate branches of the anterior cardinal veins in (E), (F), (K), and (L). Note again the apparent arrest of angiogenesis at the capillary plexus stage in the mutant (B, F, L, and N).

visualize an extensive intercalation between the two types of vessels during yolk sac morphogenesis (Figures 4H, 4L, and 9A). Such interdigitation may be essential to distribute interactions between arteries and veins throughout the developing capillary bed (Figure 9B). The availability of *ephrin-B2*^{tlacZ} mice may similarly reveal undiscovered features of the morphogenesis of arterial and venous networks during angiogenesis in the adult. It may also provide an opportunity to examine whether angiogenic or antiangiogenic drugs have artery-selective effects in vivo.

Most or all embryonic arteries express *ephrin-B2* and veins, *Eph-B4*, at the stages we examined. Furthermore, we were unable to detect expression on yolk sac or trunk endothelial cells of ephrins-B1 and -B3 as well as of their receptors Eph-B1, -3, and -A4. However, this should not be taken to imply that these are the only ephrins and Eph receptors expressed by arterial and

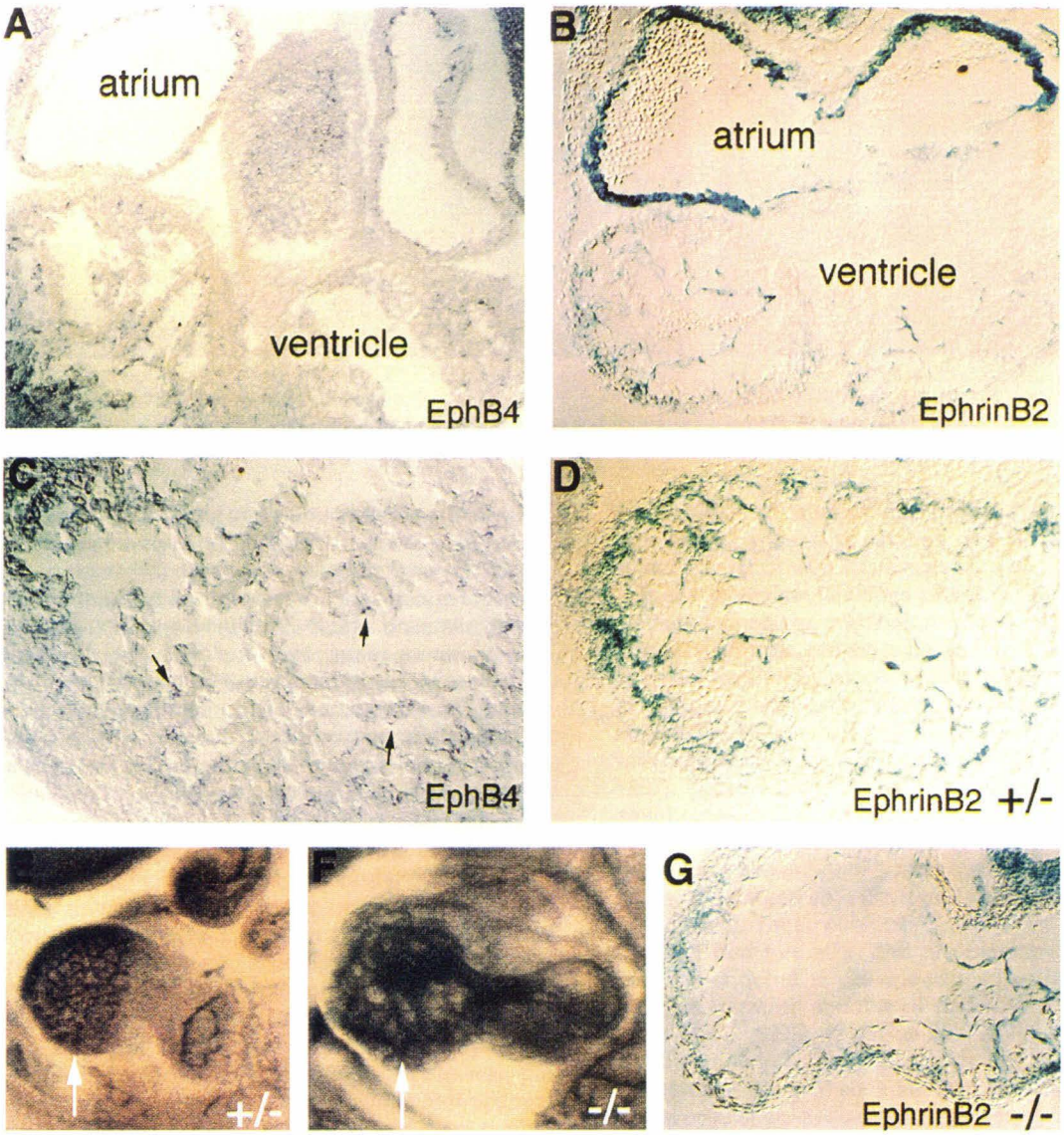

Figure 7. Receptor-Ligand Expression in the Heart and Defects in the Mutants at E10

(A and B) In situ hybridization of Eph-B4 (A) and lacZ staining of ephrin-B2 (B) in the atria and ventricles.

(C and D) Higher magnifications of receptor or ligand expression in the ventricles.

(E and F) Whole-mount views of PECAM-1-stained heterozygous (E) and homozygous mutant (F) hearts. Arrows indicate the ventricles.

(G) Section through a lacZ-stained mutant heart.

venous endothelial cells in later development or adulthood. For example, human renal microvascular endothelial cells (HRMEC) (Martin et al., 1997) have recently been shown to express *Eph-B1* and *Eph-B2* as well as *ephrin-B1* and *ephrin-B2* (Stein et al., 1998). However, the finding that both Eph-B-class receptors and ephrin-B-class ligands are expressed on this same cell population is not in contradiction to our observations, since HRMEC are not of defined arterial or venous origin (and may in fact represent a mixture of the two) or may have lost their vessel identity in vitro.

Eph-A-class receptors and their ligands have also been implicated in angiogenesis. Human umbilical vein endothelial cells (HUVECs) express Eph-A2, and TNF-α-induced angiogenesis is mediated by ephrin-A1 in vivo (Pandey et al., 1995). *Eph-A2* mutants, however, do not exhibit any detectable phenotype (Chen et al., 1996). We have not yet explored the expression of Eph-A-class receptors and their ephrin-A-class ligands on embryonic arteries and veins in vivo. However, the phenotype of the *ephrin-B2* mutant in the yolk sac, head, and heart suggests that there is not substantial functional redundancy of ephrin ligands in these regions at the embryonic stages we have examined. Nevertheless, other ephrins and their receptors could be expressed in different vessels or vascular beds at different stages of development or in the adult (Stein et al., 1998).

ephrin-B2-Mediated Interactions Are Essential for Angiogenesis of Arteries and Veins

The pattern of phenotypic defects caused by the *ephrin-B2* mutation, taken together with the complementary

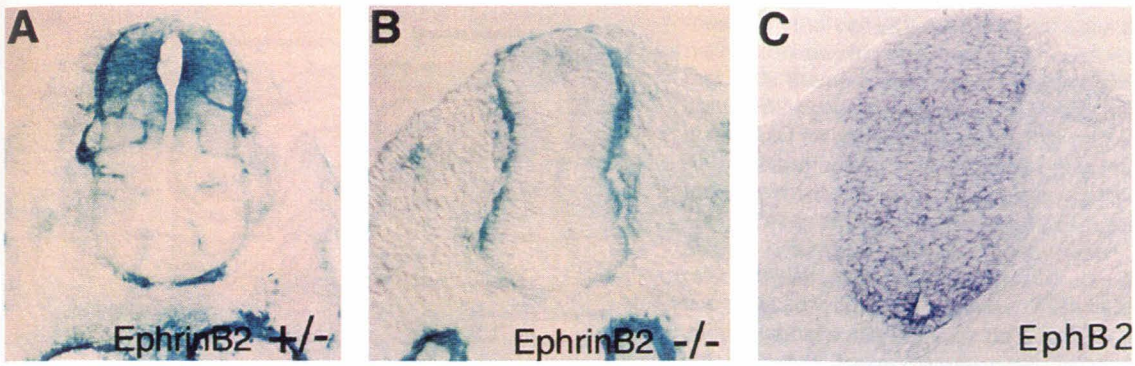

Figure 8. Neurovascular Defects in the Mutants

(A and B) Transverse sections of lacZ-stained E9.5 heterozygous (A) and homozygous mutant (B) trunk neural tube.
(C) In situ hybridization of Eph-B2 receptor in E9.5 heterozygous trunk neural tube.

expression of this ligand and its receptor by arteries and veins, respectively, suggests that reciprocal signaling between these two classes of vessels is essential for remodeling the capillary network. For example, in the head the *ephrin-B2* mutation not only blocks branching of the internal carotid artery, but it also prevents remodeling of the capillary bed of the anterior cardinal vein. This implies that ephrin-B2 provides a signal from arteries to veins that is essential for remodeling of the latter. A similar defect in venous capillary remodeling is seen in the yolk sac; here, however, remodeling of the intrinsic *arterial* capillary network is blocked as well. This suggests that a reciprocal signal from veins to arteries is also necessary for arterial angiogenesis.

Since ephrin-B2 and related transmembrane ephrin-B-type ligands have been shown capable of intracellular signaling (Holland et al., 1996; Bruckner et al., 1997), the simplest explanation for this putative reciprocal arterial–venous signaling would be that ephrin-B2 acts both as a ligand and as a receptor for Eph-B family transmembrane kinases expressed on veins. In this way, the same receptor/ligand pair would mediate bidirectional signaling between arteries and veins. We were unable to detect expression on yolk sac endodermal cells of any other ephrin-B2-interacting receptors at E9.5–10.0. However, we cannot exclude the possibility that other Eph-B class receptors are expressed below the detection limit of our in situ hybridization technique on mesenchymal or endodermal cells and also signal to arterial cells via ephrin-B2.

It is formally possible that the arterial defects in the mutant reflect an autonomous function for ephrin-B2 and that the venous defects are a secondary consequence of altered or absent blood flow in the defective arteries. We feel this is unlikely, not only because veins express the Eph-B4 receptor for ephrin-B2, but also because ephrin-B2-dependent remodeling events begin at E8.5, before the heart starts to beat regularly (E9.0; Kaufman, 1992). Conversely, the arterial defects in the mutant are unlikely to simply reflect changes in venous blood flow, because a similar angiogenic defect is observed in the neural tube, where vascularization requires an interaction between ephrin-B2$^+$ endothelial cells and Eph-B2-expressing neuroepithelial cells (Figure 8C). Targeted disruption of *Eph-B4* should directly address the question of whether this receptor is required for signaling from veins to arteries and should provide a useful marker of venous vessels as well.

The biochemical functions promoted by ephrin/eph-mediated signaling, and their role in the angiogenic remodeling process, remain to be explored. One hint, however, is provided by recent studies which indicate that the ephrin-B receptor Eph-B2/Nuk interacts directly with regulators of GTPases, including ras-GAP, and indirectly with regulators of small GTPases via Nck (Holland et al., 1997). These GTPases have in turn been implicated in membrane–actin cytoskeletal rearrangements that underly both axon guidance (Garrity et al., 1996) and the formation of membrane specializations such as focal contacts between cells (reviewed in Hall, 1998; Holland et al., 1998). These cell–cell junctions are important in capillary bed formation and are mediated, at least in part, by endothelial cell-specific adhesion molecules such as vascular endothelial cadherin (VE-CAD) (Navarro et al., 1998). It will be interesting to determine whether ephrin-B2-mediated signaling is required for the establishment of such junctions in vivo.

The cellular consequences of ephrin signaling in angiogenesis have yet to be determined. In the nervous system, ephrins have been implicated as repulsive guidance cues for axon growth and neural crest cell migration (reviewed in Holland et al., 1998). By analogy, mutually repulsive interactions between arteries and veins mediated by ephrins could be important in establishing the proper balance of these two vessel types in capillary beds. On the other hand, ephrin-A1 has been shown to promote angiogenesis in vivo as well as endothelial cell chemotaxis (Pandey et al., 1995), and very recently ephrin-B1 has been shown to promote capillary-like assembly of renal endothelial cells in vitro (Stein et al., 1998). Thus, these latter data suggest that ephrin signaling may mediate stimulatory rather than inhibitory influences on endothelial cells. Purification of ephrin-B2$^+$ arterial and Eph-B4$^+$ venous endothelial cells should permit in vitro studies that will address this issue.

Potential Interactions between ephrin and Angiopoietin Signaling

The angiogenic phenotype of the *ephrin-B2* mutation in the head and yolk sac appears similar to that of mutations in the receptor TIE2 (Sato et al., 1995) and its ligand

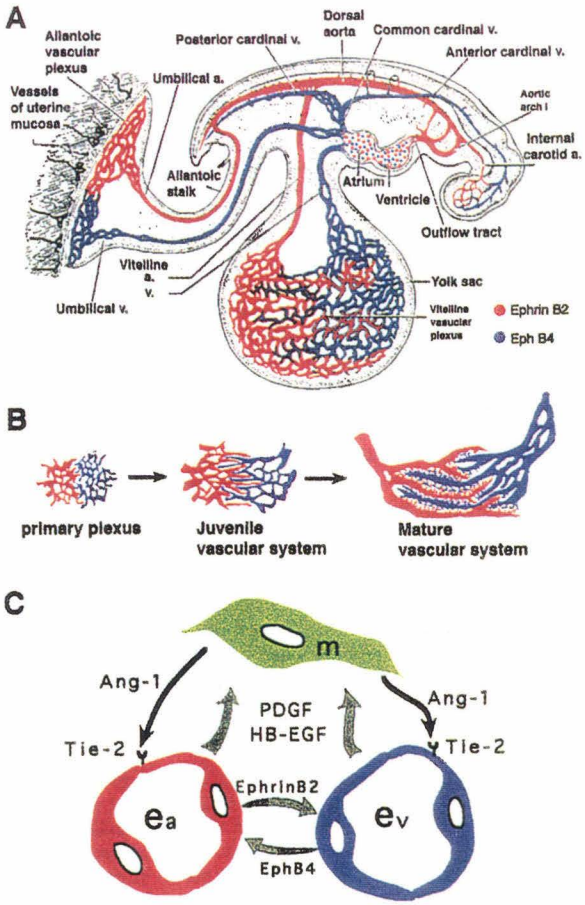

Figure 9. Summary of the Endothelial Expression of ephrin-B2 and Eph-B4, and Deduced Mechanistic Models

(A) Distinction of arteries and veins by the expression of ephrin-B2 and Eph-B4, and their coexpression in the heart in early mouse embryos. Note the intercalation of arteries and veins in the yolk sac. Modified from Carlson (1981).

(B) Ontogeny of arterial–venous intercalation during yolk sac morphorgenesis. Vascular stage nomenclature is according to Risau (1997). The *ephrin-B2* mutation arrests yolk sac angiogenesis at the primary plexus stage (see Figure 4).

(C) Revised model of cell–cell interactions in angiogenesis, modified from Folkman and D'Amore (1996).

Abbreviations: e_a, arterial endothelial cell; e_v, venous endothelial cell; m, mesenchymal cell.

Angiopoietin-1 (Suri et al., 1996). Those data have been interpreted to suggest that mesenchymal cells signal via Ang-1 to *tie-2*-expressing endothelial cells, which in turn secrete a reciprocal signal (possibly PDGF or HB-EGF) that recruits the mesenchymal cells to differentiate to smooth muscle cells and pericytes that form the vessel wall (Folkman and D'Amore, 1996). Sections of the yolk sac in *ephrin-B2* mutants reveal apparent defects in the morphological differentiation of vessel-associated support cells (Figures 5E and 5F). A more dramatic phenotype is seen in the heart where (as in the *tie-2* and *ang-1* mutants) formation of the myocardial trabeculae is disrupted, although here again both ligand and receptor are expressed by endothelial cells.

How could defective reciprocal signaling between endothelial cells produce an apparently similar defect in mesenchymal cell differentiation, as does defective signaling between the endothelial cells and the mesenchymal cells themselves? One attractive possibility is that ephrin-B2-Eph-B4-mediated interendothelial signaling is required for either production of or responsiveness to Ang-1. Alternatively, Ang-1 signaling could be necessary for the expression or function of the ephrin-B2-Eph-B4 ligand-receptor pair. Genetic epistasis experiments may help to distinguish between these possibilities. Whatever the case, what was previously conceived of as a two-way conversation between endothelial and mesenchymal cells may actually be a three-way conversation between mesenchymal cells, arteries, and veins (Figure 9C).

The Implications of Molecular Distinctions between Arteries and Veins

The finding that arterial and venous endothelial cells are genetically distinct raises new questions relevant to both basic and clinical research into vasculogenesis and angiogenesis. How are arterial and venous angioblasts initially specified? Do arterial and venous angioblasts display homotypic vasculogenic or angiogenic properties? Do activators and inhibitors of angiogenesis act equivalently on each type of endothelial cell, or do they exhibit arterial or venous specificity? The roles of ephrins and their receptors in tumor angiogenesis (Hanahan and Folkman, 1996) or myocardial neovascularization (Schumacher et al., 1998) also remain to be explored.

Finally, our results indicate that the physiological and pathological distinctions between mature arteries and veins are not due simply to differences in their anatomy, oxygenation, or blood pressure, but rather are genetically determined. This implies that arteries and veins are likely to differ in their expression of many other genes as well. The identification of such genes may not only inform our understanding of vascular physiology, but may also shed light on the different disease suceptibilities of these two types of vessels. In turn, this may lead to novel artery- or vein-specific angiogenic or antiangiogenic therapies.

Experimental Procedures

Targeted Disruption of the *ephrin-B2* Gene

A 200 bp probe starting from the ATG of the mouse *ephrin-B2* gene (Bennett et al., 1995) was used to screen a 129SVJ genomic library (Stratagene). Analysis of several overlapping clones revealed that the first exon, including the signal sequence, ends at 131 bp after the ATG. Further phage analysis and library screens revealed that the rest of the *ephrin-B2* gene was located at least 7 kb downstream from the first exon. To construct a targeting vector, a 3 kb Xba1–NcoI fragment whose 3′ end terminated at the ATG was used as the 5′ arm. A 5.3 kb tau-lacZ coding sequence (Mombaerts et al., 1996) was fused in frame after the ATG. The *PGKneo* gene (Ma et al., 1998) was used to replace a 2.8 kb intronic sequence 3′ to the first exon. Finally, a 3.2 kb downstream EcoRI–EcoRI fragment was used as the 3′ arm. Normal (6 kb) and targeted (9 kb) loci are distinguished by HindIII digestion when probed with a 1 kb HindIII–XbaI genomic fragment (Figure 1A). Electroporation, selection, and blastocyst-injection of AB-1 ES cells were performed essentially as described (Ma et al., 1998), with the exception that FIAU-selection was omitted. ES cell targeting efficiency via G418 selection was 1 out of 18 clones. Germline transmission of the targeted *ephrin-B2* locus in heterozygous males was confirmed by Southern blotting. Subsequent genotyping was done by genomic PCR. Primers for Neo are 5′-AAGATGG

ATTGCACGCAGGTTCTC-3′ (5′) and 5′-CCTGATGCTCTTCGTCCA GATCAT-3′ (3′). Primers for the replaced intronic fragment are 5′-AGGACGGAGGACGTTGCCACTAAC-3′ (5′) and 5′-ACCACCAGTT CCGACGCGAAGGGA-3′ (3′).

LacZ, PECAM-1, and Histological Staining

Embryos and yolk sacs were removed between E7.5 and E10.0, fixed in cold 4% paraformaldehyde/PBS for 10 min, rinsed twice with PBS, and stained for 1 hr to overnight at 37°C in X-Gal buffer (1.3 mg/ml potassium ferrocyanide, 1 mg/ml potassium ferricyanide, 0.2% Triton X-100, 1 mM $MgCl_2$, and 1 mg/ml X-Gal in PBS [pH 7.2]). LacZ-stained embryos were post-fixed and photographed or sectioned on a cryostat after embedding in 15% sucrose and 7.5% gelatin in PBS. Procedures for whole-mount or section staining with anti-PECAM-1 antibody (clone MEC 13.3, Pharmingen) were done essentially as described (Fong et al., 1995; Ma et al., 1998). HRP-conjugated secondary antibodies (Jackson) were used for all PECAM-1 stainings except for Figure 4, where alkaline phosphatase was the enzyme of choice. LacZ-stained yolk sacs were sectioned in gelatin and then subjected to hematoxylin counterstaining by standard procedures.

In Situ Hybridization

In situ hybridization on frozen sections was performed as previously described (Birren et al., 1993). Whole-mount in situ hybridization followed a protocol by Wilkinson (Wilkinson, 1992). pBluescript vectors (Stratagene) containing cDNAs for Eph-B2/Nuk and Eph-B4/Myk-1 were generated as described (Wang and Anderson, 1997).

Acknowledgments

We thank P. Mombaerts for the tau-lacZ plasmid, A. Bradley and R. Behringer for AB-1 ES cells, L. Wang for feeder cell culture, B. Turring for illustrations, the staff of the Caltech Transgenic Facility for mouse care, and lab members for discussion and support. We thank J. Folkman for an insightful review and J. L. Anderson for encouragement. This work was supported by a grant from the American Paralysis Association. D. J. A. is an Investigator of the Howard Hughes Medical Institute.

Received April 14, 1998; revised May 5, 1998.

References

Andres, A.-C., Reid, H.H., Zurcher, G., Blaschke, R.J., Albrecht, D., and Ziemiecki, A. (1994). Expression of two novel eph-related receptor protein tyrosine kinases in mammary gland development and carcinogenesis. Oncogene *9*, 1461–1467.

Bennett, B.D., Zeigler, F.C., Gu, Q., Fendly, B., Goddard, A.D., Gillett, N., and Matthews, W. (1995). Molecular cloning of a ligand for the Eph-related receptor protein-tyrosine kinase Htk. Proc. Natl. Acad. Sci. USA *92*, 1866–1870.

Bergemann, A.D., Cheng, H.J., Brambilla, R., Klein, R., and Flanagan, J.G. (1995). ELF-2, a new member fo the Eph ligand family, is segmentally expressed in mouse embryos in the region of the hindbrain and newly forming somites. Mol. Cell. Biol. *15*, 4921–4929.

Birren, S.J., Lo, L.C., and Anderson, D.J. (1993). Sympathetic neurons undergo a developmental switch in trophic dependence. Development *119*, 597–610.

Bruckner, K., Pasquale, E.B., and Klein, R. (1997). Tyrosine phosphorylation of transmembrane ligands for Eph receptors. Science *275*, 1640–1643.

Carlson, B.M. (1981). The circulatory system. In Patten's Foundations of Embryology, J. Vastyan and S. Wagley, eds. (McGraw-Hill).

Chen, J., Nachabah, A., Scherer, C., Ganju, P., Reith, A., Bronson, R., and Ruley, E.H. (1996). Germ-line inactivation of the murine Eck receptor tyrosine kinase by gene trap retroviral insertion. Oncogene *12*, 979–988.

Dumont, D.J., Gradwohl, G., Fong, G.H., Puri, M.C., Gertsenstein, M., Auerbach, A., and Breitman, M L. (1994). Dominant-negative and targeted null mutations in the endothelial receptor tyrosine kinase, tek, reveal a critical role in vasculogenesis of the embryo. Genes. Dev. *8*, 1897–1909.

Evans, H.M. (1909). On the development of the aortae, cardinal and umbilical veins, and the other blood vessels of vertebrate embryos from capillaries. Anat. Rec. *3*, 498–518.

Folkman, J., and Klagsbrun, M. (1987). Angiogenic factors. Science *235*, 442–447.

Folkman, J., and D'Amore, P.A. (1996). Blood vessel formation: what is its molecular basis? Cell *87*, 1153–1155.

Fong, G.-H., Rossant, J., Gertsenstein, M., and Breitman, M.L. (1995). Role of the Flt-1 receptor tyrosine kinase in regulating the assembly of vascular endothelium. Nature *376*, 66–70.

Gale, N.W., Holland, S.J., Valenzuela, D.M., Flenniken, A., Pan, L., Ryan, T.E., Henkemeyer, M., Strebhard, K., Hirai, H., Wilkinson, D.G., et al. (1996). Eph receptors and ligands comprise two major specificity subclasses, and are reciprocally compartmentalized during embryogenesis. Neuron *17*, 9–19.

Garrity, P.A., Rao, Y., Salecker, I., McGlade, J., Pawson, T., and Zipursky, S.L. (1996). *Drosophila* photoreceptor axon guidance and targeting requires the dreadlocks SH2/SH3 adapter protein. Cell *85*, 639–650.

Gassmann, M., Casagranda, F., Orioli, D., Simon, H., Lai, C., Klein, R., and Lemke, G. (1995). Aberrant neural and cardiac development in mice lacking the erbB4 neuregulin receptor. Nature *378*, 390–394.

Gilbert, S.F. (1997). Developmental Biology, Fifth Ed., (transl.) (Sunderland, MA: Sinauer Associates, Inc.).

Goto, F., Goto, K., Weindel, K., and Folkman, J. (1993). Synergistic effects of vascular endothelial growth factor and basic fibroblast growth factor on the proliferation and cord formation of bovine capillary endothelial cells within collagen gels. Lab. Invest. *69*, 508–517.

Hall, A. (1998). Rho GTPases and the actin cytoskeleton. Science *279*, 509–514.

Hanahan, D. (1997). Signaling vascular morphogenesis and maintenance. Science *277*, 48–50.

Hanahan, D., and Folkman, J. (1996). Patterns and emerging mechanisms of the angiogenic switch during tumorigenesis. Cell *86*, 353–364.

Henkemeyer, M., Marengere, L.E.M., McGlade, J., Olivier, J.P., Conlon, R.A., Holmyard, D.P., Letwin, K., and Pawson, T. (1994). Immunolocalization of the Nuk recepter tyrosin kinase suggests roles in segmental patterning of the brain and axonogenesis. Oncogene *9*, 1001–1014.

Holland, S.J., Gale, N.W., Mbamalu, G., Yancopoulos, G.D., Henkemeyer, M., and Pawson, T. (1996). Bidirectional signaling through the Eph-family receptor Nuk and its membrane ligands. Nature *383*, 722–725.

Holland, S.J., Gale, N.W., Gish, G.D., Roth, R.A., Songyang, Z., Cantley, L.C., Henkemeyer, M., Yancopoulos, G.D., and Pawson, T. (1997). Juxtamembrane tyrosine residues couple the Eph family receptor Eph-B2/Nuk to specific SH2 domain proteins in neuronal cells. EMBO J. *16*, 3877–3888.

Holland, S.J., Peles, E., Pawson, T., and Schlessinger, J. (1998). Cell-contact-dependent signaling in axon growth and guidance: Eph receptor tyrosine kinases and receptor protein tyrosine phosphatases. Curr. Opin. Neurobiol. *8*, 117–127.

Kaufman, M.H. (1992). The atlas of mouse development. edit. transl. Academic Press.

Krull, C.E., Lansford, R., Gale, N.W., Collazo, A., Marcelle, C., Yancopoulos, G.D., Fraser, S.E., and Bronner-Fraser, M. (1997). Interactions of Eph-related receptors and ligands confer rostrocaudal pattern to trunk neural crest migration. Curr. Biol. *7*, 571–580.

Lee, K.-F., Simon, H., Chen, H., Bates, B., Hung, M.-C., and Hauser, C. (1995). Requirement for neuregulin receptor erbB2 in neural and cardiac development. Nature *378*, 394–398.

Ma, Q., Chen, Z., del Barco Barrantes, I., de la Pompa, J.L., and Anderson, D.J. (1998). Neurogenin1 is essential for the determination of neuronal precursors for proximal cranial sensory ganglia. Neuron *20*, 469–482.

Martin, M.M., Schoecklmann, H.O., Foster, G., Barley-Maloney, L., McKanna, J., and Daniel, T.O. (1997). Identification of a subpopulation of human renal microvascular endothelial cells with capacity to form capillary-like cord and tube structures. In vitro Cell Dev. Biol. *33*, 261–269.

Meyer, D., and Birchmeier, C. (1995). Multiple essential functions of neuregulin in development. Nature *378*, 386–390.

Mombaerts, P., Wang, F., Dulac, C., Chao, S.K., Nemes, A., Mendelsohn, M., Edmondson, J., and Axel, R. (1996). Visualizing an olfactory sensory map. Cell *87*, 675–686.

Navarro, P., Ruco, L., and Dejana, E. (1998). Differential localization of VE- and N-Cadherins in human endothelial cells: VE-Cadherin competes with N-Cadherins for junctional localization. J. Cell Biol. *140*, 1475–1484.

Pandey, A., Shao, H., Marks, R.M., Polverini, R.J., and Dixit, V.M. (1995). Role of B61, the ligand for the Eck receptor tyrosine kinase, in TNF-alpha-induced angiogenesis. Science *268*, 567–569.

Risau, W. (1997). Mechanisms of angiogenesis. Nature. *386*, 671–674.

Risau, W., and Flamme, I. (1995). Vasculogenesis. Annu. Rev. Cell. Dev. Biol. *11*, 73–91.

Sabin, F.R. (1917). Origin and development of the primitive vessels of the chick and of the pig. Contrib. Embryol. Carnegie Inst. Washington *6*, 61–124.

Sato, T.N., Tozawa, Y., Deutsch, U., Wolburg-Buchholz, K., Fujiwara, Y., Gendron-Maguire, M., Gridley, T., Wolburg, H., Risau, W., and Qin, T. (1995). Distinct roles of the receptor tyrosine kinases Tie-1 and Tie-2 in blood vessel formation. Nature *376*, 70–74.

Schumacher, B., Pecher, P., von Specht, B.U., and Stegmann, T.H. (1998). Induction of Neoangiogenesis in ischemic myocardium by human growth factors, first clinical results of a new treatment of coronary heart disease. Circulation *97*, 645–650.

Shalaby, F., Rossant, J., Tamaguchi, T.P., Gertsenstein, M., Wu, X.-F., Breitman, M.L., and Schuh, A.C. (1995). Failure of blood-island formation and vasculogenesis in Flk-1-deficient mice. Nature *376*, 62–66.

Smith, A., Robinson, V., Patel, K., and Wilkinson, D.G. (1997). The EphA4 and EphB1 receptor tyrosine kinases and EphrinB2 ligand regulate targeted migration of branchial neural crest cells. Curr. Biol. *7*, 561–570.

Stein, E., Lane, A.A., Cerretti, D.P., Schoecklmann, H.O., Schroff, A.D,, Van Etten, R.L., and Daniel, T.O. (1998). Eph receptors discriminiate specific ligand oligomersto determine alternative signaling complexes, attachment, and assembly responses. Genes Dev. *12*, 667–678.

Suri, C., Jones, P.F., Patan, S., Bartunkova, S., Maisonpierre, P.C., Davis, S., Sato, T.N., and Yancopoulos, G.D. (1996). Requisite role of angiopoietin-1, a ligand for the Tie-2 receptor, during embryonic angiogenesis. Cell *87*, 1171–1180.

Wang, H.U., and Anderson, D.J. (1997). Eph family transmembrane ligands can mediate repulsive guidance of trunk neural crest migration and motor axon outgrowth. Neuron *18*, 383–396.

Wilkinson, D.G. (1992). Whole-mount in situ hybridization of vertebrate embryos. In In Situ Hybridization: A Pratical Approach, D.G. Wilkinson, ed. (Oxford: IRL Press), pp. 75–83.

Xu, Q., Alldus, G., Holder, N., and Wilkinson, D.G. (1995). Expression of truncated Sek-1 receptor tyrosine kinase disrupts the segmental restriction of gene expression in the Xenopus and zebrafish hindbrain. Development *121*, 4005–4016.

Chapter 6

Current and future studies of arteries and veins

Based on our discovery of a molecular distinction between arterial and venous endothelial cells, we have initiated a series of experiments to expand our studies on the development of arteries and veins. We are interested in the basic questions such as how ephrinB2-EphB4 mediated interactions between arterial and venous endothelial cells might promote vascular remodeling in the capillary beds. We are interested in probing the mechanisms of identity specification of arterial and venous endothelial cells originated at different embryonic locations. We are eager to identify more molecules that are differentially expressed in arteries and veins. Such molecules may help us understand the functional and pathological differences between mature arteries and veins. Finally, we hope to develop practical applications based on our findings. We want to know whether ephrinB2 and EphB4 are expressed in the vessels of growing tumors. If so, inhibition of the ephrin signaling system by monoclonal antibodies or soluble receptors or ligands may be an effective approach in blocking abnormal angiogenesis and associated tumor growth.

A) EphrinB2 expression in neonatal and adult mice

The arterial endothelial restricted expression of ephrinB2 in embryos was established in our recent studies. However, its vascular expression in the newborn mice or adults are not known. To examine the expression in the later stages of development, I took different tissues and performed wholemount or section staining for ephrinB2-lacZ. For a pan-endothelial marker, I used PECAM-1 monoclonal antibody (MEC13.3, Pharmingen).

In the newborn mice, ephrinB2 shows strong expression in the vascular system. Fresh frozen tissues were sectioned immediately, and air dried at room temperature for 45

minutes. After a very brief fixation (5 minutes in cold 4% paraformaldehyde), LacZ staining were carried out for overnight at 37^{0}C. Intense staining of ephrinB2 were observed in all major arteries, and not veins, confirming its arterial specificity (Figure 1). In the newly developed lungs, ephrinB2 is likewise restricted to the pulmonary arteries.

For adult expression patterns, different tissues were fresh frozen and sectioned immediately. LacZ staining was performed after brief air-drying and fixation. Intense lacZ signals were observed in all major arteries (Figure 2), small arterioles (Figure 3), and even in numerous capillaries in different tissues (Figure 4 and 5).

An unique site of ephrinB2 expression is in the capillaries. Capillary vessels have not been subdivided into arterial and venous populations based on traditional physiological definitions. Our data now shows that ephrinB2 is expressed only in the capillaries closely connected to the arterioles, and not in those closely connected to the venules. These results suggest that capillaries have distinct identities based on their connection or association with larger arteries or veins, even in the center of the capillary beds where physiological parameters such as oxygen or blood pressure should be uniform. This suggests that arterial and venous endothelial cells of the capillaries may have homophilic properties or repulsive actions against each other, so that the two populations of endothelial cells do not intermingle at the A-V vessel junctions.

It will be interesting to examine postnatal and adult expression patterns of EphB4 receptor. The question is whether EphB4 is expressed in endothelial cells of large veins, venules and venous capillaries. If EphB4 shows persistent expression in adult veins, then ephrinB2-EphB4 mediated signaling may continue to play roles in adult angiogenesis such as wound healing, or tumor vascularization.

Figure 1. Arterial specificity of ephrinB2 expression in newborn mice.

Newborn tissues were freshly frozen, sectioned, and processed for lacZ staining. **A,** A cross trunk section at thoracic level. EphrinB2-lacZ signals were observed in aortic arches (AA), descending dorsal aorta (DA), but not in right or left superior vena cava (RSV, LSV). **B** and **C**, In cross sections of the neck region, ephrinB2 is positive in right and left carotid arteries (RCA, LCA), but negative in right or left jugular veins (RJV, LJV). **D** and **E**, In the newly developed lungs, ephrinB2 is expressed in right or left pulmonary arteries (RPA, LPA), but not in right or left pulmonary veins (RPV, LPV).

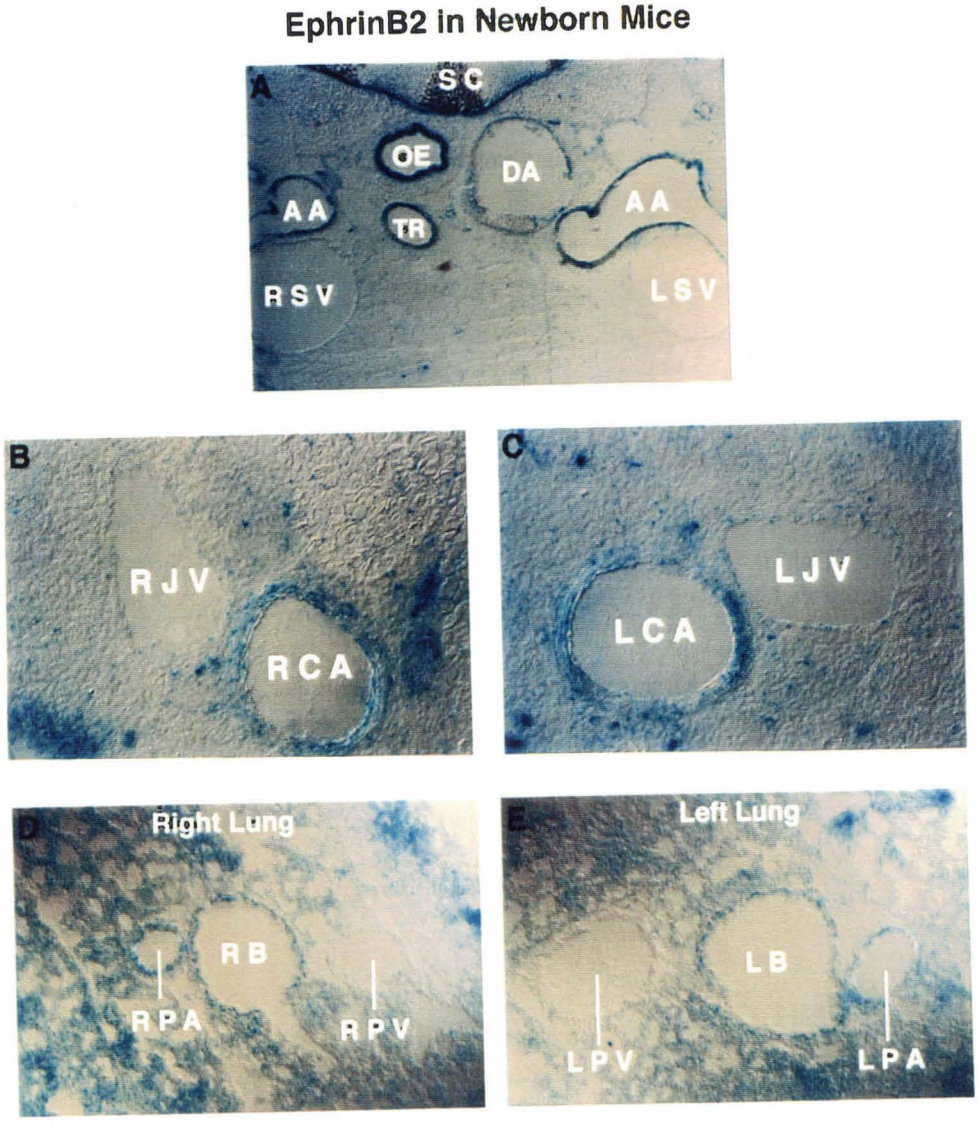

Figure 2. EphrinB2 expression in aorta and coronary artery.

A, EphrinB2 (lacZ blue) and PECAM1 (brown) double labeling of adult descending dorsal aorta and adjacent inferior vena cava. **B,** Double labeling of femoral artery and vein. **C,** Single lacZ staining of coronary artery, but not vein. **D,** An adjacent section of **C**, labeled by PECAM1, to show both coronary artery and vein.

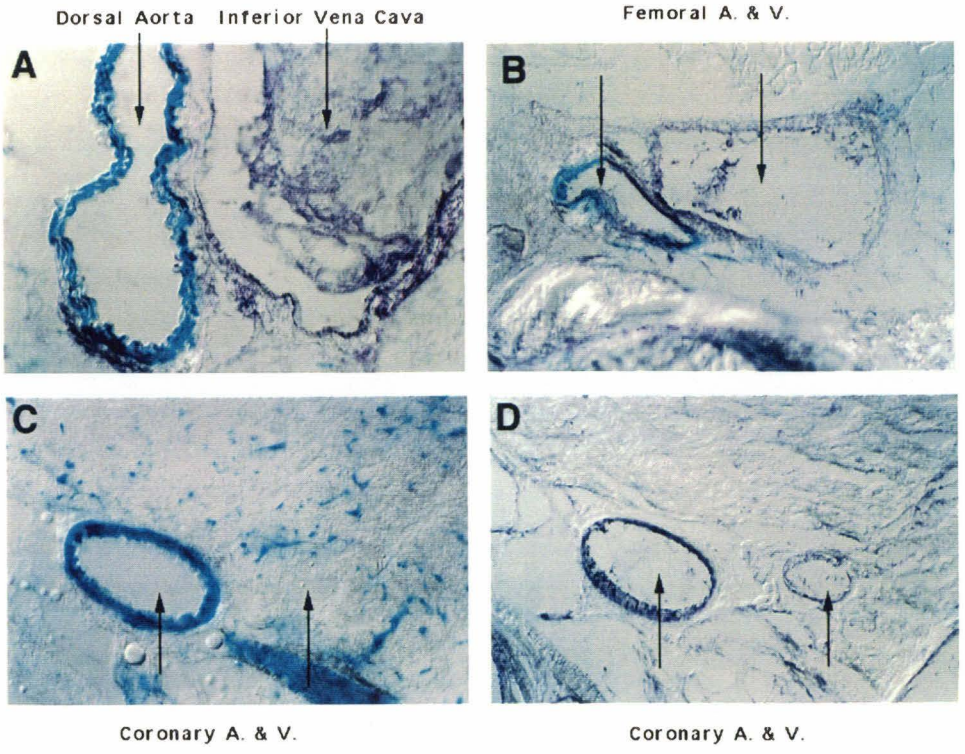

Figure 3. EphrinB2 expression in arteries of kidney, liver, and muscle.

In this figure, white arrowheads point to arterioles, and white arrows point to venules. **A**, Double labeling of kidney arteriole and venule. Also noted is the ephrinB2 signal in glomeruli.(black arrow). **B**, In liver, most vessels are hepatic veins. Small arteriole are labeled by ephrinB2. **C**, Embedded in leg muscle is ephrinB2 positive arteries and PECAM1 positive veins. **D**, A pair of capillaries in the leg muscle.

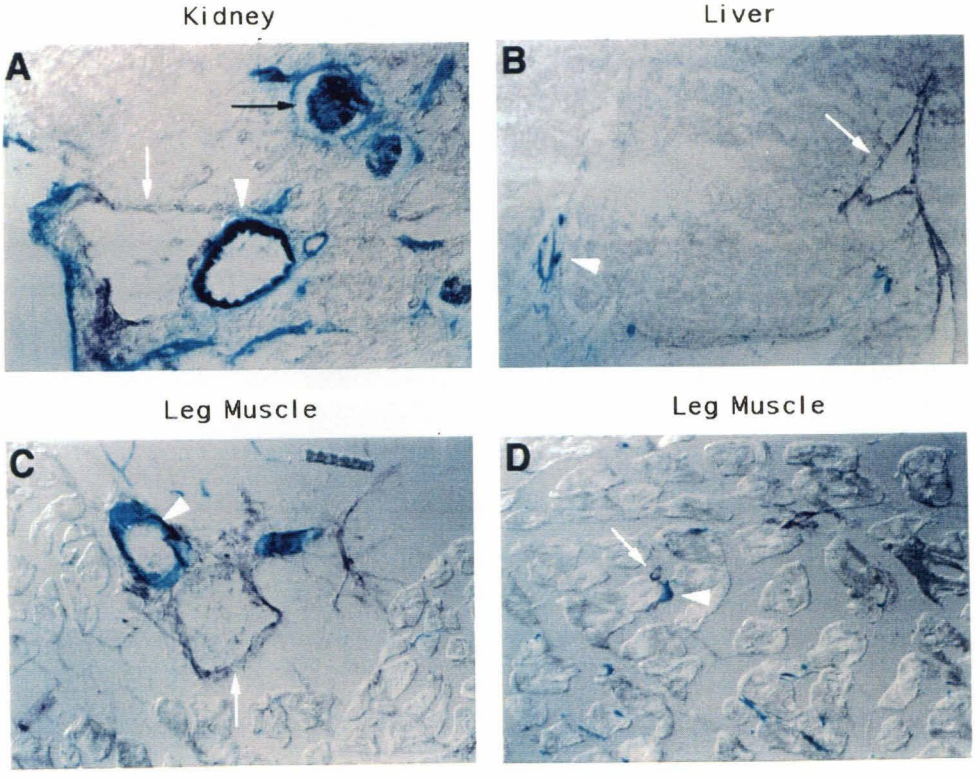

Figure 4. EphrinB2 expression in arterial capillaries in fat.

A, A whole mount view of arterioles (arrow head) and arterial capillaries (arrow) revealed by ephrinB2-lacZ in the fat tissue. **B**, Another wholemount view of the fat tissue similar to **A**. **C**, A section of double labeled fat tissue shows ephrinB2 positive arteriole (black arrowhead) and PECAM1 positive venule (black arrow). **D**, Higher magnification view of **C** shows blue arterial capillaries (black arrow) and brown venous capillaries (black arrowhead).

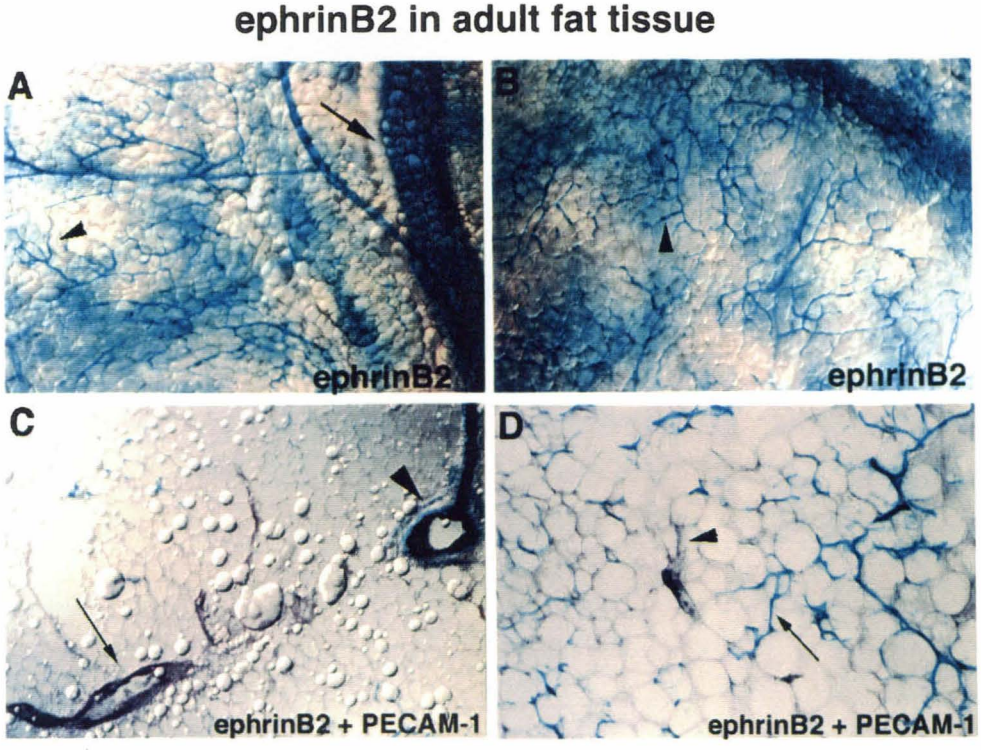

Figure 5. EphrinB2 expression in arterial capillaries in muscle fiber.

A, EphrinB2 signals in arterial capillaries (arrowheads) of the leg muscle fibers. **B**, PECAM-1 reveals all capillaries (arrowheads) in the muscle fibers in an adjacent section to that of **A**. PECAM-1 positive vessels outnumber ephrinB2 positive ones, suggesting ephrinB2 is only expressed in a subset of the total capillaries.

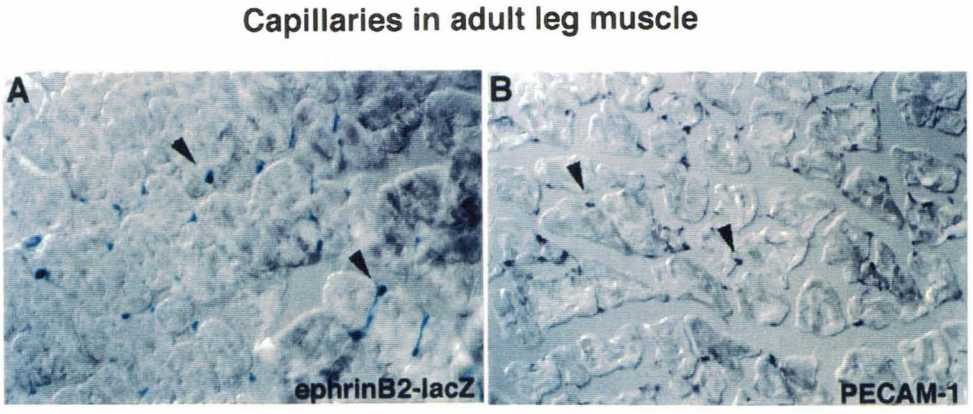

B) Nature of ephrinB2-EphB4 signaling in angiogenesis

Vascular angiogenesis consists of two processes: the synthesis of new vessels by sprouting and splitting, and remodeling or maturation of existing ones (For review, see Risau, 1997). Sprouting, the outgrowth of new vessels from existing ones (Figure 6A, arrowhead), involves proliferation and migration of endothelial cells, and the subsequent formation of endothelial lumen. Splitting involves proliferation of endothelial cells inside a vessel and formation of transcapillary lumen (Figure 6A, arrow). The remodeling of pre-existing capillaries involves vessel enlargement and pericyte coating. The expansion of capillary endothelial lumen is probably contributed by both endothelial cell proliferation and incorporation of endothelial cells newly differentiated from mesoderm or migrated from adjacent capillaries. To counter balance the vessel enlargement, local mesenchymal cells are attracted to coat the forming vessels. Differentiation of pericyte or smooth muscle cells outside of vessel leads to an inhibition of endothelial proliferation and accumulation of extracellular matrix (Folkman and D'Amore, 1996). Balanced expansion and inhibition result in the formation of mature vascular tree. Figure 6 illustrates the angiogenic process seen in the developing yolk sac. Primary capillary network (Figure 6A) expands into a matured one (Figure 6B) through sprouting, splitting, and remodeling.

In the absence of ephrinB2, both the expansion and remodeling of the primary capillary plexus were affected (See Chapter 5). Mutant yolk sacs lacked the normal vascular density as well as larger vessels typically seen in the mature vascular tree. Sections of homozygous mutant yolk sacs also revealed a lack of recruitment of mesenchymal cells to the blood vessels. In the absence of a normal pericyte or smooth muscle cell coating, the integrity of the vascular network was defective and leakage of blood cells was observed.

EphrinB2 and EphB4 signaling occurs between arterial and venous endothelial cells at the junction of the two types of capillaries (Figure 6C). One hypothesis is that the ligand-receptor signaling in contacting A-V endothelial cells may lead to a secretion of certain soluble factors that act on local capillaries. Such factors may have stimulatory effects on the

synthesis of new capillaries near the A-V junction as well as the remodeling of pre-existing vessels. The positive roles of ligand-receptor signaling at artery-vein junction is consistant with the active angiogenesis in the capillary beds. Expansion of embryonic capillary beds is then counter balance by the decrease of expression of angiogenic growth factors such as VEGF in the adult. Almost all adult endothelial cells cease proliferation, only to be activated during neovascularization events such as wound healing and tumor angiogenesis. Thus, ephrinB2-EphB4 signaling primarily functions in embryonic vascular growth and neovascularization.

There are a couple of situations where endothelial-mesenchymal cell interactions and ephrinB2-EphB4 signaling are not correlated. First, vessel maturation does occur away from the A-V interface. Large arteries and veins such as aorta and cardinal veins don't interact with each other. The smooth muscle layer formation on these vessels is likely independent of ephrinB2-EphB4 signaling. Second, ephrinB2 is persistently expressed in the adult arterial capillaries. Adult capillaries, however, are not sheathed for allowing an efficient exchange of oxygen and nutrients with the surrounding tissues. Why shouldn't adult capillaries be coated by smooth muscle cells as a consequence of ephrinB2 signaling? One possibility is that receptor EphB4 is not normally expressed in adult venous capillaries. EphB4 could be then induced in the event of neovascularization. We will examine EphB4's expression in the normal vascular networks and tumor vessels by in situ hybridization. Another possibility is that is mesenchymal cells in the adult don't normally respond to ephrinB2 signaling. Only in the event of neovascularization that they are attracted to newly developed vascular plexus.

What is then the role of ephrinB2 in the endothelial cells of main arteries? These endothelial cells can interact with smooth muscle cells. Our data, however, suggested that smooth muscle cells doesn't express any of EphB type receptors for ephrinB2. One possibility is that ephrinB2 in the arteries mediates interactions of arterial endothelial cells and certain receptor-bearing blood cells such as lymphocytes and macrophages. This

hypothesis is consistant with the preferential plaque formation on the arteries through macrophage or lymphocyte deposition. One way to study the potential role of ephrinB2 in endothelial-blood cell interactions is to systemic inject ephrinB2 antibodies or soluble ephrinB2 extracellular protein in atherosclerosis transgenic mice to observe the changes in blood vessel clotting.

Figure 6. EphrinB2-EphB4 signaling in angiogenesis. Angiogenic growth and remodeling of a primary plexus (**A**) into a mature plexus (**B**) is accompanied by synthesis of new vessels through splitting (**A**, arrow) and sprouting (**A**, arrowhead), and by vessel lumen enlargement and formation of arteries (**B**, a) and veins (**B**, v). In **C**, deduced interactions between ephrinB2$^+$ arterial and EphB4$^+$ venous capillaries and between endothelial and mesenchymal cells are illustrated. A hypothetical angiogenic stimulator secreted by endothelial cells at A-V junction is shown as "factor ?." EphrinB2-EphB4 signaling at A-V junction may trigger endothelial proliferation and new vessel sprouts from the surrounding capillaries. Ligand-receptor signaling may also help to recruit mesenchymal cells which will differentiate into pericytes or smooth muscle cells.

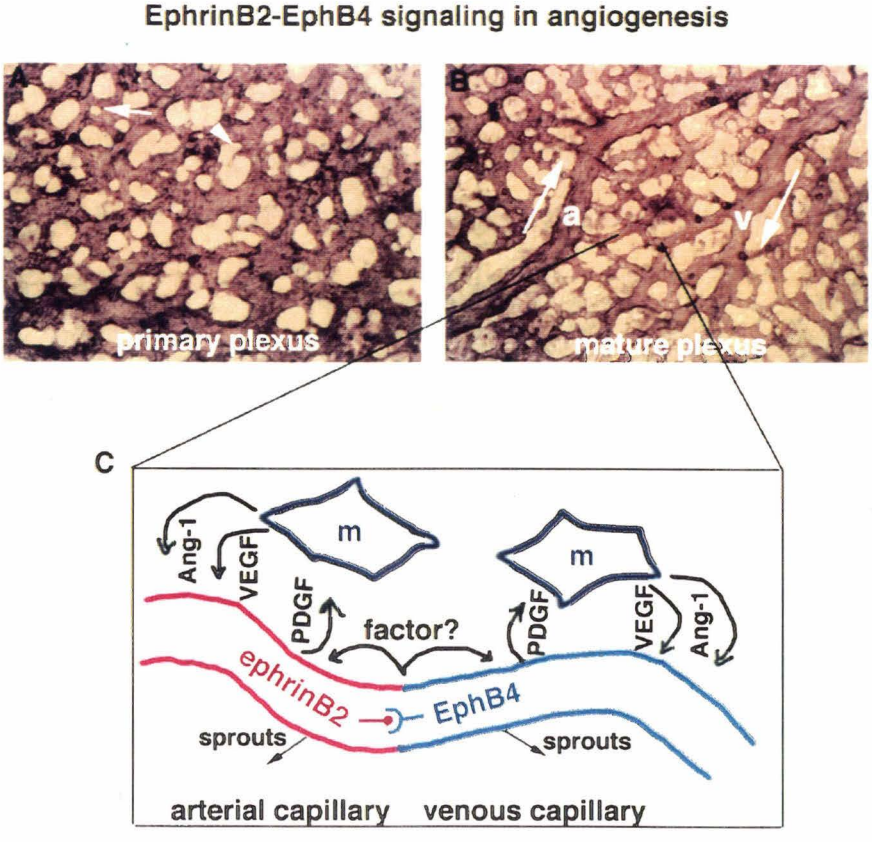

C) Targeted deletion of EphB4 receptor

EphrinB2-EphB4 ligand-receptor signaling system provides us a starting point to study the interactions between arterial and venous endothelial cells, and the angiogenesis of the two types of vessels in the capillary beds. EphB4 knockout mice would serve as an important complementary study to ephrinB2 deficient mice. Is EphB4 essential for vein development? Would capillary beds of the yolk sac and head region be defective in terms of remodeling like the phenotypes seen in ephrinB2 mutants? What would happen in ephrinB2 and EphB4 double heterozygous mice where the strength, though not entirety, of the signaling system is reduced? Addition to the genetical analysis, EphB4 targeting, by an inframe insertion of lacZ gene, would provide us a useful enzymatic marker for venous endothelial cells. EphB4 targeting project is currently pursued by Sebastian Gerety in our lab.

D) Gene hunt for artery or vein restricted molecules

One immediate implication of the molecular distinction of arterial and venous endothelial cells is that more genes are likely expressed differentially in arteries and veins during development. To isolated such genes, we plan to build cDNA libraries from arterial and venous endothelial cells from early stages of the embryonic development. There are two simple ways to do this. One way is to take mid-gestation embryonic umbilical arteries and veins, physically separate them, and isolate endothelial cells by FACS via staining of cell surface markers. The other way is to isolate E10 yolk sacs, dissociate the tissue, and sort out mixed arterial and venous endothelial cells by FACS. With either approach, we run into the problem of a small number of endothelial cells (around $3x10^4$) that could be sorted out

from a given tissue. Single cell PCR amplification could be a useful tool in constructing desired libraries.

E10 yolk sacs have been tested by staining with PECAM-1 antibody and sorting by FACS. Roughly 5% positive cells can be sorted out of the total viable population (figure). I plan to sort out single positive cells into individual wells of 96 well-plates that contain lyse buffer. Reverse transcription and single cell PCR would be then used for cDNA amplification and library construction. Quality of such libraries will be examined by southern blot probing with various endothelial markers such as pan-endothelial Flk1, Flt1 and Tie2, arterial ephrinB2, and venous EphB4. Quality checked libraries from single cells of arterial or venous origin will be screened against each other through differential hybridization.

E) In vitro culture studies of arterial and venous endothelial cells

Our finding on the distinction of arterial and venous endothelial cells suggests that they may response differently to growth factors and angiogenic stimuli. In vitro culture studies would be useful to test the growth and angiogenic potentials of arterial and venous endothelial cells isolated by FACS.

For pilot experiments, we (Sebastian Gerety and I) dissociated E9.5 yolk sacs, and plate cells in fibronectin coated dishes. Culture medium was composed of 10% FBS, 10ng/ml VEGF, and 10ng/ml bFGF. Two morphologically distinct cell types were observed after overnight culture. One type was smooth muscle cells that were larger and spread-out. Another type of cells were smaller, with cobblestone morphology. To confirm that the latter type of cells were endothelial, as well as a portion of them were arterial, I performed PECAM-1 and ephrinB2-lacZ double labeling. Figure 7 shows PECAM-1 (brown) and ephrinB2-lacZ (blue) co-labeled endothelial cells that had been cultured for 3 days in vitro. Adjacent smooth muscle cells were negative for both markers. Venous endothelial cells,

positive for PECAM-1, but negative for lacZ, were also observed in such cultures (not shown). This result suggested that arterial expression of ephrinB2 can be maintained for short term in culture.

I was not successful in establishing longer term culture (one week and more) of mixed populations of yolk sac cells (endothelial and smooth muscle), or pure endothelial cells sorted by FACS. Endothelial cells did not proliferate enough to generated large clones in several different media I tested. Neither FBS nor hypothalamic protein extract (Upstate) promoted endothelial cell proliferation. We think that oncogene mediated immortalization could be used to generate cell lines (arterial or venous) from these primary endothelial cultures.

Figure 7. PECAM-1 and ephrinB2-lacZ double labeling of 3-day cultured yolk sac endothelial cells.

PECAM-1 (brown) and ephrinB2-lacZ (blue) co-labeled endothelial cells are shown in **A** and **C** by arrows. Adjacent smooth muscle cells were negative for both markers shown in phase photos in **B** and **D** by arrowheads.

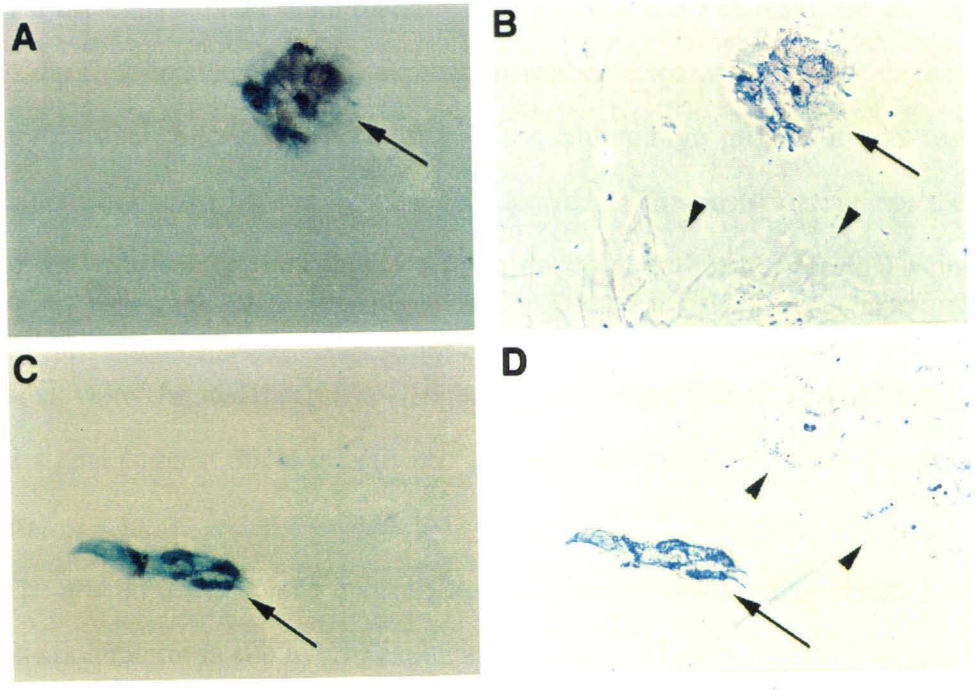

F) Specification of arteries and vein in an early embryo

The specification of arterial and venous endothelial cells and the subsequent establishment of their primary plexi may require patterning events yet unexplored. Two lines of evidence suggest that the expression of ephrinB2 is activated as a result of arterial identity specification of the early endothelial cells. First, ephrinB2 is not expressed at E7.5 and E8.0 when the earliest endothelial markers such as Flk1 and PECAM1 are expressed (not shown). The first notable ephrinB2 expression was detected around E8.5 in the yolk sac and embryo proper. Second, in both the yolk sac and embryo proper, it was restricted in arterial endothelial cells, i.e., endothelial cells located in the posterior but not the anterior region of the yolk sac, or endothelial cells in dorsal aorta but not cardinal veins. Aortic endothelial cells are located centrally, in vicinity to neural tube and notochord, in contrast to the cardinal veins located laterally. Together, the temporal and spatial distribution of ephrinB2 signal suggest that it is activated in committed endothelial cells located near the central axis.

The arterial restriction of ephrinB2 expression is conserved in chick. I performed ephrinB2 wholemount in situ hybridization in 2 to 3 day old chick embryos. Figure 8 shows that chick ephrinB2 is expressed in aorta, but not in lateral cardinal veins. Weaker expression of ephrinB2 was observed in dorsal neural tube and myotome. Intense chick ephrinB2 staining was detected in eye lense and dorsal retina region, like the pattern seen in mouse.

One hypothesis is that diffusible axial signals from the notochord, such as Sonic Hedgehog (Shh), may activate ephrinB2 in aortic endothelial cells. Endothelial cells of the laterally located cardinal veins may respond to a lower level of Shh, and/or receive instructions from lateral mesoderm derived signals such as BMPs. To test the roles of

notochord and Shh in ephrinB2 activation, we plan to use Shh knockout mouse embryos for loss-of-function studies. For gain-of-function studies in chick, we plan to ectopically graft notochords, or implant Shh soaked bead, in the lateral mesoderm next to the forming cardinal veins. Unlike mouse ephrinB2, the chick homolog has no detectable expression in sclerotome of the caudal somite halves (not shown). The absence of sclerotomal signals provides a clear background for the assay of ectopic chick ephrinB2 induction in the cardinal veins.

Figure 8. Expression of chick ephrinB2 in aorta and retina.

Whole mount in situ hybridization was used to study ephrinB2 expression in 3 day old chick embryos. C-ephrinB2 showed strong expression in dorsal retina (**A**, arrow), and in developing lens (**A**, arrowhead). In trunk region, c-ephrinB2 is expressed in roof plate of neural tube (**B**, asterisk) and developing dermamyotome (**B**, dm). In the vascular system, its expression is restricted to the artery / dorsal aorta (da), and not in the bilateral cardinal veins (**B**, arrowheads).

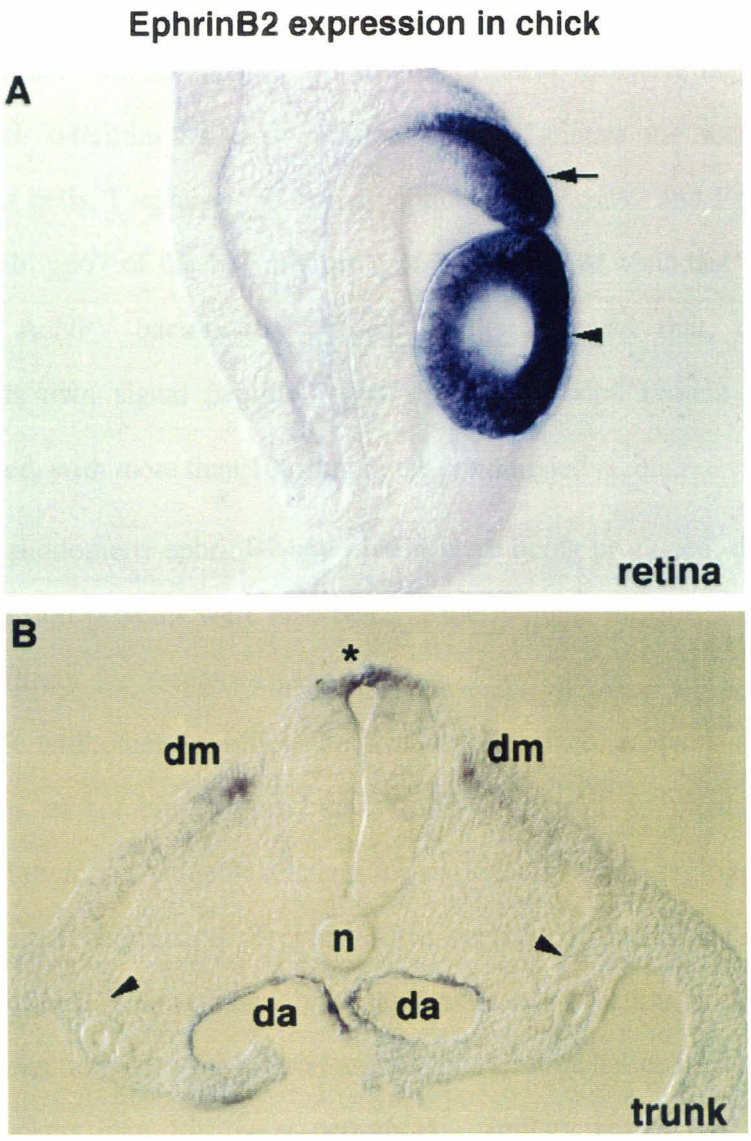

G) Antibodies, soluble ligands, and anti-angiogenic perturbations

EphB4 and ephrinB2 are cell surface molecules that distinguish arterial and venous endothelial cells. We are interested in generating monoclonal antibodies to the extracellular domains of these two molecules. Such antibodies would be useful for a variety of studies, such as cell or section staining, FACS analysis, and anti-angiogenic perturbations. To produce soluble proteins for immunization, I made a series of baculovirus vectors containing the extracellular domains of ephrinB2 and EphB4, that were tagged with multiple Histidines at their c-termini for easy purification. To facilitate the secretion of soluble proteins by insect cells, I replaced the signal peptides of ephrinB2 and EphB4 with that of acidic glycoprotein gp67 of the baculovirus. gp67 is the most abundant envelope surface glycoprotein of AcNPV baculovirus. Present results indicated that, compared to the ephrinB2 with its own signal peptide, gp67-ephrinB2 fusion protein was much more efficiently secreted, with more than 10μg/ml in the conditioned media.

Not only monomeric ephrinB2 and EphB4 were being produced, dimeric ephrinB2- and EphB4-Fc fusion proteins were also being made. Soluble dimeric fusion proteins will have a higher affinity for receptor-ligand binding. They can be further multimerized via polyclonal anti-Fc antibodies for efficient activation of surface receptors or ligands. These different versions of soluble ephrinB2 and EphB4, as well as monoclonal antibodies generated against them, are valuable reagents for angiogenic or anti-angiogenic experiments.

The persistent expression of ephrinB2 in arterial endothelial cells in adult tissues suggests that ephrinB2 mediated signaling may continue to function in adult angiogenesis. Inhibiting the interactions between arterial and venous endothelial cells in the capillary beds by ephrinB2 blockers may selectively perturb the capillary vessel development. Several assays will be used to evaluate the above reagents in terms of their antiangiogenic potentials.

First, chorioallantoic membrane (CAM) assay can be used to test those soluble proteins in the chick extra-embryonic vascular system. They can be tested for their ability to inhibit endogenous vessel growth or remodeling in the CAM. Or they can be tested in combination with bFGF or VEGF, for inhibition of bFGF or VEGF induced ectopic vessel growth in the CAM.

Second, rabbit or mouse corneal assays can be utilized for testing their abilities to inhibit vessel growth in mammals. Other antiangiogenic substance such as angiostatin have been tested in this assay (O'Reilly et al., 1994). Hydron pellets soaked in angiogenic factors such as bFGF or VEGF were inserted under corneal micropockets. Within 6 days, neovascularization from the corneal lime bud to the pellet would occur. When hydron pellet was saturated with both angiogenic factors and angiostatin, and then implanted, neovascularization was inhibited (O'Reilly et al., 1994). Our soluble proteins of monomeric/dimeric ephrinB2 and EphB4, as well as monoclonal antibodies generated against them could be tested in this fashion, for their abilities to block endogenous artery-vein interactions.

Third, the antiangiogenic potentials of our reagents could be tested in tumor cell line implantation assays. Various cell lines of Lewis Lung Carcinoma (LLC) can be injected subcutaneously into C57BL6/J mice (O'Reilly et al., 1997). Primary tumor formation by such cell lines is associated with extensive tumor vascularization. One way to inhibit such tumor growth in vivo, is to transfect LLC cells in vitro with our vectors expressing soluble ephrinB2 or EphB4. We can then transplant the engineered LLC cells, and their tumor growth rate will be compared with that of normal LLC cells. An alternative experiment is to mix LLC cells with our monoclonal antibody secreting hybridoma cells for co-implantation. Antibody against ephrinB2 or EphB4 secreted within the tumor implants may reduce the vessel infiltration by endogenous arteries and veins.

H) Concluding remarks

EphrinB2 and EphB4 distinguish embryonic arterial and venous endothelial cells. EphrinB2 is also stablely expressed in adult arteries, big and small. EphrinB2 mediated signaling between arteries and veins may persist in adult tissues and tumors. The nature of ephrinB2-EphB4 signaling between arterial and venous endothelial cells in angiogenesis remain unexplored. There are several implications and applications based on our finding. First, more genes are likely expressed differentially in arteries and veins, which is consistant with the physiological and pathological differences between the types of vessels, i.e., arterial hypertension and arteriosclerosis. Second, the specification of arterial or venous endothelial cells and the subsequent establishment of the aorta or veins in the embryo suggest novel inductive or patterning events. Third, the ephrinB2-EphB4 signaling system between arteries and veins is a potential antiangiogenic target for controlling abnormal vascular development such as tumor angiogenesis. These and other aspects of the arteries and veins are subjects of ongoing and future studies that may enhance our understanding of the vascular system.

Appendix I

Nep-Fc, its decoration studies and collagen ligands

This appendix describes our attempt to clone ligand for receptor tyrosine kinase Nep/DDR1. It documents the production of Nep-Fc fusion proteins, using such fusion proteins as affinity probes to decorate cells and embryo sections, and our interpretation of the staining results in the light of the recent identification of collagens as ligands for Nep/DDR1.

Nep is one of the known receptor tyrosine kinases (RTK) identified in my neural crest survey experiments (Chapter 2). Nep is expressed in the neuroepithelia and early dorsal root ganglia (Zerlin et al., 1993). Nep and tyro10 are two related orphan RTKs identified during 1993 to 1994. They are distinguished by a structural domain in their extracellular portions homologous to discoidin 1 protein of the slime mold Dictyostelium discoideum (Poole et al., 1981). These discoidin 1 domains are also found in other vertebrate proteins such as coagulation factors V and VIII, and a neural recognition molecule in Xenopus call A5 (Eaton et al., 1987; Jenny et al., 1987; Takagi et al., 1987). Nep and tyro10 have now been renamed as DDR1 and DDR2, respectively.

As one of my expression cloning projects several years ago, identification of a ligand for Nep seemed attractive due to its strong expression in early DRG and neuroepithelia. To produce an affinity probe for Nep ligand, I constructed fusion protein between Nep extracellular domain and human IgG1 Fc. The fusion construct was transiently transfected into 293 cells, and conditioned media were collected and assayed by western blotting. Figure 1 shows the Nep-Fc fusion proteins identified by polyclonal antibodies again Fc. Under non-reducing condition, Nep-Fc is a dimer of 180 Kd. I also constructed a monomeric Nep-Fc fusion molecule by using the Fc domain without the hinge region which contains 2 cysteins for dimerization. Such fusion protein was secreted as a monomer in

conditioned media at a higher level than the dimers (not shown). The unconcentrated conditioned media contained about 10 μg/ml dimeric Nep-Fc or 20 μg/ml for the monomeric Nep-Fc.

Conditioned media were typically filtered and stored at 4^0C for up to 2 weeks, or Nep-Fc fusion proteins were purified over protein-A columns (Pierce). Figure 2 shows a coomassie staining of 1 μg of purified Nep-Fc dimers on a non-reducing gel.

Both conditioned media and purified Nep-Fc were tested for staining of cells and embryo sections. Culture staining of various freshly dissociated tissues have failed to reveal any signal (not shown). No specific staining were observed for Nep-Fc over control Fc proteins. Next, I performed decorations on embryo sections. Intense staining were observed on fresh frozen tissue sections of various embryonic stages. Staining signals were obtained by both conditioned media or purified Nep-Fc proteins. The signals were consistently associated with connective and cartilage tissues, such as peri-aorta smooth muscle cells (Figure 3A, arrowhead), gut mesenchyme (3A, arrow), connective linings of sciatic nerves (3B, arrow), and all embryonic cartilage (3C, arrows). These results suggested that the ligand(s) for Nep was located in non-neuronal tissues. The abundance of such ligand in cartilage and connective tissues suggested a nature of extracellular matrix, either in a membrane form or a secreted component of the ECM.

The identification of Nep ligands was published in December 1997 by researchers of Regeneron and of Tony Pawson lab in Toronto (Shrivastava et al., 1997; Vogel et al., 1997). Various subtypes of collagens are ligands for Nep/DDR1 and tyro10/DDR2. Interestingly, the Pawson group has showed that matrigel, a commercially available preparation of basal membrane proteins from mouse sarcoma, can induce autophosphorylation of Nep receptor. They actually used matrigel as the source for ligand purification. Nep/DDR1 was shown to interact with all types of collagen tested (Vogel et al., 1997), consistent with our results of the Nep-Fc decoration studies on embryo sections.

Figure 1. Western blot analysis of Nep-Fc fusion protein.

Conditioned media containing Nep-Fc fusion proteins were collected from transfected 293 cells, and subjected to western blot analysis with HRP-conjugated polyclonal antibodies against Fc (Jackson). Lane 1 to 4 are 1ng, 5ng, 10ng and 20ng of human IgG1 control proteins, respectively. Land 5 and 6 are 5 μl and 20 μl of conditioned media containing Nep-Fc. Under non-reducing condition, control IgG1 were dimers of 180 Kd, and Nep Fc fusion proteins were dimers of 170 Kd. The unconcentrated conditioned media contained about 10 μg/ml dimeric Nep-Fc.

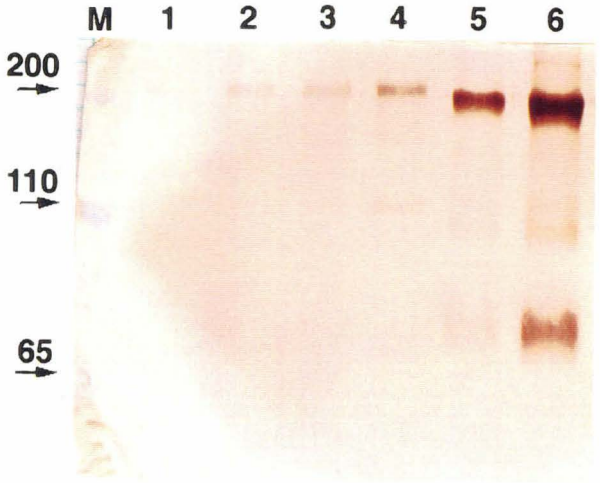

Figure 2. Coomassie staining of purified Nep-Fc fusion protein.

Dimeric Nep-Fc fusion proteins purified by protein-A column were visualized on a non-reducing gel by commossie staining. Lanes 1 and 2 contained 10 and 1 μg of BSA, respectively. 5 μl of PBS solution containing purified Nep-Fc was loaded into lane 3. The estimated concentration of purified Nep-Fc was 100 μg/ml.

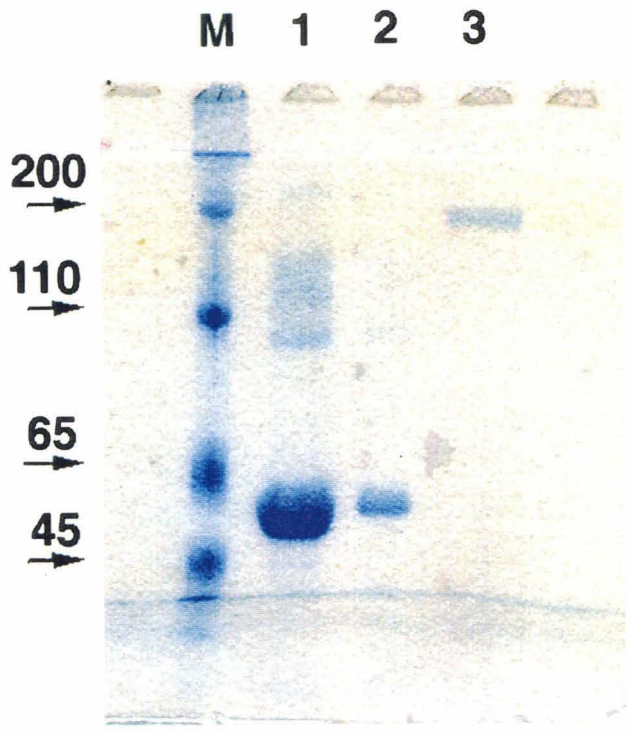

Figure 3. Section staining by Nep-Fc fusion proteins.

Fresh frozen tissues were sectioned and stained by Nep-Fc protein. Purified Nep-Fc or conditioned medium gave identical specific staining results. **A**, Transverse section of E14 mouse trunk region. Aorta lining (arrowhead) and gut mesenchyme (arrow) cells were labeled. **B**, Newborn sciatic nerves were isolated, frozen, sectioned and stained. Connective linings (arrow) were strongly labeled. **C**, Cross section of mouse E14 caudal trunk region. All embryonic cartilage were strongly labeled (arrows).

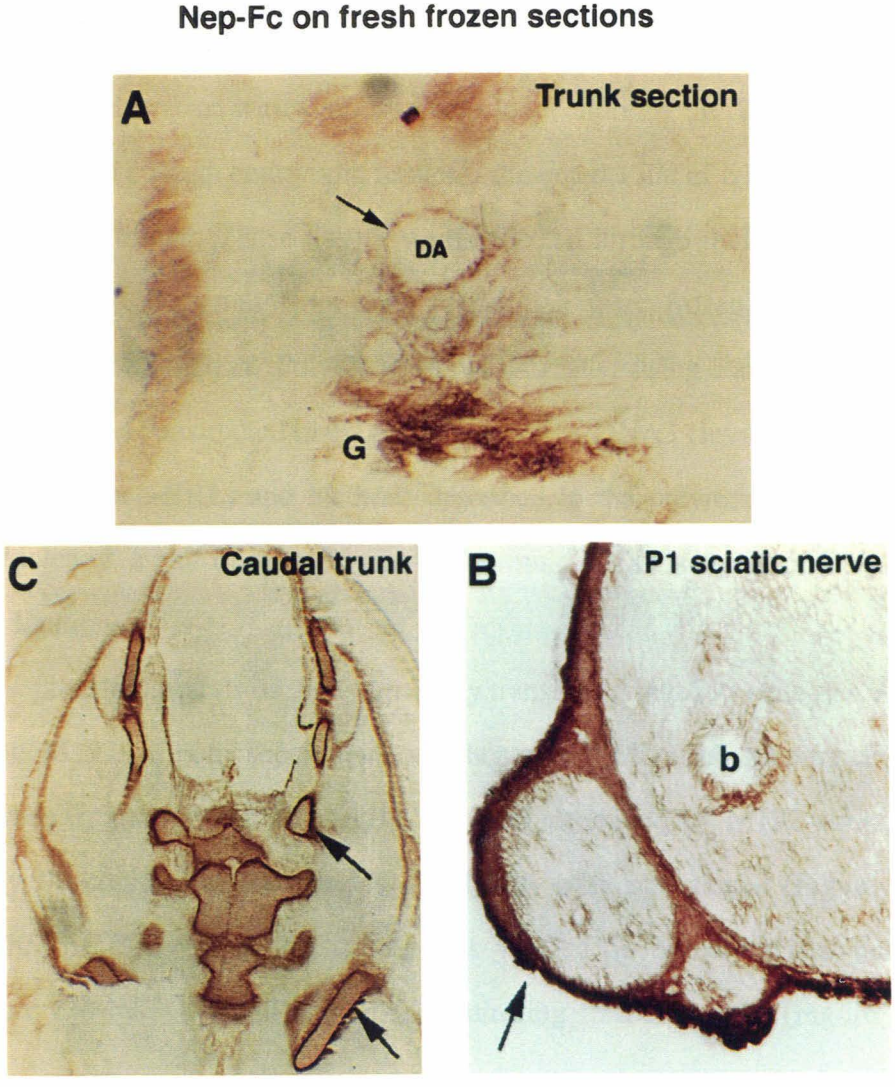

Appendix II

An expression library of rat-E14 DRG, and a p75 screen

One of the earliest application of expression library is cloning surface antigens by monoclonal antibodies (Aruffo and Seed, 1987; Aruffo and Seed, 1987; Seed, 1987). For a pilot experiment prior to several of my expression cloning projects, I made an expression library from rat embryonic DRG which is rich in glia progenitors and the low affinity NGF receptor p75 molecule. The quality of this expression library was then checked by transient transfection and decoration with a mouse monoclonal antibody -M192, against rat p75.

To isolated enough embryonic tissues, I dissected 1500 of E14 rat DRGs from about 100 embryos (10 litters). Those tissues were collected through multiple dissections over a period of 2 weeks. Materials from each preparation were frozen in -80^{0}C until pooled together for RNA extraction. Poly-A RNA was isolated using Fastrack kit (Invitrogen). Plasmid library was constructed in expression vector pCDNA3 (Invitrogen) using synthesis reagents from Gibco-BRL, and methods described in the previous chapters. To increase cloning efficiency, a pair of inverted non-palindromic BstX1 sites in pCDNA3 were used for cDNA ligations.

The plasmid library was then transiently transfected into 293 cells as a whole without subdivision. M192 antibody supernatant was then used for live cell staining. Figure 1C and 1D (arrowheads) show a pair of positive 293 cells decorated by M192 antibody that was detected by PE-conjugated secondaries. Dead cells were not stained (Figure 1C and 1D, arrow). The specificity of m192 staining was verified on primary sciatic nerve schwann cells (Figure 1A and 1B), and not on contaminating fibroblast cells (Figure 1A and 1B, arrow).

The ease of cloning surface antigens by a monoclonal antibody in a given expression library depends on the abundant of the antigen in the tissue source. Through limited dilution experiments, I found that if the percentage of the desired antigen plasmid is more than 0.1% of the library (1 out of 1000), no subdivision is needed. For p75 cloning, a pure source such as cultured sciatic nerve schwann cells or a tissue containing abundant glia progenitors such as early DRG, would be ideal. For a complex tissue, one need to subdivide the plasmid library into pools of 1000 plasmids, and screen 50 to 100 pools. In any case, these results encouraged me to pursue other expression cloning projects involving Fc-tagged receptor bodies.

Figure 1. Expression screening by low affinity NGF receptor p75 monoclonal antibody M192. Rat DRG expression library was transfected into 293 cells which were stained with M192 hybridoma supernatant, detected by PE-conjugated polyclonal antibodies against mouse IgG (Jackson). **C** and **D**, Arrowheads point to a pair of positive 293 cells decorated by M192 antibody. Arrow shows negative dead cells. **A** and **B**, Primary schwann cell culture confirmed the staining specificity of M192 on schwann cells, but not on fibroblast cells (arrow).

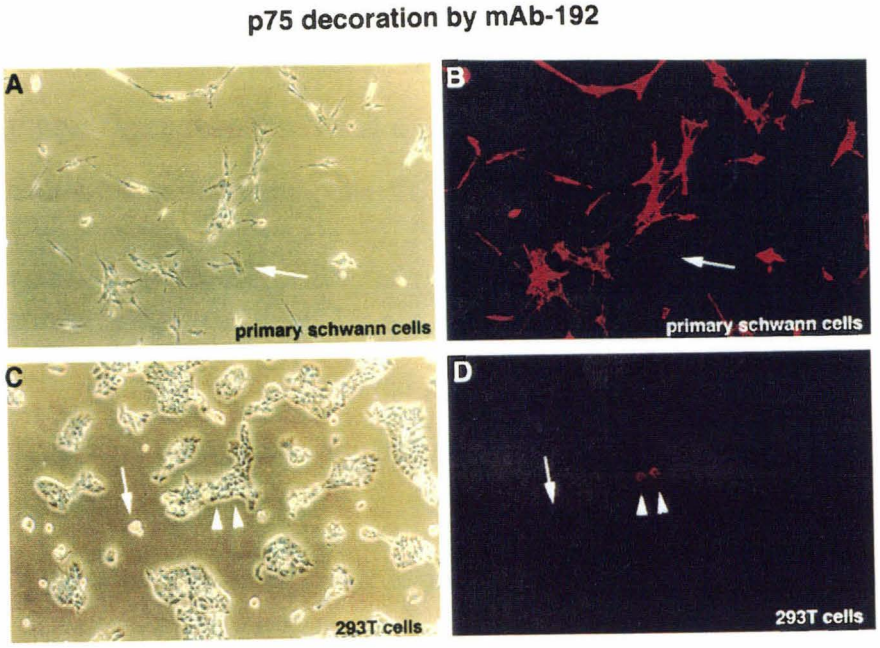

Appendix III

A) Degenerate bHLH primers and screen

Basic helix-loop-helix proteins play important roles in neural development, particularly in lineage restrictions. Mash1 and Neurogenins, two types of related bHLH transcription factors, are essential regulators in vertebrate autonomic and sensory neuron lineage (Fode et al., 1998; Guillemot et al., 1993; Ma et al., 1998). In the peripheral nervous system, glial cells consist of another important neural lineage. Mash1 or Neurogenin related bHLHs in the glia cell lineage, however, were not identified so far. The bHLH superfamily is composed of many subfamilies such as MyoD, NeuroD, Twist and SCL/TAL groups. One possibility is that a novel subfamily of bHLH proteins exist in glia progenitors and/or mature schwann cells. To identify such novel bHLH genes, we decided to use a degenerate PT-PCR approach.

My primer design was based on a survey of many different bHLH subfamilies. I found that there are two motifs conserved across all subfamilies, but also with enough residue variations for creating subfamily biased primers.

The 5' epitope is around the basic region. seven primers were designed for unbiased or biased primers.

A N A/E/D R E R

an almost unbiased primer for almost all subfamilies

A S E R E K

a variation of the first primer. The last a.a. "K" biases a new subfamily consisting Mesogenin and its related members.

A N A R E R N/K

1 a.a. extension on the first primer, biasing NeuroD and Neurogenin related members.

A N A/E R E R R

1 a.a extension on the first primer, biasing dHand, PTF1, and MyoD related members.

A N A R E R T/S

1 a.a extension on the first primer, biasing MATH3/Atonal3 and related bHLHs.

A N A R E R D/E

1 a.a extension on the first primer, biasing Scleraxis and Paraxis related proteins.

A N A R E R Q

1 a.a extension on the first primer, biasing Twist, Mist, and Sustagenin (see below) related members.

The 3' primers are around a.a behind the second helix region. Two primers were designed to cover majority of the bHLH genes.

K I/V E T/I L R L/F A

for majority of the bHLH genes.

L T K I E/Q T L

for majority of the bHLH genes. The bHLH members that not covered by the above 3' primer would be likely covered by this one, and vice versa.

B) Cloning of Sustagenin and a targeting construct

Degenerate PCR with above primers were performed on cDNA prepared from primary rat sciatic nerve schwann cells, and from GGF treated neural crest cells. Different primer combinations were used in this experiment, and appropriate bands were purified and re-amplified for cloning. Sequencing of 60 or so PCR inserts revealed several different bHLH products, among which is a novel gene fragment we now named Sustagenin (SGN) based on its unique expression in olfactory sustentacular cells. SGN showed up 20 or so times in the 60 inserts, thus representing one third of the total.

Sequence search against genebank revealed a close homology between the bHLH regions of SGN and Mash1, with a 60% a.a. identity. SGN could represent an additional family member of the Mash1 subgroup. However, as described below, its sequence outside of the bHLH domain is very divergent from that of Mash1. SGN could be the first member of a new subfamily.

To get full length cDNA of SGN, a 129SVJ genomic library (Stratagene) was screened with the 130 base pair bHLH fragment of the rat SGN. Because bHLH genes usually consist of a single exon, genomic libraries represent convenient sources for cDNA cloning. Under high stringency washes (0.2 x SSC), several phage clones were isolated. Analysis revealed that they were overlapping genomic fragments. One clone contained a full length ORF of SGN, and was chosen for further mapping and creating a targeting construct (see below).

The ORF of SGN is 174 a.a, with bHLH region located near the c-terminal (Figure 1A). Genebank search and sequence alignment confirmed that SGN is closely related to Mash1 at their bHLH domains (Figure 1B). But due to the divergence of SGN to other members at its sequence outside bHLH domain, it is likely a member of a new subfamily. Such hypothesis promoted me to screen SGN related genes using various methods, such as

degenerate PCR, and low stringency hybridization of genomic libraries. Repeated PCR and hybridization using both the bHLH and the non-bHLH SGN sequences all failed to obtain SGN related genes (not shown).

The expression pattern of SGN in development was studied in various embryonic tissues at different developmental stages. Between E8.5 to E13.5, no signal was detected anywhere in wholemount embryos or tissue sections by using digoxigenin based in situ probes. The riboprobes used in these experiments were good, since they have subsequently given excellent signals in the olfactory epithelia in older embryos (see below). It is very possible that SGN is expressed at low level in developing glia cells in the sensory ganglia or sciatic nerves, but below the detection of our methods. Krox-20, a zinc-finger transcription factor is such an example. It is expressed at very low level in developing glial cells. Thin section in situs were unable to demonstrate its expression. Better visualization of krox-20 was achieved by in-frame gene targeting with lacZ gene, and followed by prolonged lacZ staining (Topilko et al., 1994). Krox-20 knockout mice revealed its important role in schwann cell myelination. Likewise, I think the expression and the function of SGN in the peripheral nervous system can be better examined in knockout animals with an in-frame lacZ insertion.

From E14.5 stage onward, SGN has a persistent expression in sustentacular cells (Figure 2A) which are glia-like supporting cells of the olfactory epithelium (Crews and Hunter, 1994). In comparison, mash1 is expressed in basal stem cells (Figure 2B), and SCG10, a pan-neuronal marker, is expressed in the mature olfactory neuron zone (Figure 2C). There are two interesting features of the SGN expression pattern. First, SGN was expressed as early as E14.5, the stage when first sustentacular cells were reported (Crews and Hunter, 1994). Second, the expression of SGN is absent in the majority of the sustentacular cells. Only 10% of the mature sustentacular cells in the apical olfactory epithelium express SGN. Together, the temporal and spatial distribution of the SGN expression pattern suggest it could be restricted to a minor population of sustentacular

progenitors. The fact that SGN and Mash1 share sequence homology in their bHLH regions suggests SGN may have a similar function to Mash1 in lineage restriction. While Mash1 is expressed in neuronal stem cells in the basal olfactory layer, SGN may control development of the sustentacular progenitors in the apical supporting layer.

To study SGN's role in olfactory epithelium, and to provide a sensitive gene marker for the possible low level of expression in the developing glial cells, I generated a gene targeting construct with an in-frame insertion of tau-lacZ. Figure 3 shows a diagram of the genomic region surrounding SGN gene, a targeting construct, and the 3' probe for checking the recombination.

Mash1 deficient mice suffer from a depletion of olfactory neurons, but the sustentacular cells remained intact (Guillemot et al., 1993). It will be very interesting to have a conversed situation where sustentacular supporting cells are specifically deleted. Sustentacular cells have been shown to express Steel ligand for the kit tyrosine kinase receptor expressed by underlying olfactory neurons (Guillemot et al., 1993). Deletion of SGN in sustentacular progenitors could potentially delete all supporting cells, and result in a subsequent degeneration of olfactory neurons. Sustentacular cells are also thought to help regulate ions, oxidize toxic compounds on the mucosal surface, and play some role in chemoreception (Zielinski et al., 1988). SGN knockout mice could provide additional insights into aspects of the olfactory physiology that are specifically related to the sustentacular cells.

Figure 1. Peptide sequence and alignment of Sustagenin (SGN).

A, Deduced peptide sequence of SGN from genomic sequence. The ORF is 174 a.a. long. **B**, SGN shares homologous bHLH domain with mouse Mash1. There is a 57% identity over the bHLH region.

A

```
  1  MDTRSYPSPP DRLSVFAESA HLPLSRPFYL DPMVTVHLCP ETPVPASYTD
 51  ELPLLPFSSD TLIMNNYGDP YPFPFPMPYT NYRRCDYTYG PAFIRKRNER
101  ERQRVKCVNE GYARLRRHLP EDYLEKRLSK IETLRAAIKY ISYLQSLLYP
151  DESETKKNPR TASCGSLDPA LRVI*
```

B

```
               70        80        90       100       110       120
SGN   . TLIMNNYGDPYPFPFPMPYTNYRRCDYTYGPAFIRKRNERERQRVKCVNEGYARLRRHLP
                                     || : :||||||:||| || |:| || |:|
Mash1. KRQRSSSPELMRCKRRLNFSGFGYSLPQQQPAAVARRNERERNRVKLVNLGFATLREHVP
            90        100       110       120       130       140

              130       140       150       160       170
SGN   . EDYLEKRLSKIETLRAAIKYISYLQSLLYPDESETKKNPRTASCGSLDPALRVIX
       ::  :|::||:||||:|::||: || ||
Mash1. NGAANKKMSKVETLRSAVEYIRALQQLLDEHDAVSAAFQAGVLSPTISPNYSNDLNSMAG
           150       160       170       180       190       200
```

Figure 2. Sustagenin expression in the newborn olfactory epithelium.

Sustagenin is expressed in sustentacular supporting cells in the apical layer (**A**). Mash1 is restricted to basal stem cells (**B**). SCG10 is strongly expressed in mature olfactory neurons located in the middle zone (**C**).

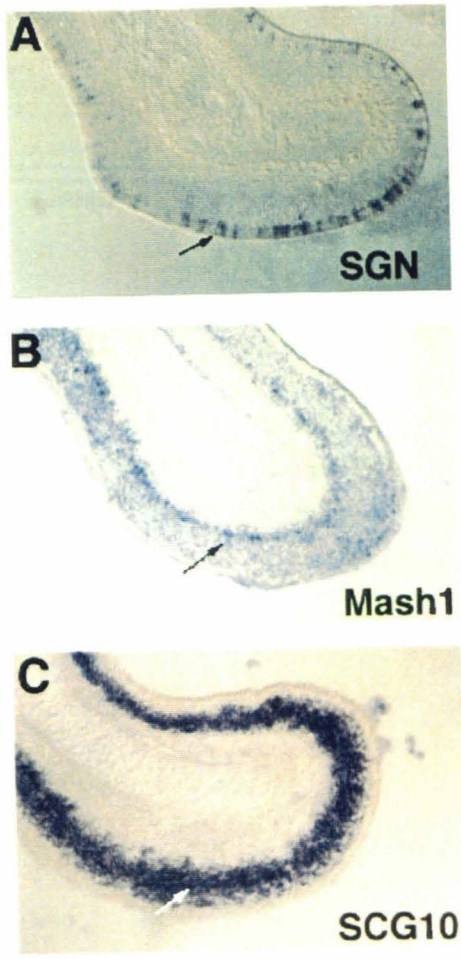

Figure 3. Genomic region of sustagenin and a targeting construct.

SGN is encoded by a single axon, with NCOI site located at its ATG. Tau-lacZ was in-frame inserted at NCOI site, and was followed by pGK-NEO. A 3' probe will distinguish the 7.5 kb wild type and the 4.0 kb targeted fragment, by EcoRI restriction.

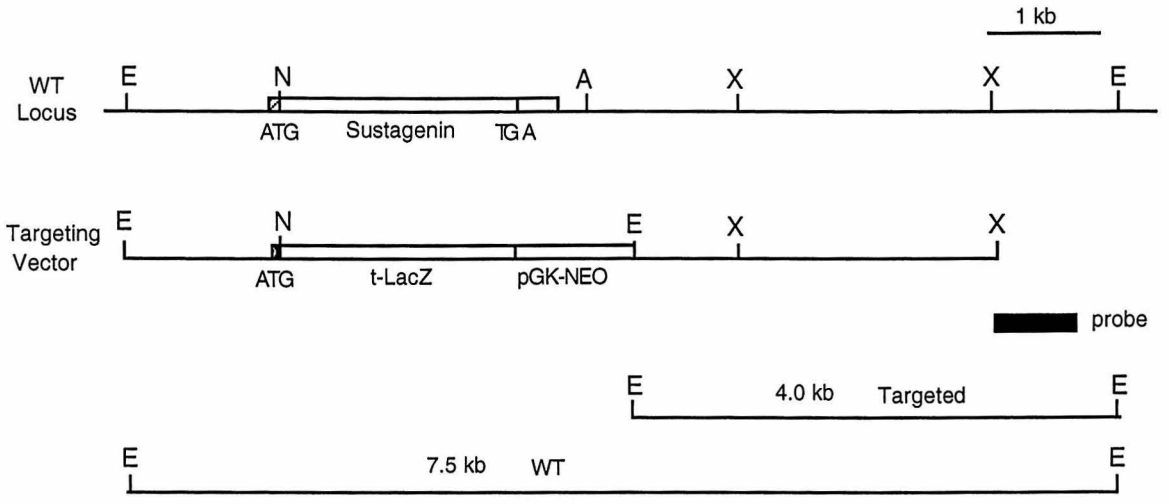

C) Cloning of m- & x-Hes6 and a targeting construct

There are four classes of helix-loop-helix proteins (Benezra et al., 1990; Murre et al., 1989). Class A contains the ubiquitously expressed proteins such as E12/E47. Class B molecules such as those in the bHLH superfamily are expressed in a lineage restricted fashion. Class C proteins such as MYC do not form heterodimers with either class A or B molecules. Class D is composed of negative HLH regulators such as Id-1 and Id-2 that lack the basic region.

In Class B, in addition to those positive acting bHLH molecules such as MyoD and NeuroD, there is a small group of negative players that include Hairy and Enhancer-split (E(spl))related molecules. This second group share a divergent bHLH domain to that of the first one.

To search for novel Hairy and E(spl) related molecules, I designed degenerate primers biased for their bHLH domains and performed RT-PCR on crest cDNA.

For 5' primer biased to Hairy related molecules:

K P/T I M E K

For 5' primers biased to E(spl) related molecules:

K P L/M L E R

or

H P L L/I E K

For 3' primers biased to Hairy related ones:

R L E K A E/D

or

K L E K A E/D

For 3' primers biased to E(spl) related ones:

K F E/D K A E/D

or

H L E K A E/D

One novel Hairy related molecule was cloned from neural crest cDNA, which we named Hes6. Genebank search conveniently revealed one matching cDNA clone in the est database. The est clone, which I called New3c-PAC, was requested and analyzed. It had a 1.2 kb of cDNA insert which contained the entire Hes6 ORF. The ORF is 224 a.a. long, with bHLH domain located near the n-terminal (Figure 1A). At its c-terminal, it has the typical WRPW sequence (underlined) conserved in several Hairy/Hes related molecules. Figure 1B shows the sequence alignment between Hes6 and Hes1. The two related molecules are 57% similar, and 32% identical.

To study the functions of Hes6 in neural crest development, I performed three sets of experiments.

1) cloning of Xenopus Hes6 for gain-of-function experiments in frog embryos.

2) expression studies in early mouse embryos.

3) generating a mouse gene targeting vector.

A xenopus gt10 phage library (gift from Dr. Chris Kintner) was screened under reduced stringency with mouse Hes6 probe. Several strong positive phages were isolated and analyzed. One clone contained a 1.9 kb insert that has the entire xHes6 ORF, and the 3' untranslated sequence including a poly-A stretch. Sequence alignment between mouse and

xenopus Hes6 revealed high homology in their n-terminal halves (Figure 2). xHes6 also has the typical WRPW motif at its c-terminal. xHes6 clone has been sent to Dr. Chris Kintner at UCSD, for expression and functional studies.

Wholemount and section in situ hybridization were used to study Hes6 expression in early mouse embryos. At E9.5 stage, Hes6 is expressed in the migrating crest cells in the trunk (Figure 3). The Hes6 signals in the neural crest cells start at the 10th somite (Arrow. Newly generated somite as the first), and increase in strength more rostrally. Hes6 expression was also observed in cranial ganglia such as the trigeminals (arrowhead). Section staining at E11.5 stage revealed Hes6 expression in the early DRGs (Figure 4A, arrowhead). Strong signals were also located in trigeminal and facial ganglia (4C, arrowheads). In the CNS, signals were observed in marginal zone of the neural tube at the caudal trunk level (4A, arrows). At the rostral trunk level, it is expressed in ventricular zone of the neural tube, with stronger signals in progenitors migrating outward (4B, arrows). In the developing forebrain cortical plate, signals were restricted to newly formed neurons in the marginal layer, and differentiating progenitors migrating towards the marginal layer (4D). In E13.5 olfactory epithelium, the expression of Hes6 is located in marginal layer and in cells migrating outwards (Figure 5A), a very similar pattern to that of forebrain plate. Additional strong expression was observed in developing vomeronasal organ (Figure 5B, arrows) and retina (Figure 5C). In the later stages, Hes6 expression in the mature neurons was reduced. For example, a lower level of expression was seen in the E17.5 olfactory neurons (not shown). Together, these results indicated that Hes6 is expressed by differentiating neuronal progenitors, and the expression is then down regulated in mature neurons. The spatial distribution of Hes6 signals suggests that it may act later in neural differentiation pathway than related members such as Hes1 and Hes5, which are mainly located in ventricular zones (Akazawa et al., 1992; Ishibashi et al., 1995). One possible function of Hes6 is to delay, but not inhibit, the differentiation of committed progenitors and prolong their proliferative phase.

To study its role in neural crest and cranial ganglia development in vivo, I generated a Hes6 targeting construct. Screening and analysis of the Hes6 genomic region revealed that the Hes6 cDNA is encoded by 5 exons. The bHLH domain is located in 2nd and 3rd exons. Stop codon is near the end of the 4th exon. The 5th exon encodes the 3' non-translated sequence. The targeting vector and Hes6 genomic structure are shown in Figure 6. Tau-lacZ, as a cell body and axonal marker, was in frame fused to Hes6 ATG. ES cell targeting and mutant analysis is currently performed by Dr. Jae Kim in our lab.

Figure 1. Peptide sequence of mouse Hes6 and its alignment with mouse Hes1.

A, The mouse Hes6 is 224 a.a. long, with the **WRPW** motif at its c-terminal.

B, Alignment between mouse Hes6 and Hes1 shows a 57% similarity and a 32% identity. The bHLH domains are located near n-terminal for both molecules.

A

```
  1  MAPSQAPSRD RAGQEDEDRW EARGDRKARK PLVEKKRRAR INESLQELRL
 51  LLAGTEVQAK LENAEVLELT VRRVQGALRG RAREREQLQA EASERFAAGY
101  IQCMHEVHTF VSTCQAIDAT VSAELLNHLL ESMPLREGSS FQDLLGDSLA
151  GLPGGSGRSS WPPGGSPESP LSSPPGPGDD LCSDLEEIPE AELNRVPAEG
201  PDLVSTSLGS LTAARRAQSV WRPW*
```

B

```
                .         .         .         .         .
  1 .........MAPSQAPSRDRAGQEDEDRWEARGDRKARKPLVEKKRRARI 41
             ... |:..... ..:....|.:.||..||::||:|||||
  1 MPADIMEKNSSSPVAATPASVNTTPDKPKTASEHRKSSKPIMEKRRRARI 50
            .         .         .         .         .
 42 NESLQELRLLL.....AGTEVQAKLENAEVLELTVRRVQGALRGRARERE 86
    |||| :|: |:      :.. :.|||.|::||:||:::..  |:.  .
 51 NESLSQLKTLILDALKKDSSRHSKLEKADILEMTVKHLRNLQRAQMTAAL 100
            .         .         .         .         .
 87 QLQAEASERFAAGYIQCMHEVHTFVSTCQAIDATVSAELLNHLLESMPLR 136
      ::.. ::: ||: :||:||  |:|||:::::..|.. ||.|| ::|.
101 STDPSVLGKYRAGFSECMNEVTRFLSTCEGVNTEVRTRLLGHLANCMTQI 150
            .         .         .         .         .
137 EGSSFQDLLGDSL.......AGLPGGSGRSSW.............PPGG 165
    :: .:.:   ..|       :: |||..:.:.             ||.|
151 NAMTYPGQAHPALQAPPPPPPSGPGGPQHAPFAPPPPLVPIPGGAAPPPG 200
            .         .         .         .         .
166 SPESPLSSPPGPGDDLCSDLEEIPEAE..................... 192
    |:.:.|:|.:|.:..: :::: :|.::
201 SAPCKLGSQAGEAAKVFGGFQVVPAPDGQFAFLIPNGAFAHSGPVIPVYT 250
            .         .         .
193 LNRVPAEGPDLVSTSLGSLTAARRAQSVWRPW.. 224
     |.... ||: ||.| ||   .  |:|:||||
251 SNSGTSVGPNAVSPSSGS...SLTADSMWRPWRN 281
```

Figure 2. Peptide sequence of xenopus Hes6 and its alignment with mouse Hes6.

Xenopus Hes6 (top) is compared with mouse Hes6 (bottom). High identity is located in the n-terminal half. Overall similarity is 72%, and overall identity is 58%.

Figure 3. Hes6 expression in E9.5 mouse embryo.

Specific signals were detected in cranial ganglia (arrowheads), and migrating trunk neural crest cells. The earliest neural crest expression is located in the 10th somite (arrow). The newly formed somite counts as the first.

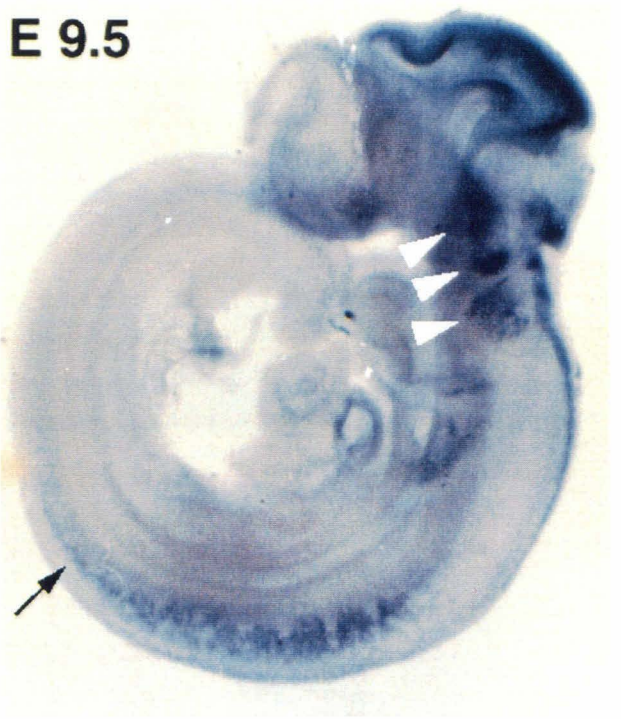

Figure 4. Hes6 expression in E11.5 mouse embryo sections.

In the peripheral nervous system, trunk DRG cells (**A**, arrowhead) and cranial ganglia (**C**, arrowheads) are labeled strongly with Hes6 probe. In the central nervous system, hes6 is expressed in differentiating neural progenitors in the neural tube (**A** and **B**), and in the forebrain cortical plate (**D**). Arrows point to the committed progenitor cells migrating outwards to the marginal zone in the neural tube as well as forebrain.

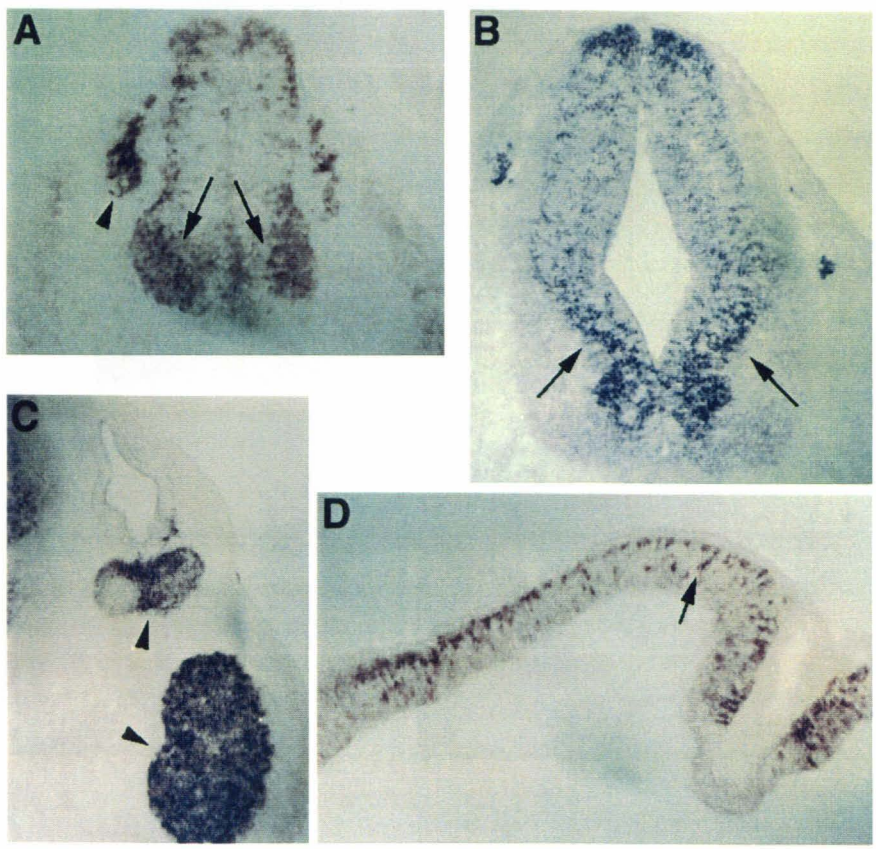

Figure 5. Hes6 expression in E13.5 mouse olfactory epithelium and retina.

Main olfactory epithelium (**A**) as well as accessory vomeronasal organ (**B**) show strong expression in differentiating progenitors located near the basal layer. These hes6 positive cells seem to be migrating toward mature neuron zone, where the expression is down regulated. Strong signals were also observed in developing retina.

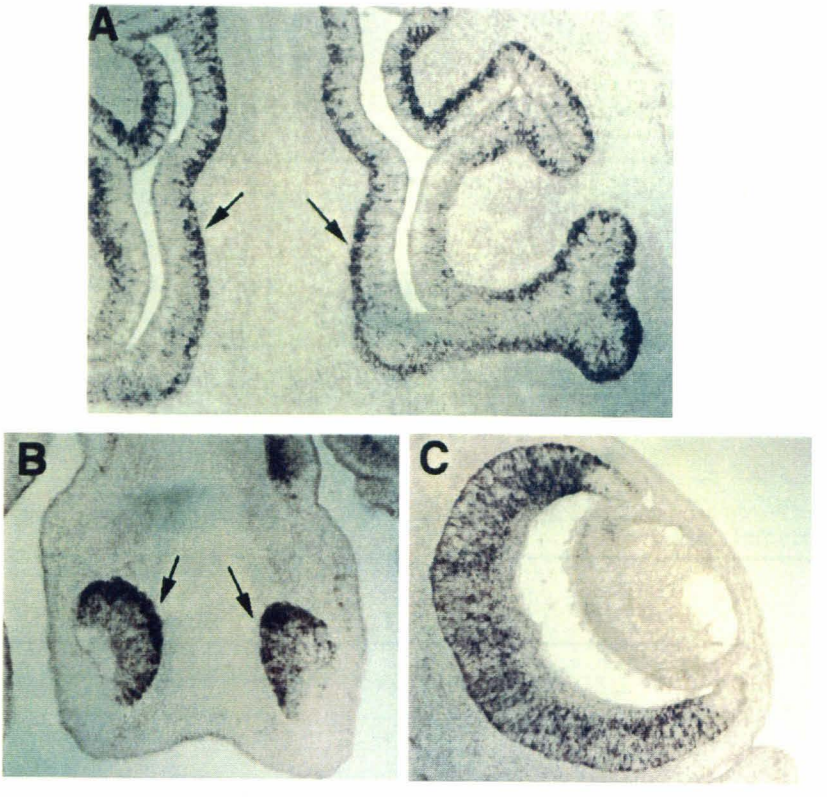

Figure 6. Genomic structure of mouse Hes6 and a targeting construct.

Mouse Hes6 gene is encoded by 5 exons. Coding regions are located in exon 1 to 4. Exon 5 has 3' untranslated sequence. To disrupt the hes6 gene, exon 1 to 3 are replaced with tau-lacZ which is in-frame inserted with the Hes6 ATG in a NCOI site. The 3' probe will distinguish a 5kb targeted or a 10kb wild type fragment, by XbaI restriction.

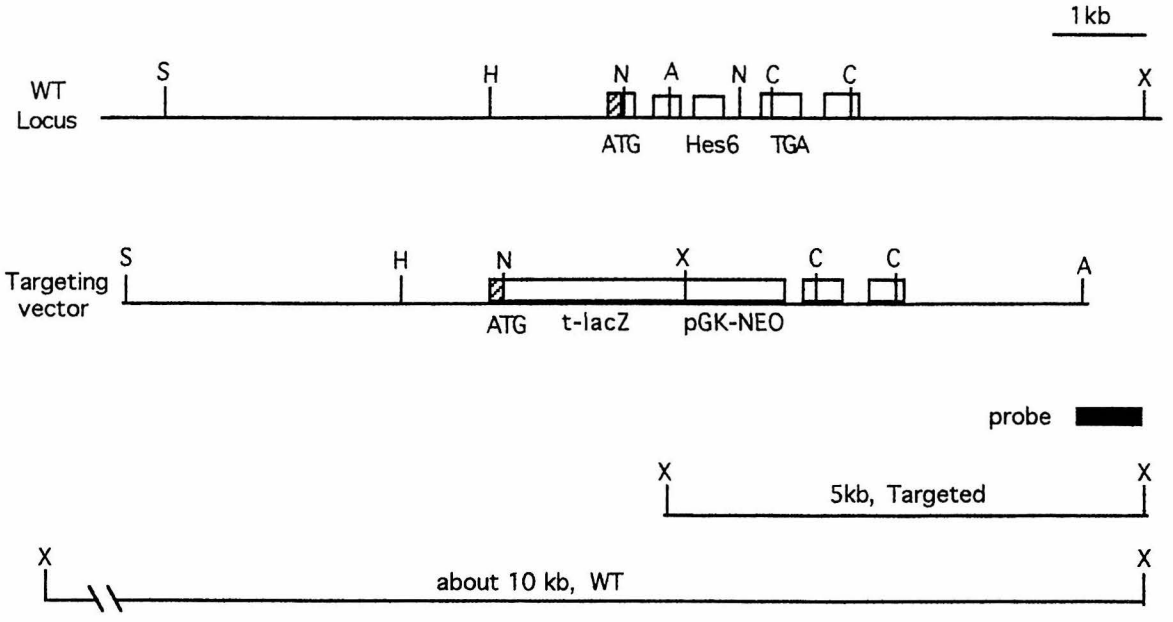

References

Akazawa, C., Sasai, Y., Nakanishi, S., and Kageyama, R. (1992). Molecular characterization of a rat negative regulator with a basic helix-loop-helix structure predominantly expressed in the developing nervous system. J. Biol. Chem. *267*, 21879-21885.

Alvarado-Mallart, R. M. (1993). Fate and potentialities of the avian mesencephalic/metencephalic neuroepithelium. J. Neurobiol. *24*, 1341-1355.

Aruffo, A., and Seed, B. (1987). Molecular cloning of a CD28 cDNA by a high-efficiency COS cell expression system. Proc. Natl. Acad. Sci. *84*, 8573-8577.

Aruffo, A., and Seed, B. (1987). Molecular cloning of two CD7 (T-cell leukemia antigen) cDNAs by a COS cell expression system. EMBO J. *6*, 3313-3316.

Bannerman, P. G., and Pleasure, D. (1993). Protein growth factor requirements of rat neural crest cells. J. Neurosci. Res. *36*, 46-57.

Bartley, T. D., Hunt, R. W., Welcher, A. A., Boyle, W. J., Parker, V. P., Lindberg, R. A., Lu, H. S., Colombero, A. M., Elliott, R. L., and et al. (1994). B61 is a ligand for the ECK receptor protein-tyrosine kinase. Nature *368*, 558-560.

Becker, N., Seitanidou, T., Murphy, P., Mattei, M. G., Topilko, P., Nieto, M. A., Wilkinson, D. G., Charnay, P., and Gilardi-Hebenstreit, P. (1994). Several receptor tyrosine kinase genes of the Eph family are segmentally expressed in the developing hindbrain. Mech. Dev. *47*, 3-17.

Beckmann, M. P., Cerretti, D. P., Baum, P., Vanden Bos, T., James, L., and et al. (1994). Molecular characterization of a family of ligands for eph-related tyrosine kinase receptors. EMBO. J. *13*, 3757-3762.

Benezra, R., Davis, R. L., Lockshon, D., Turner, D. L., and Weintraub, H. (1990). The protein Id: a negative regulator of helix-loop-helix DNA binding proteins. Cell *61*, 49-59.

Bergemann, A. D., Cheng, H. J., Brambilla, R., Klein, R., and Flanagan, J. G. (1995). ELF-2, a new member of the Eph ligand family, is segmentally expressed in mouse embryos in the region of the hindbrain and newly forming somites. Mol. Cell. Biol. *15*, 4921-4929.

Bergemann, A. D., Zhang, L., Chiang, M. K., Brambilla, R., Klein, R., and Flanagan, J. G. (1998). Ephrin-B3, a ligand for the receptor EphB3, expressed at the midline of the developing neural tube. Oncogene *16*, 471-480.

Breier, G., Albrecht, U., Sterrer, S., and Risau, W. (1992). Expression of vascular endothelial growth factor during embryonic angiogenesis and endothelial cell differentiation. Development *114*, 521-532.

Breier, G., Clauss, M., and Risau, W. (1995). Coordinate expression of vascular endothelial growth factor receptor-1 (flt-1) and its ligand suggests a paracrine regulation of murine vascular development. Dev. Dyn. *204*, 228-239.

Bruckner, K., Pasquale, E. B., and Klein, R. (1997). Tyrosine phosphorylation of transmembrane ligands for Eph receptors. Science *275*, 1640-1643.

Carmeliet, P., Ferreira, V., Breier, G., Pollefeyt, S., Kieckens, L., Gertsenstein, M., Fahrig, M., Vandenhoeck, A., Harpal, K., Eberhardt, C., Declercq, C., Pawling, J., Moons, L., Collen, D., Risau, W., and Nagy, A. (1996). Abnormal blood vessel development and lethality in embryos lacking a single VEGF allele. Nature *380*, 435-439.

Chen, J., Nachabah, A., Scherer, C., Ganju, P., Reith, A., Bronson, R., and Ruley, E. H. (1996). Germ-line inactivation of the murine Eck receptor tyrosine kinase by gene trap retroviral insertion. Oncogene *12*, 979-988.

Cheng, H. J., Nakamoto, M., Bergemann, A. D., and Flanagan, J. G. (1995). Complementary gradients in expression and binding of ELF-1 and Mek4 in development of the topographic retinotectal projection map. Cell *82*, 371-381.

Crews, L., and Hunter, D. (1994). Neurogenesis in the olfactory epithelium. Perspect. Dev. Neurobiol. *2*, 151-161.

Davies, J. A., Cook, G. M. W., Stern, C. D., and Keynes, R. J. (1990). Isolation from chick somites of a glycoprotein fraction that causes collapse of dorsal root ganglion growth cones. Neuron *2*, 11-20.

Davis, S., Aldrich, T. H., Jones, P. F., Acheson, A., Compton, D. L., Jain, V., Ryan, T. E., Bruno, J., Radziejewski, C., Maisonpierre, P. C., and Yancopoulos, G. D. (1996). Isolation of Angiopoietin-1, a ligand for the Tie-2 receptor, by secretion-trap expression cloning. Cell *87*, 1161-1169.

Davis, S., Gale, N. W., Aldrich, T. H., Maisonpierre, P. C., Lhotak, V., Pawson, T., Goldfarb, M., and Yancopoulos, G. D. (1994). Ligands for the EPH-related receptor tyrosine kinases that require membrane attachment or clustering for activity. Science *266*, 816-819.

Drescher, U., Bonhoeffer, F., and Muller, B. K. (1997). The Eph family in retinal axon guidance. Curr. Opin. Neurobiol. *7*, 75-80.

Drescher, U., Kremoser, C., Handwerker, C., Loschinger, J., Noda, M., and Bonhoeffer, F. (1995). In vitro guidance of retinal ganglion cell axons by RAGS, a 25 kDa tectal protein related to ligands for Eph receptor tyrosine kinases. Cell *82*, 359-370.

Dumont, D. J., Fong, G. H., Puri, M. C., Gradwohl, G., Alitalo, K., and Breitman, M. L. (1995). Vascularization of the mouse embryo: a study of flk-1, tek, tie, and vascular endothelial growth factor expression during development. Dev. Dyn. *203*, 80-92.

Dumont, D. J., Gradwohl, G., Fong, G. H., Puri, M. C., Gertsenstein, M., Auerbach, A., and Breitman, M. L. (1994). Dominant-negative and targeted null mutations in the endothelial receptor tyrosine kinase, tek, reveal a critical role in vasculogenesis of the embryo. Genes. Dev. *8*, 1897-1909.

Eaton, D. L., Hass, P. E., Riddle, L., Mather, J., Wiebe, M., Gregory, T., and Vehar, G. A. (1987). Characterization of recombinant human factor VIII. J. Biol. Chem. *262*, 3285-3290.

Erickson, C. A., Duong, E. D., and Tosney, K. W. (1992). Descriptive and experimental analysis of the dispersion of neural crest cells along the dorsolateral path and their entry into ectoderm in the chick embryo. Dev. Biol. *151*, 251-272.

Evans, H. M. (1909). On the development of the aortae, cardinal and umbilical veins, and the other blood vessels of vertebrate embryos from capillaries. Anat. Rec. *3*, 498-518.

Ferrara, N., Carver-Moore, K., Chen, H., Dowd, M., Lu, L., O'Shea, K. S., Powell-Braxton, L., Hillan, K. J., and Moore, M. W. (1996). Heterozygous embryonic lethality induced by targeted inactivation of the VEGF gene. Nature *380*, 439-442.

Flanagan, J. G., and Vanderhaeghen, P. (1998). The ephrins and Eph receptors in neural development. Annu. Rev. Neurosci. *21*, 309-345.

Fode, C., Gradwohl, G., Morin, X., Dierich, A., LeMeur, M., Goridis, C., and Guillemot, F. (1998). The bHLH protein NEUROGENIN 2 is a determination factor for epibranchial placode-derived sensory neurons. Neuron *20*, 483-494.

Fong, G.-H., Rossant, J., Gertsenstein, M., and Breitman, M. L. (1995). Role of the Flt-1 receptor tyrosine kinase in regulating the assembly of vascular endothelium. Nature *376*, 66-70.

Fredette, B. J., Miller, J., and Ranscht, B. (1996). Inhibition of motor axon growth by T-cadherin substrata. Development *122*, 3163-3171.

Gale, N. W., Flenniken, A., Compton, D. C., Jenkins, N., Copeland, N. G., Gilbert, D. J., Davis, S., Wilkinson, D. G., and Yancopoulos, G. D. (1996). Elk-L3, a novel transmembrane ligand for the Eph family of receptor tyrosine kinases, expressed in embryonic floor plate, roof plate and hindbrain segments. Oncogene *13*, 1343-1352.

Gale, N. W., Holland, S. J., Valenzuela, D. M., Flenniken, A., Pan, L., Ryan, T. E., Henkemeyer, M., Strebhardt, K., Hirai, H., Wilkinson, D. G., Pawson, T., Davis, S., and Yancopoulos, G. D. (1996). Eph receptors and ligands comprise two major specificity subclasses and are reciprocally compartmentalized during embryogenesis. Neuron *17*, 9-19.

Gale, N. W., and Yancopoulos, G. D. (1997). Ephrins and their receptors: a repulsive topic? Cell Tissue Res *290*, 227-241.

Guillemot, F., Lo, L.-C., Johnson, J. E., Auerbach, A., Anderson, D. J., and Joyner, A. L. (1993). Mammalian achaete-scute homolog-1 is required for the early development of olfactory and autonomic neurons. Cell *75*, 463-476.

Henkemeyer, M., Marengere, L. E., McGlade, J., Olivier, J. P., Conlon, R. A., Holmyard, D. P., Letwin, K., and Pawson, T. (1994). Immunolocalization of the Nuk receptor tyrosine kinase suggests roles in segmental patterning of the brain and axonogenesis. Oncogene *9*, 1001-1014.

Henkemeyer, M., Orioli, D., Henderson, J. T., Saxton, T. M., Roder, J., Pawson, T., and Klein, R. (1996). Nuk controls pathfinding of commissural axons in the mammalian central nervous system. Cell *86*, 35-46.

Holland, S. J., Gale, N. W., Mbamalu, G., Yancopoulos, G. D., Henkemeyer, M., and Pawson, T. (1996). Bidirectional signaling through the EPH-family receptor Nuk and its transmembrane ligands. Nature *383*, 722-725.

Holzman, L. B., Marks, R. M., and Dixit, V. M. (1990). Mol. Cell. Biol. A novel immediate-early response gene of endothelium is induced by cytokines and encodes a secreted protein. Mol. Cell. Biol. *10*, 5830-5838.

Hrabe de Angelis, M., McIntyre, J. N., and Gossler, A. (1997). Maintenance of somite borders in mice requires the Delta homologue DII1. Nature *386*, 717-721.

Ishibashi, M., Ang, S. L., Shiota, K., Nakanishi, S., Kageyama, R., and Guillemot, F. (1995). Targeted disruption of mammalian hairy and Enhancer of split homolog-1 (HES-1) leads to up-regulation of neural helix-loop-helix factors, premature neurogenesis, and severe neural tube defects. Genes Dev *9*, 3136-3148.

Jenny, R. J., Pittman, D. D., Toole, J. J., Kriz, R. W., Aldape, R. A., Hewick, R. M., Kaufman, R. J., and Mann, K. G. (1987). Complete cDNA and derived amino acid sequence of human factor V. Proc. Natl. Acad. Sci. *84*, 4846-4850.

Kalcheim, C., and Neufeld, G. (1990). Expression of basic fibroblast growth factor in the nervous system of early avian embryos. Development *109*, 203-215.

Krull, C. E., Collazo, A., Fraser, S. E., and Bronner-Fraser, M. (1995). Segmental migration of trunk neural crest: time-lapse analysis reveals a role for PNA-binding molecules. Development *121*, 3733-3743.

Krull, C. E., Lansford, R., Gale, N. W., Collazo, A., Marcelle, C., Yancopoulos, G. D., Fraser, S. E., and Bronner-Fraser, M. (1997). Interactions of Eph-related receptors and ligands confer rostrocaudal pattern to trunk neural crest migration. Curr. Biol. *7*, 571-580.

Le Douarin, N. M. (1993). Embryonic neural chimaeras in the study of brain development. Trends. Neurosci. *16*, 64-72.

Lhotak, V., and Pawson, T. (1993). Biological and biochemical activities of a chimeric epidermal growth factor-Elk receptor tyrosine kinase. Mol. Cell Biol. *13*, 7071-7079.

Ma, Q., Chen, Z., del Barco Barrantes, I., de la Pompa, J. L., and Anderson, D. J. (1998). neurogenin1 is essential for the determination of neuronal precursors for proximal cranial sensory ganglia. Neuron *20*, 469-482.

Maisonpierre, P. C., Goldfarb, M., Yancopoulos, G. D., and Gao, G. (1993). Distinct rat genes with related profiles of expression define a TIE receptor tyrosine kinase family. Oncogene *8*, 1631-1637.

Meyer, D., and Birchmeier, C. (1995). Multiple essential functions of neuregulin in development. Nature *378*, 386-390.

Mori, T., Wanaka, A., Taguchi, A., Matsumoto, K., and Tohyama, M. (1992). Differential expressions of the eph family of receptor tyrosine kinase genes (sek, elk, eck) in the developing nervous system of the mouse. Mol. Brain Res. *29*, 325-335.

Murphy, M., Reid, K., Ford, M., Furness, J. B., and Bartlett, P. F. (1994). FGF2 regulates proliferation of neural crest cells, with subsequent neuronal differentiation regulated by LIF or related factors. Development *120*, 3519-3528.

Murre, C., McCaw, P. S., Vaessin, H., Caudy, M., Jan, L. Y., Jan, Y. N., Cabrera, C. V., Buskin, J. N., Hauschka, S. D., Lassar, A. B., Weintraub, H., and Baltimore, D. (1989). Interactions between heterologous helix-loop-helix proteins generate complexes that bind specifically to a common DNA sequence. Cell *58*, 537-544.

Nakamoto, M., Cheng, H. J., Friedman, G. C., McLaughlin, T., Hansen, M. J., Yoon, C. H., O'Leary, D. D., and Flanagan, J. G. (1996). Topographically specific effects of ELF-1 on retinal axon guidance in vitro and retinal
axon mapping in vivo. Cell *86*, 755-766.

Nieto, M. A., Gilardi-Hebenstreit, P., Charnay, P., and Wilkinson, D. G. (1992). A receptor protein tyrosine kinase implicated in the segmental patterning of the hindbrain and mesoderm. Development *116*, 1137-1150.

O'Reilly, M. S., Boehm, T., Shing, Y., Fukai, N., Vasios, G., Lane, W. S., Flynn, E., Birkhead, J. R., Olsen, B. R., and Folkman, J. (1997). Endostatin: an endogenous inhibitor of angiogenesis and tumor growth. Cell *88*, 277-285.

O'Reilly, M. S., Holmgren, L., Shing, Y., Chen, C., Rosenthal, R. A., Moses, M., Lane, W. S., Cao, Y., Sage, E. H., and Folkman, J. (1994). Angiostatin: a novel angiogenesis inhibitor that mediates the suppression of metastases by a Lewis lung carcinoma. Cell *79*, 315-328.

Pandey, A., Shao, H., Marks, R. M., Polverini, R. J., and Dixit, V. M. (1995). Role of B61, the ligand for the Eck receptor tyrosine kinase, in TNF-alpha-induced angiogenesis. Science *268*, 567-569.

Poole, S., Firtel, R. A., Lamar, E., and Rowekamp, W. (1981). Sequence and expression of the discoidin I gene family in Dictyostelium discoideum. J. Mol. Biol. *153*, 273-289.

Rickmann, M., Fawcett, J. W., and Keynes, R. J. (1985). The migration of neural crest cells and the growth of motor axons through the rostral half of the chick somite. J. Embryol. Exp. Morph. *90*, 437-455.

Ring, C., Hassell, H., and Halfter, W. (1996). Expression pattern of collagen IX and potential role in the segmentation of the peripheral nervous system. Dev. Biol. *180*, 41-53.

Risau, W. (1997). Mechanisms of angiogenesis. Nature *386*, 671-674.

Ruiz, J. C., and Robertson, E. J. (1994). The expression of the receptor-protein tyrosine kinase gene, eck, is highly restricted during early mouse development. Mech. Dev. *46*, 87-100.

Sabin, F. R. (1909). The lymphatic system in human embryos, with a consideration of the morphology of the system as a whole. American J. Anatomy *9*, 43-91.

Sabin, F. R. (1917). Origin and development of the primitive vessels of the chick and of the pig. Contrib. Embryol. Carnegie Inst. Washington *6*, 61-124.

Sabin, F. R. (1920). Studies on the origin of blood vessels and of red blood corpuscules as seen in the living bastoderm of chicks during the second day of incubation. Contrib. Embryol. Carnegie Inst. Washington *9*, 214-262.

Saga, Y., Yagi, T., Ikawa, Y., Sakakura, T., and Aizawa, S. (1992). Mice develop normally without tenascin. Genes Dev. *6*, 1821-1831.

Sato, T. N., Qin, Y., Kozak, C. A., and Audus, K. L. (1993). Tie-1 and tie-2 define another class of putative receptor tyrosine kinase genes expressed in early embryonic vascular system. Proc. Natl. Acad. Sci *90*, 9355-9358.

Sato, T. N., Tozawa, Y., Deutsch, U., Wolburg-Buchholz, K., Fujiwara, Y., Gendron-Maguire, M., Gridley, T., Wolburg, H., Risau, W., and Qin, T. (1995). Distinct roles of the receptor tyrosine kinases Tie-1 and Tie-2 in blood vessel formation. Nature *376*, 70-74.

Seed, B. (1987). An LFA-3 cDNA encodes a phospholipid-linked membrane protein homologous to its receptor CD2. Nature *329*, 840-842.

Serbedzija, G. N., Fraser, S. E., and Bronner-Fraser, M. (1990). Pathways of trunk neural crest cell migration in the mouse embryo as revealed by vital dye labeling. Development *108*, 605-612.

Shah, N. M., Marchionni, M. A., Isaacs, I., Stroobant, P., and Anderson, D. J. (1994). Glial growth factor restricts mammalian neural crest stem cells to a glial fate. Cell *77*, 349-360.

Shalaby, F., Rossant, J., Tamaguchi, T. P., Gertsenstein, M., Wu, X.-F., Breitman, M. L., and Schuh, A. C. (1995). Failure of blood-island formation and vasculogenesis in Flk-1-deficient mice. Nature *376*, 62-66.

Shepherd, I., Luo, Y., Raper, J. A., and Chang, S. (1996). The distribution of collapsin-1 mRNA in the developing chick nervous system. Dev. Biol. *173*, 185-199.

Shrivastava, A., Radziejewski, C., Campbell, E., Kovac, L., McGlynn, M., Ryan, T. E., Davis, S., Goldfarb, M. P., Glass, D. J., Lemke, G., and Yancopoulos, G. D. (1997). An orphan receptor tyrosine kinase family whose members serve as nonintegrin collagen receptors. Mol. Cell *1*, 25-34.

Sieber-Blum, M., and Zhang, J. M. (1997). Growth factor action in neural crest cell diversification. J. Anat. *191*, 493-499.

Smith, A., Robinson, V., Patel, K., and Wilkinson, D. G. (1997). The EphA4 and EphB1 receptor tyrosine kinases and EphrinB2 ligand regulate targeted migration of branchial neural crest cells. Curr. Biol. *7*, 561-570.

Suri, C., Jones, P. F., Patan, S., Bartunkova, S., Maisonpierre, P. C., Davis, S., Sato, T. N., and Yancopoulos, G. D. (1996). Requisite role of angiopoietin-1, a ligand for the Tie-2 receptor, during embryonic angiogenesis. Cell *87*, 1171-1180.

Takagi, S., Tsuji, T., Amagai, T., Takamatsu, T., and Fujisawa, H. (1987). Specific cell surface labels in the visual centers of Xenopus laevis tadpole identified using monoclonal antibodies. Dev. Biol. *122*, 90-100.

Topilko, P., Schneider-Maunoury, S., Levi, G., Baron-Van Evercooren, A., Chennoufi, A. B., Seitanidou, T., Babinet, C., and Charnay, P. (1994). Krox-20 controls myelination in the peripheral nervous system. Nature *371*, 796-799.

Vogel, W., Gish, G. D., Alves, F., and Pawson, T. (1997). The discoidin domain receptor tyrosine kinases are activated by collagen. Mol. Cell *1*, 13-23.

Wang, H. U., and Anderson, D. J. (1997). Eph family transmembrane ligands can mediate repulsive guidance of trunk neural crest migration and motor axon outgrowth. Neuron *18*, 383-396.

Wang, H. U., Chen, Z. F., and Anderson, D. J. (1998). Molecular distinction and angiogenic interaction between embryonic arteries and veins revealed by ephrin-B2 and its receptor Eph-B4. Cell *93*, 741-753.

Xu, Q., Alldus, G., Holder, N., and Wilkinson, D. G. (1995). Expression of truncated Sek-1 receptor tyrosine kinase disrupts the segmental restriction of gene expression in the xenopus and zebrafish hindbrain. Development *121*, 4005-4016.

Yamaguchi, T. P., Dumont, D. J., Conlon, R. A., Breitman, M. L., and Rossant, J. (1993). flk-1, an flt-related receptor tyrosine kinase is an early marker for endothelial cell precursors. Development *118*, 489-498.

Zerlin, M., Julius, M. A., and Goldfarb, M. (1993). NEP: a novel receptor-like tyrosine kinase expressed in proliferating neuroepithelia. Oncogene *8*, 2731-2739.

Zielinski, B. S., Getchell, M. L., and Getchell, T. V. (1988). Ultrastructural characteristics of sustentacular cells in control and odorant-treated olfactor mucosae of the salamander. Anat. Rec. *221*, 769-779.